Senescence and senotherapies in pediatric biliary cirrhosis

Giulia Jannone

Cover figure:

Multiple immunofluorescence staining of a biliary atresia liver fragment obtained at the time of liver transplantation, evidencing important ductular reaction and established biliary cirrhosis. The staining identifies hepatocytes (HNF4-α; green), cholangiocytes (CK-19; yellow), myofibroblasts (α-SMA; light blue), cells containing DNA-damage foci (γH2AX; orange) and proliferative cells (Ki67; pink). The section was counterstained with Hoechst to evidence all cellular nuclei (dark blue).

Composition of the jury

President	Pr Isabelle Leclercq, UCLouvain
Promotor	Pr Etienne Sokal, UCLouvain
Co-promotor	Pr Anabelle Decottignies, UCLouvain
Secretary	Dr Mustapha Najimi, UCLouvain
Members	Pr Stefan Constantinescu, UCLouvain
	Pr Emmanuel Gonzales, Université Paris-Saclay
	Dr Florence Debacq-Chainiaux, UNamur
	Pr Ruth De Bruyne, Ghent University

This work was supported by the Fonds de la Recherche Scientifique (FRS-FNRS):
Formation à la Recherche dans l'Industrie et dans l'Agriculture (FRIA)

À celles et ceux qui œuvrent pour un monde meilleur,

À maman

Dans la vie, rien n'est à craindre,
tout est à comprendre.

Marie Curie

Je remercie les Pr Vincent Blondel, recteur de l'UCLouvain, Frédéric Houssiau, vice-recteur du Secteur des Sciences de la Santé, Françoise Smets, doyenne de la Faculté de Médecine et Médecine Dentaire, Isabelle Leclercq, présidente de l'Institut de Recherche Expérimentale et Clinique, et Jean-Louis Vanoverschelde, directeur médical des Cliniques universitaires Saint-Luc, de m'avoir offert l'opportunité de mener à bien ce projet de recherche académique au sein de l'UCLouvain, en collaboration avec les Cliniques universitaires Saint-Luc. Merci à eux également pour la formation qui m'a été donnée tout au long de mon parcours académique et clinique.

Je remercie le Fonds de la Recherche Scientifique (FRS-FNRS) pour son soutien financier ayant permis la réalisation de cette thèse, ainsi que la Fondation Saint-Luc grâce à laquelle le projet a pu débuter.

Je tiens à adresser un sincère et immense merci à mon promoteur, le Pr Etienne Sokal, qui m'a accompagnée depuis les bancs de médecine puis tout au long de mon parcours. Lorsque je lui ai fait part de mon envie de réaliser un mémoire de recherche clinique, je n'imaginais pas que cette rencontre allait progressivement faire naitre chez moi une passion pour l'hépatologie pédiatrique et pour la recherche. Son enthousiasme et son œil innovant m'ont donné l'envie d'en savoir toujours plus, et c'est presque logiquement que j'ai commencé une thèse sous sa supervision. Malgré un agenda chargé, il a toujours trouvé le temps de m'accompagner et de partager avec moi ses conseils avisés, ainsi que ses avis parfois tranchés mais toujours bienveillants. J'ai également l'immense privilège d'apprendre l'hépatologie pédiatrique à ses côtés, le partage de ses connaissances est un réel cadeau que je tenterai d'honorer du mieux possible tout au long de ma carrière. Sans lui rien de tout cela n'aurait été possible, et pour ça je lui adresse toute ma reconnaissance et ma gratitude.

Merci également à ma co-promotrice, le Pr Anabelle Decottignies, d'avoir accepté de superviser mon travail et de partager son expertise de la sénescence avec moi. Son esprit pratique et ses conseils toujours précis et efficaces m'ont remise à maintes reprises sur le droit chemin quand je n'arrivais plus à y voir clair. Je la remercie aussi de m'avoir permis d'apprendre et de réaliser certaines expérimentations dans son laboratoire, ainsi que pour sa disponibilité et son soutien.

Je remercie le Pr Isabelle Leclercq, présidente de mon comité d'accompagnement de thèse, pour ses conseils avisés et ses remarques toujours pertinentes, ainsi que pour son soutien moral mais également technique. Merci d'avoir partagé cellules et anticorps avec moi, et surtout merci pour vos paroles encourageantes.

Merci aux membres de mon comité d'accompagnement et de mon jury de thèse pour leur accompagnement et pour le temps qu'ils m'ont accordé. Merci aux Pr Stefan Constantinescu et Emmanuel Gonzales pour leurs précieux conseils et leur expertise. Merci au Dr Florence Debacq-Chainiaux et au Pr Ruth De Bruyne d'avoir accepté de rejoindre le train en route et de faire partie de mon jury, ainsi que pour leurs remarques et commentaires avisés et bienveillants qui m'ont permis d'améliorer ce manuscrit. Enfin, un merci particulier à Mustapha Najimi de m'avoir encadrée et de m'avoir ouvert la porte de son bureau à maintes reprises lorsque je toquais à l'improviste pour obtenir l'un ou l'autre conseil.

Merci à tous mes collègues présents et passés du laboratoire PEDI. À Louise qui m'a confortée dans mon envie de faire une thèse lors de mon stage de recherche, à Milena qui m'a tout appris quand je suis arrivée, à Caroline, Valéry, Adil, Nawfal et Nawal pour leur gentillesse et leur disponibilité. Merci à Paola, Sophie, Antoine et Brieuc d'avoir fait régner la bonne humeur dans notre bureau, Brieuc par

contre je dois avouer que le fait t'avoir à proximité n'a pas amélioré ma consommation de sucre… Merci à Olivier pour les nombreux partages de galères et pour m'avoir fait gagner des jours de travail grâce à ses talents de codeur, à Grégory d'avoir réinstauré la pause lunch et pour son oreille attentive, to Ananya for sharing her amazing culture with us, aux étudiants qui sont passés par le laboratoire et particulièrement à Marie de m'avoir aidée en culture cellulaire. Merci à Jonathan et Joachim pour votre aide précieuse et d'avoir répondu avec patience à mes questions souvent naïves de néo-doctorante, le laboratoire ne serait pas pareil sans vous. Enfin, un merci tout particulier à Tanguy qui a toujours été présent et disponible pour répondre à mes nombreuses questions pratiques et techniques, mais aussi pour son écoute attentive et pour nos nombreux partages enrichissants. Même depuis Montréal tu continues à me guider et à partager tes astuces avec moi, je ne sais pas ce que j'aurais fait sans toi !

Merci à Xavier Stephenne et Isabelle Scheers pour leur présence soutenante et leurs conseils avisés. Merci de vous être rendus toujours disponibles pour partager avec bienveillance vos parcours de chercheurs et de cliniciens, vous avez été une aide et un soutien précieux pour moi. Merci aussi de m'accueillir à bras ouverts dans le service, je me réjouis de commencer cette nouvelle aventure avec vous même si mes débuts sont un peu plus mouvementés que je ne l'avais espéré. Je remercie également Philippe Lysy et Françoise Smets pour leur intérêt scientifique et humain, et enfin Ilse van Elewijck pour sa gentillesse et son travail toujours efficace.

Je remercie Eliano Bonaccorsi d'avoir accepté de m'aider et de palier à mes talents inexistants de microchirurgienne, grâce à toi j'ai découvert qu'opérer des rats peut être un art ! Merci à Cathy de Magnée et à Roberto Tambucci pour leur gentillesse et leur disponibilité, et surtout merci d'avoir toujours pensé à

m’appeler au bon moment malgré les prouesses techniques que vous êtes en train de réaliser au moment où je viens récupérer mes petits morceaux de foie… Merci aussi à Aude pour sa serviabilité.

J’adresse par ailleurs mes chaleureux remerciements à Caroline Bouzin pour son aide précieuse et son partage de connaissances toujours empreint de gentillesse, ainsi que pour les nombreux bonbons ingurgités pendant mes sessions Visiopharm,

À Aurélie Daumerie et Michèle de Beukelaer pour leur assistance technique et leur disponibilité,

À Guillaume Courtois pour avoir accepté de partager son algorithme Visiopharm,

À Olivier Van Kerk et à toute l’équipe de GYNE, toujours prêts à aider,

À Marc de Bournonville pour sa serviabilité et sa musique revigorante,

Au Pr Jean-Paul Dehoux et à Magali Crutzen d’avoir partagé avec moi leurs compétences *in vivo*,

Au Dr Pamela Baldin d’avoir toujours essayé de m’aider au mieux dans ma collecte d’échantillons,

Au Pr Philippe Gailly et à ses doctorantes Caren et Farah d’avoir mis à disposition leur laboratoire pour mes Western Blot et de m’avoir aidée dans leur réalisation,

Au Pr Frédérique Lemaigre et à Rita Manco d’avoir accepté de me rencontrer et de partager avec moi leurs connaissances des voies biliaires et de la réaction ductulaire.

À l’institut de Duve, je tiens à remercier Hara Episkopou et Manon Mahieu de m’avoir tenu la main au début de ma thèse, Patrick van der Smissen de m’avoir initiée à la microscopie confocale, ainsi que Laurent Gatto et Axelle Loriot d’avoir rendu les biostatistiques un tout petit peu moins obscures pour moi.

I want to offer my sincere thanks to Fotios Sampaziotis and Teresa Brevini for their warm hospitality when I visited them in Cambridge. Thank you so much for sharing your expertise about cholangioids, for all your precious advices and help, and for making sure that I did not miss Cambridge's traditions and pubs. It was also a pleasure to meet Claudia in your lab.

Many thanks to Pr Kathleen Schwarz, who encouraged me on the path of pediatric hepatology and research many years ago, and who continued to follow my work all along the years with a lot of kindness. It was a real pleasure to meet you again in Bruges.

A tous ceux qui de près ou de loin m'ont apporté leur soutien et leur aide durant ces années de thèse, j'adresse un sincère merci. Merci également aux jeunes patients et à leurs familles de renouveler sans cesse notre motivation à faire progresser la médecine pour leur offrir un avenir meilleur.

Enfin, je dédie cette thèse à ma mère, qui m'a entourée d'un amour et d'une force sans limites tout au long de ma vie et qui a été d'un soutien inconditionnel durant mon parcours académique et professionnel, depuis mes 12 ans lorsque j'ai décidé de devenir pédiatre. Merci pour tout maman.
Merci aussi évidemment à Quentin, mon meilleur allié, de me soutenir dans tout ce que je fais et de me permettre de réaliser mes rêves. Et enfin – last but not least – merci à Gabriel et à son petit frère à naitre de me donner chaque jour l'envie et le courage de me dépasser un peu plus.

Table of contents

List of abbreviations

β-gal: β-galactosidase

γGT: gamma-glutamyl transferase

A-MSC: adipose-derived mesenchymal stem cells

ALGS: Alagille syndrome

ALT: alanine transaminase

AST: aspartate transaminase

BA: biliary atresia

BASM: biliary atresia splenic malformation

BDL: bile duct ligation

BDR: bile duct resection

BM-MSC: bone marrow-derived mesenchymal stem cells

CAR: chimeric antigen receptor

CDK: cyclin-dependent kinases

D: dasatinib

DAB: 3,3′-diaminobenzidine

DDR: DNA damage response

DSB: double-strand break

DSP: digital spatial profiling

FA: formaldehyde

FC: fold change

FFPE: formalin-fixed paraffin-embedded

GA: glutaraldehyde

GO: gene ontology

GPX-1: glutathione peroxidase 1

GSEA: gene set enrichment analysis

HALPC: human allogenic liver-derived progenitor cells

HCC: hepatocellular carcinoma

HNF4-α: hepatocyte nuclear factor 4-alpha

HSC: hepatic stellate cells

IF: immunofluorescence

IHC: immunohistochemistry

IL-6: interleukin 6

IL-8: interleukin 8

LLN: lower limit of normal

LSEC: liver sinusoidal endothelial cells

MDA: malondialdehyde

MMP: matrix metalloproteinases

MSC: mesenchymal stem cells

N1ICD: notch1 intracellular domain

NAFLD: non-alcoholic fatty liver disease

NES: normalized enrichment score

O/N: overnight

OIS: oncogene-induced senescence

p-adj: adjusted *p*-value

PBC: primary biliary cholangitis

PCA: principal component analysis

PFIC: progressive familial intrahepatic cholestasis

PSC: primary sclerosing cholangitis

Q: quercetin

ROI: region of interest

ROS: reactive oxygen species

RT: room temperature

RT-qPCR: reverse transcription quantitative polymerase chain reaction

SA-β-gal activity: senescence-associated β-galactosidase activity

SASP: senescence-associated secretory phenotype

SEM: standard error of the mean

SIPS: stress-induced premature senescence

SOD: superoxide dismutase

TGF-β1: transforming growth factor β1

ULN: upper limit of normal

uPAR: urokinase-type plasminogen activator receptor

WTA: whole transcriptome analysis

Summary

Cholestatic liver diseases – and especially biliary atresia (BA) – are the first cause of liver transplantation in the pediatric population. Although the outcomes of liver transplantation improved in the last years, there is still important mortality and morbidity related to this heavy procedure, generating a need for alternative therapies. Premature senescence has emerged as an important feature of adult chronic hepatobiliary diseases since this phenomenon was associated to disease severity and prognosis. Numerous preclinical studies were conducted in this context and demonstrated that liver disease improves when senescence decreases. A few studies also suggested the presence of liver senescence in BA, but the possibility of using anti-senescence therapies was never explored in pediatric biliary cirrhosis. In this context, and since there is an urgent need for new therapies to avoid or postpone liver transplantation in pediatric biliary cirrhosis, the aim of our work was to deeply investigate premature senescence in BA and to assess translatable anti-senescence therapies in a preclinical model of biliary cirrhosis.

We first developed multiple techniques to assess senescence since no single marker is completely specific of this phenomenon. In this process, we developed an optimized protocol allowing us to detect senescence-associated β-galactosidase activity on cryopreserved liver (see Chapter 2). We also performed the first spatial whole transcriptomic analysis on BA livers and demonstrated that liver senescence and the senescence-associated secretory phenotype (SASP) are already present from early stage in BA and continue to progress until liver transplantation, supporting the potential benefit of senotherapeutic interventions following hepatoportoenterostomy (see Chapter 3). The next step was to develop a preclinical model of biliary cirrhosis and senescence in which we could test senotherapies that would be ready for clinical applications. We demonstrated that the bile duct ligation (BDL) model in two-months-old rats displayed liver disease

and senescence progression that were in many aspects comparable to BA, and administrated the operated animals with human allogenic liver-derived progenitor cells (HALPC) or with the senolytic combination dasatinib (D) + quercetin (Q) (see Chapter 3). HALPC decreased the early marker of senescence p21 and improved liver disease in BDL rats, providing promising results regarding the use of senotherapeutics in biliary cirrhosis. However, a longer experiment with repeated administrations of HALPC did not confirm those preliminary results, and D+Q did not have any effect on liver senescence in the experiments (see Chapters 3 & 4). Finally, we report for the first time that the livers of patients suffering from Alagille syndrome – another leading cause of liver transplantation due to pediatric cholestasis – display premature senescence at the time of liver transplantation, despite Jagged1 mutation and the involvement of the Notch pathway in senescence induction and propagation (see Chapter 5).

In conclusion, we provide the first report suggesting a potential interest of anti-senescence therapies in pediatric biliary cirrhosis. However, proof of efficacy regarding therapeutic interventions that act on early and late senescence through identified mechanisms and thereby improve liver disease will be needed before translating senotherapies to pediatric biliary cirrhosis.

Chapter 1: introduction

Background

Liver transplantation in pediatric cholestatic diseases

Cholestatic liver diseases in the neonate or the young infant are a group of rare diseases inducing conjugated hyperbilirubinemia due to bile flow impairment (1). Those diseases affect approximately 1/2500 infants and the principal etiology is biliary atresia (BA), which is involved in 25-55% of the cases (1). Other conditions inducing cholestatic jaundice in infants include alpha1-antitrypsin deficiency, Alagille syndrome (ALGS) and progressive familial intrahepatic cholestasis (PFIC). Despite the existence of supportive therapies – mainly choleretics and antipruritics – there are currently no curative treatments for chronic cholestasis and the only therapeutic option in case of end-stage liver disease remains liver transplantation (1). According to the European Liver Transplantation Registry (ELTR) website, that reports the results of 17117 children transplanted between 1988 and 2020, cholestatic diseases alone represent 70.6% of the liver transplantation indications in children under 2 years old. The SPLIT registry reports results from 1911 pediatric liver recipients in North America from 2011 to 2018 (2). Cholestatic diseases were the first cause of liver transplantation in the total pediatric population of this database (0-18 years of age) as they were responsible for 47.3% of the transplantations. Within cholestatic diseases, the main etiology was BA (38.5%), followed by ALGS (4.1%) and PFIC (2.8%) (2). The outcomes of liver transplantation have progressed as the SPLIT registry reported a 5-years patient's survival rate of 94.2% and a 5-years graft survival rate of 87.7% (2). However, the 20-years graft survival rate drops to 55% in the ELTR long-term data and the life-long

immunosuppressive therapy required after liver transplantation still induces substantial morbidity (3). Also, the cognitive and behavioral development of transplanted children is significantly affected (3). Although the outcomes of pediatric liver transplantation notably improved in the last years, there is still considerable mortality and morbidity related to this procedure and therapeutic alternatives are urgently needed.

Senescence and the senescence-associated secretory phenotype

Senescence development

Senescence is a process of cellular aging, which may occur following different mechanisms. Replicative senescence results from a progressive decline in the cell's ability to proliferate (4). It occurs in response to telomere shortening after a number of cellular doublings depending on various parameters (cellular type and donor's species, age or genotype). On the other side, stress-induced premature senescence (SIPS) can be triggered at any time by a large diversity of factors promoting cellular stress, including telomere dysfunction, non-telomere DNA damage, oxidative stress or oncogene activation (5). A DNA damage response (DDR) occurs in response to DNA double-strand breaks (DSBs) and leads to cell-cycle arrest until the damage has been repaired (6). DDR signaling kinases such as ATM and ATR accumulate at the damaged site and phosphorylate DDR proteins including H2AX and 53BP1. If the damage persists, ATM and ATR activate the tumor suppressor p53, which leads to a permanent cell-cycle arrest and cellular senescence through p21 activation. When DSBs are located at telomeric regions due to telomere shortening or to genotoxic agents, the DNA repair is much less efficient and cellular senescence quickly occurs (6). DNA altered replication and DSBs can also be a consequence of the hyperproliferative phase triggered by

oncogene expression – such as RAS or BRAF – and lead to oncogene-induced senescence (OIS) (6).

The senescent phenotype

Senescent cells display a specific structural and functional phenotype (Figure 1). Those cells typically show an enlarged and flattened morphology, associated to the upregulation of cell cycle inhibitors such as p21 and p16, which lead to permanent cell cycle arrest through Rb-E2F modulation. Both p21 and p16 inhibit cyclin/cyclin-dependent kinases (CDK) complexes and thereby prevent Rb phosphorylation (7). The unphosphorylated form of Rb represses E2F family transcription factor activity, resulting in a cell cycle arrest as E2F is normally required for cell-cycle progression. Other CDK inhibitors include p15 and p27 and can also be used as senescence markers in selected situations (7). Senescent cells also display a higher activity of the lysosomal enzyme beta-galactosidase (β-gal), as a consequence of the increase in the number and activity of lysosomes due to the accumulation of damaged macromolecules (8). Other hallmarks of senescence include the accumulation of DNA-damage foci, telomere shortening and/or dysfunction, metabolic modifications including mitochondrial dysfunction, upregulation of anti-apoptotic pathways and a senescence-associated secretory phenotype (SASP) (9, 10). DNA-damage foci are nuclear structures containing proteins associated to the DDR such as ATM, ATR, γH2AX (histone H2AX phosphorylated on Ser-139) or 53BP1 (7). Telomere shortening mainly occurs in replicative senescence, while telomere dysfunction consists in the accumulation of DNA-damage foci at telomeric sites (telomere dysfunction-induced foci – TIFs) and can be detected in all types of senescence (5). Mitochondrial dysfunction in senescent cells leads to an increase in reactive oxygen species (ROS), which causes oxidative stress that can in turn reinforce senescence (7). Senescent cells also upregulate anti-apoptotic/pro-

survival pathways, mediated amongst others by the increased expression of Bcl2 family members (7). Finally, the SASP includes pro-inflammatory cytokines and chemokines, angiogenic factors, growth modulators and matrix metalloproteinases (MMPs) amongst others (11). It allows developmental senescence during embryogenesis, as well as wound healing, tissue plasticity, and the activation of immune responses resulting in the clearance of senescent cells. However, the SASP also contributes to reinforcing and spreading senescence through autocrine and paracrine effects, which can lead to deleterious tissue remodeling and cellular dysfunction (7). Furthermore, chronic activation of the SASP can cause sustained inflammation and be pro-tumorigenic through angiogenesis stimulation. Interestingly, the SASP profile can vary widely according to the cell type, senescence induction stimulus and duration of senescence (12, 13). Various cytokines are represented in the SASP of cirrhotic livers, including transforming growth factor β1 (TGF-β1), C–C motif chemokine ligand 2 (CCL2), interleukin 6 (IL-6) and 8 (IL-8), which are important promotors of the paracrine and autocrine transmission of senescence (10, 14, 15). Since no senescence markers are completely specific, the identification of senescent cells classically relies on a selected combination of markers reflecting various hallmarks of the senescent phenotype (5).

Altogether, the senescent phenotype causes an irreversible inhibition of cell proliferation with the inability to induce apoptosis and a modulation of the cell metabolic activity. While acute senescent cells are beneficial (embryogenesis, tumour suppression, wound repair), the accumulation of chronic senescent cells can be harmful and result in cell and tissue dysfunction (16).

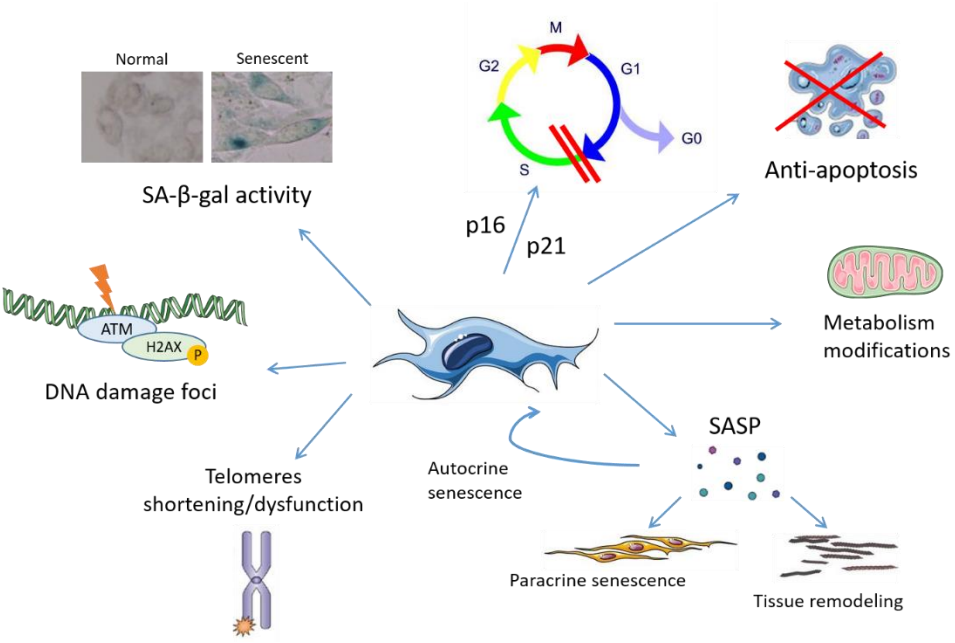

Figure 1. Hallmarks of cellular senescence. SA-β-gal: senescence-associated β-galactosidase; SASP: senescence-associated secretory phenotype.

Premature senescence in adult hepatobiliary diseases and in preclinical models of liver disease

Senescence worsens the prognosis of biliary diseases

Premature liver senescence occurs in numerous chronic hepatobiliary diseases and has been associated to disease severity and cirrhosis (17-20). Cholangiocytes senescence was associated with disease severity and prognosis in primary sclerosing cholangitis (PSC) (18). In primary biliary cholangitis (PBC), cholangiocytes senescence increased with disease severity, modulated the response to choleretic therapy and induced paracrine transmission of senescence in other cholangiocytes (21, 22). Hepatocytes senescence was also demonstrated in numerous chronic liver diseases including PSC, PBC, non-alcoholic fatty liver disease (NAFLD) and chronic

viral hepatitis, and also correlated with disease severity and prognosis (17, 20). Current knowledge about senescence in cholangiopathies suggests that the initial biliary injury induces the activation of cholangiocytes and the formation of a ductular reaction, but also directly causes stress-induced premature senescence in cholangiocytes (Figure 2) (23-25). The SASP of senescent cholangiocytes not only worsens the inflammation and fibrosis related to the biliary injury and ductular reaction, but also causes paracrine transmission of senescence in surrounding cholangiocytes and hepatocytes. Those paracrine effects of the SASP reinforce cholangiocytes senescence and lead to hepatic dysfunction due to hepatocytes senescence. Ultimately, the accumulation of senescent cholangiocytes – due to SIPS or paracrine senescence – and the exhaustion of the proliferative ability of the ductular reaction cells that undergo replicative senescence can lead to ductular paucity. This theory underlies the fact that senescence is a consequence and not a cause of the biliary damage, but also allows us to understand how senescence and the SASP can substantially worsen the disease evolution and prognosis.

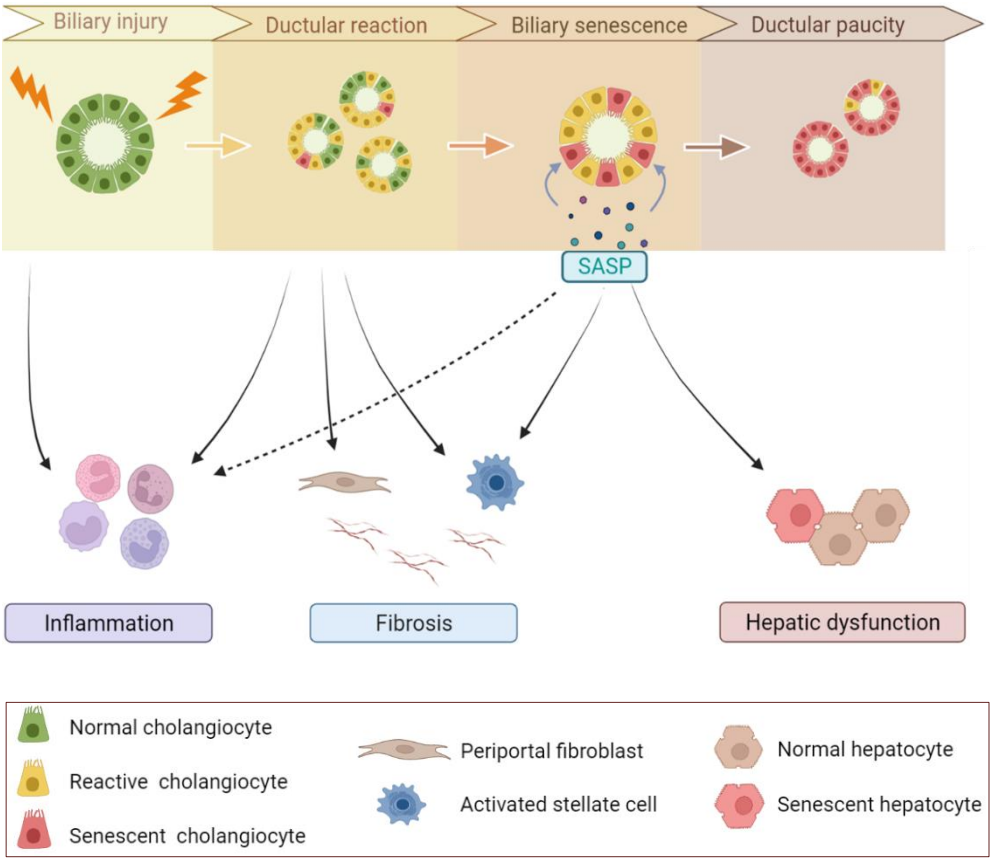

Figure 2. Senescence physiopathology in biliary diseases. SASP: senescence-associated secretory phenotype. Created with Biorender.com.

Liver disease improves when senescence decreases

Several preclinical studies clearly emphasized the connection between senescence and hepatobiliary diseases (Figure 3). In a mouse model of liver injury induced by CCl_4, shortened hepatocyte telomeres caused by telomerase knockout were associated with cellular senescence and an accelerated onset of cirrhosis (26). In the same model, reintroduction of telomerase activity improved the liver function and the histological fibrosis. In another study, clearance of senescent cells by

suicide gene-mediated ablation of p16Ink4a-expressing senescent cells or by treatment with senolytic drugs dasatinib (D) and quercetin (Q) reduced steatosis in mice (27). More recently, anti-senescence urokinase-type plasminogen activator receptor (uPAR)-specific chimeric antigen receptor (CAR) T cells improved liver function and fibrosis in mice models of liver disease induced chemically (CCl_4) or by diet (28). Also, suppressing paracrine senescence through TGF-β receptor 1 inhibition allowed to improve liver regeneration and mouse survival following acetaminophen liver injury (29). Notably, in a mouse model of biliary senescence based on the conditional deletion of *Mdm2* (an inhibitor of p53) in bile ducts under the control of the *Krt19* promoter, cholangiocytes senescence induced liver fibrosis and impaired liver function and regeneration through paracrine transmission of senescence from cholangiocytes to hepatocytes (15). Suppressing the paracrine transmission of senescence by inhibiting TGF-β receptor 1 allowed to improve liver function and regeneration in this model. In another model of biliary injury ($Mdr2^{-/-}$ mice), removal of senescent cells through ablation of p16Ink4a-expressing cells or fisetin administration reduced liver inflammation and fibrosis (30). Altogether, existing data demonstrate that liver disease improves when senescence decreases and generate a need for anti-senescence therapies that can be translated to clinical applications.

Even if the deleterious effects of senescent hepatocytes and cholangiocytes have been extensively demonstrated in chronic hepatobiliary diseases, it is important to know that other senescent cell types might be beneficial for liver homeostasis. For example, in $p53^{-/-}$ mice treated with CCl_4, liver fibrosis increased due to a reduction of senescent hepatic stellate cells (HSC) as compared to wild type CCl_4-treated mice (31). Senescent HSC also promoted liver regeneration after partial hepatectomy in mice through IL-6 and ligands of CXCR2 (32). HSC senescence thus seems to be beneficial as it limits liver fibrosis progression and improves liver regeneration. Liver sinusoidal endothelial cells (LSEC) senescence also has beneficial effects as the

removal of senescent LSEC in aged mice resulted in perivascular fibrosis (33). In this context, anti-senescence therapies should be developed with special attention payed to the senescent cell type targeted.

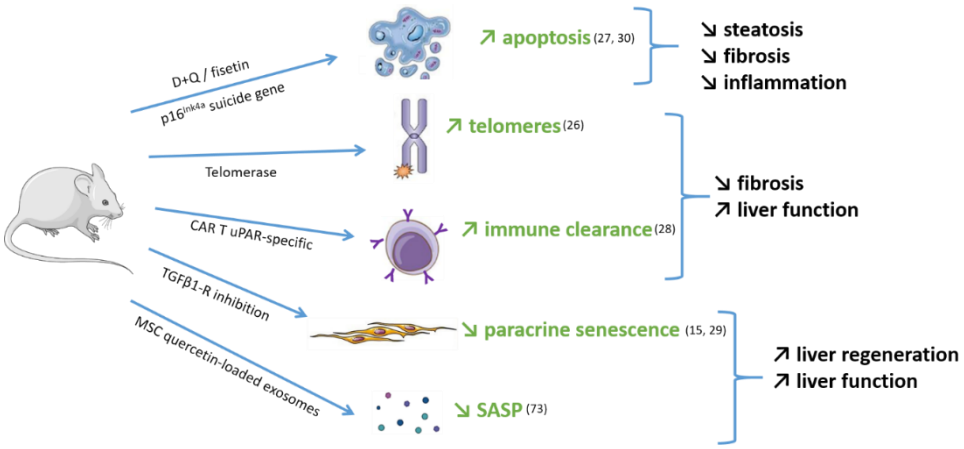

Figure 3. Liver disease improves when senescence decreases in preclinical models. D: dasatinib; MSC: mesenchymal stem cells; Q: quercetin; SASP: senescence-associated secretory phenotype.

Biliary atresia and senescence in pediatric biliary cirrhosis

Biliary atresia

BA is a severe pediatric disease caused by the progressive fibro-inflammatory obliteration of extrahepatic bile ducts (34). The biliary obstruction leads to cholestasis, hepatocellular injury and ultimately cirrhosis and end-stage liver disease. Despite the fact that BA is the first cause of liver transplantation in children, its underlying mechanisms are still not completely elucidated (34, 35). Multiple potential etiological factors have been incriminated, such as viral infection (CMV,

EBV and HPV amongst others), environmental toxins, genetic susceptibility, immune dysfunction or disruption of the apical-basal polarization of cholangiocytes (36). The diseased phenotype is most likely multifactorial, with significant involvement of viral infection and immune dysregulation in isolated BA. CMV is the most frequently incriminated viral agent and CMV-associated BA has even been proposed as a BA subgroup (37). In the rhesus rotavirus (RRV)-induced mouse model of BA, the SRL peptide of VP4 protein has been shown to be responsible for the biliary damage, and this peptide is also found in CMV proteins (38). In syndromic BA, genetic mutation(s) leading to primary cilia dysfunction such as *PDK1L1*, *PCNT*, *KIF3B* or *TTC17* probably play an important part in the physiopathology (36). Recently, a mouse model of *Pdk1l1* intrahepatic deletion was able to reproduce some pathological aspects of BA (39). Syndromic BA is not clearly defined as it can include either the typical BA splenic malformation (BASM) syndrome or various other malformations such as esophageal atresia (37). Either way, the polymalformative phenotype suggests that the disease already develops in utero and a prenatal diagnosis is sometimes possible. Children with BASM syndrome inconsistently display polysplenia, absence of the inferior vena cava, preduodenal portal vein and/or situs inversus (37). Finally, a cystic form of BA can occur and must not be mistaken for an obstructed choledochal cyst as the evolution and prognosis of those diseases are completely different (37).

Premature senescence in biliary atresia

Premature senescence has been described in pediatric BA in isolated cases or through single techniques. Gutierrez-Reyes et al evidenced senescence-associated β-galactosidase (SA-β-gal) activity and increased p53 protein expression in the cholangiocytes cell population of two children who underwent liver transplantation for BA (40). Both livers did not display protein expression of senescence markers p16 and p21 through immunohistochemistry (IHC). In contrast, other authors

reported an upregulation of p16 and p21 IHC protein expression in the cholangiocytes of 63 children transplanted for BA (41). Senescence in BA was also evidenced through a reduction of the telomere/centromere ratio in the hepatocytes of 20 transplanted children, but the Q-FISH method used for this study did not show any reduction in telomere length (42). Finally, another group investigated the gene expression of IGFBP-rP1 (or IGFBP7), a protein playing an important role in Ras- and p53-mediated senescence (43-45). They observed an increase in IGFBP-rP1 cDNA microarray expression in 11 BA children, and confirmed this result in two patients through semi-quantitative reverse transcription polymerase chain reaction (RT-PCR). The hypothesis underlying the development of senescence in BA is that continuous activation of TLR3 by double strand viral RNA would lead to N-Ras activation and ultimately to OIS (19). Of note, senescence was never investigated in other pediatric cholangiopathies such as ALGS or PFIC.

Because no senescence markers are completely specific, the gold standard is now to assess cellular senescence through multiple indicators (5). No study ever demonstrated a full senescence pattern in BA nor investigated the possibility of developing senotherapies in pediatric biliary cirrhosis to date.

Senotherapies

Substantial research has been conducted in the last years to develop therapeutic agents able to alleviate the senescent burden, so called senotherapeutics agents or senotherapies. Different subcategories of senotherapies have been proposed according to their mechanism of action (46). The main subcategories of senotherapeutics are described hereafter with special attention payed to their potential translatability to clinical applications.

Senolytics

Senolytic therapies aim at specifically targeting and eliminating senescent cells (47). Proof of concept of senolytics efficacy was first achieved through the INK-ATTAK transgene mouse model, in which elimination of p16Ink4a-positive senescent cells induced by a drug allowed to delay the onset of age-related pathologies and to attenuate the progression of already established age-related disorders (48). First-generation senolytics were subsequently developed by inhibiting the anti-apoptotic pathways that are upregulated in senescent cells (49, 50). The multityrosine kinase inhibitor D (EPHB1 inhibition) and the flavonoid Q (PI3K pathway inhibition), used in combination, demonstrated to synergistically reduce the senescent cell burden in chronologically aged, radiation-exposed, and progeroid mice (50). The Bcl-2 inhibitor navitoclax as well as the combination of Bcl-2, Bcl-xL and Bcl-w siRNAs also demonstrated to have a senolytic activity in selected cell types (51). Fisetin, a flavonoid that targets the PI3K/AKT/mTOR pathway, and the specific Bcl-xL inhibitors A1331852 and A1155463 subsequently confirmed the senolytic potential of pro-apoptotic drugs on selected senescent cell types (52). More recently, immune-mediated clearance of senescent cells through cytotoxic CAR T cells primed against uPAR efficiently ablated senescent cells *in vitro* and *in vivo*, uPAR being a cell-surface protein that is broadly induced during senescence (28).

The considerable advantage of senolytic therapies is that an intermittent use is possible as a “hit and run” strategy allows to successfully remove senescent cells with spaced administrations (46). However, despite intermittent administration, off-target side effects caused by the removal of non-senescent cells or beneficial senescent populations can still occur. For example, navitoclax can induce thrombopenia and neutropenia due to off-target effects on platelets and neutrophils (47). Still, D+Q, fisetin and navitoclax are currently being studied in clinical trials about age-related diseases. The combination of D+Q is being tested in Alzheimer’s disease (NCT04785300), diabetic kidney disease (NCT02848131),

idiopathic pulmonary fibrosis (NCT02874989), osteoporosis (NCT05313634) and NAFLD (NCT05506488). Fisetin is studied in osteoporosis (NCT05313634), osteoarthritis (NCT04210986) and diabetic kidney disease (NCT03325322), while navitoclax is investigated in solid tumors in combination with senescence-inducing chemotherapy (NCT00445198; NCT02591095; NCT02520778; NCT02079740). New strategies are being developed to increase senolytics specificity for senescent cells, for example through galactose-conjugated nanoparticles or prodrugs cleaved in cells with increased SA-β-gal activity (46). However, as mentioned before, particular attention will have to be paid in the future to the specific cell type targeted by senolytics in specific disease conditions to better avoid off-target side effects.

Senoblockers

Senoblockers inhibit or prevent the primary damage that induces senescence development or artificially reverse senescence (46). This category includes Mdm2/p53 pathway modulators, viral reactivation of telomerase or reprogramming of senescent cells into pluripotent stem cells (53-55). However, bypassing senescence raises obvious concerns about a potential oncogenic risk and those strategies are difficult to translate into clinical applications.

Senomorphics

Senomorphic therapies aim at modulating the SASP and its downstream effects (46). This subgroup includes inhibitors of molecular pathways inducing the SASP, for example mTOR inhibition through rapamycin (and analogs) or NF-kB inhibition through metformin or glucocorticoids (49). However, the effects of those drugs are often multiple and it is very difficult to attribute any beneficial effect to SASP inhibition only. Metformin was tested in clinical trials about aging (NCT02432287), frailty (NCT03451006) and muscle strength in the elderly (NCT02308228) among

others. More specific senomorphics can act on single SASP components, including monoclonal antibodies or molecules inhibiting TGF-β (SB525334), IL-6 (tocilizumab), IL6-R/JAK-STAT (ruxolitinib) or IL-1 (anakinra) (49). Still, it is very difficult to discriminate if the effect of those compounds is related to anti-inflammatory or anti-SASP effects. The main advantage of senomorphics is that they do not induce side effects related to the removal of senescent cells. However, since senescent cells are not removed and continue to produce the SASP, continuous administration could be necessary to achieve a significant effect. Also, a better understanding of individual SASP components will be needed to translate senomorphics in clinics, especially since the SASP can be beneficial and allow tissue regeneration in specific conditions (56).

Mensenchymal stem cells

Mesenchymal stem cells (MSC) (Figure 4) and MSC-derived extracellular vesicles can improve age-related diseases through anti-oxidative and anti-inflammatory properties that limit the development of senescence (57). Bone marrow-derived MSC (BM-MSC) decreased senescence in a mouse model of idiopathic pulmonary fibrosis and in cardiomyocytes of aging rats through anti-oxidative properties (NAD+ and NADPT increase or ROS and malondialdehyde – MDA – reduction) (58, 59). In an ischemia-reperfusion model of kidney injury in rats, umbilical cord-derived MSC (UC-MSC) and adipose-derived MSC (A-MSC) also reduced senescence through anti-oxidative and anti-inflammatory effects reflected by an increase in superoxide dismutase (SOD) and Klotho (60). Furthermore, A-MSC decreased adipocytes and skin senescence in aging mice through anti-oxidative properties (SOD increase and MDA reduction), and A-MSC extracellular vesicles improved ultraviolet B-induced skin senescence through anti-oxidative and anti-inflammatory effects (reduction of ROS and immune cell infiltrate) (61-63). Some evidence suggests that MSC could also have anti-senescence effects through SASP

modulation. Extracellular vesicles from human embryonic stem cell-derived MSC reduced senescence and SASP components such as IL-6 and IL-1β in various organs of aged mice (64). In addition to their anti-oxidative senoblocking effects, MSC could thus modulate the SASP through anti-inflammatory senomorphic properties. Again, discriminating senescence improvement related to SASP modulation versus anti-inflammatory properties remains a real challenge. Also, MSC anti-senescence effects were attributed to global anti-oxidative and anti-inflammatory properties in preclinical studies, but the molecular pathways underlying those effects are still not elucidated. On the other side, MSC can induce senescence in selected cell types as demonstrated in a mouse model of systemic lupus erythematosus in which human UC-MSC increased CD4+ T cells senescence via MiR-199a-5p/Sirt1/p53 axis (65). Special attention also has to be payed to the donor's age and to MSC manipulations *in vitro* since MSC senescence occurs with age or due to prolonged culture conditions (66, 67). Still, MSC already reached clinical applications and their effect was or is currently being investigated in numerous human pathologies including age-related diseases such as Alzheimer's disease (NCT02600130), osteoporosis (NCT01532076), osteoarthritis (NCT01504464), myocardial infarction (NCT05043610) and frailty syndrome (NCT04914403). MSC transplantation in chronic liver disease repeatedly demonstrated to improve liver function and histology (68-71). Recently, MSC-derived exosomes improved senescence in cholangioids treated with H2O2 and in the CCl_4 mouse model of liver injury (72, 73). However, the effect of MSC on liver senescence has never been investigated.

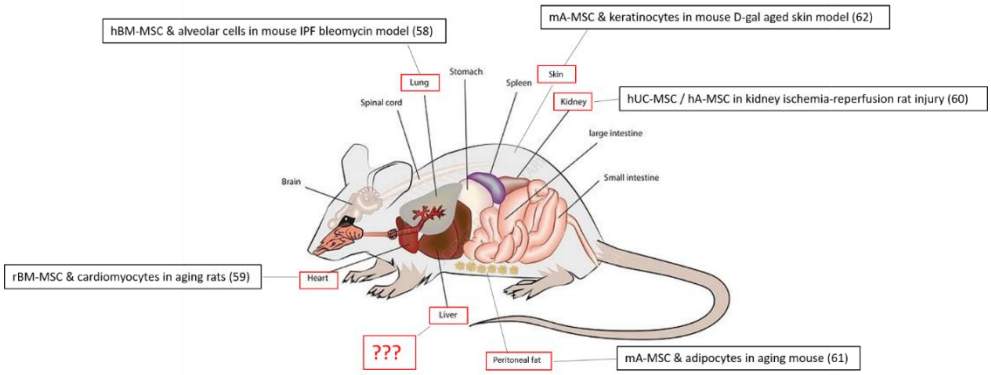

Figure 4. Anti-senescence properties of MSC. A-MSC: adipose-derived MSC; BM-MSC: bone marrow-derived MSC; h: human; IPF: idiopathic pulmonary fibrosis; m: mouse; MSC: mesenchymal stem cells; r: rat; UC-MSC: umbilical cord-derived MSC. Image modified from Science Photo Library.

Human allogenic liver-derived progenitor cells

The PEDI laboratory has reproducibly obtained a population of MSC derived from healthy adult human liver, so called human allogenic liver-derived progenitor cells (HALPC) (74). Those cells have been extensively characterized both *in vitro* and in preclinical studies, and have reached clinical application (75, 76). Before the cryopreservation step, the cells undergo strict quality control regarding various parameters: (1) identity (≥ 85% of CD90+CD73+ and sum of cell impurities < 15% in flow cytometry, expression of vimentin and αSMA in immunocytochemistry), (2) biological activity (viability ≥ 70% and PGE2 secretion ≥ 10 ng/106 total cells) and safety (karyotype verification, microbiology, testing for endotoxin and mycoplasma). HALPC display a hepatocytic differentiation ability and have multi-target properties through the secretion of important bioactive factors with paracrine activity, including anti-inflammatory, anti-fibrotic and pro-regenerative effects (Figure 5) (77-82). Their immunogenicity is low as they do not express HLA class II nor costimulatory molecules such as CD40 and CD80, which allows to

administrate them in preclinical models without concomitant immunosuppressive therapy (79). The main effects of the cells are mediated by paracrine mechanisms as they displayed pro-regenerative effects in mice livers after partial hepatectomy even in the absence of engraftment and proliferation of their own (81). Importantly, the cells secrete hepatocyte growth factor (HGF), an inhibitor of the cytokine TGF-β (80). TGF-β has pro-fibrotic properties through HSC activation, but it also demonstrated to be a critical element for the establishment of paracrine senescence through the SASP by inducing p21 expression (15, 29). Moreover, TGF-β alone is able to induce senescence in well-differentiated hepatocarcinoma cell lines (83). HALPC anti-inflammatory secretome could also suppress the pro-inflammatory effect of the SASP. However, the potential anti-senescence and anti-oxidative properties of HALPC have never been investigated to date.

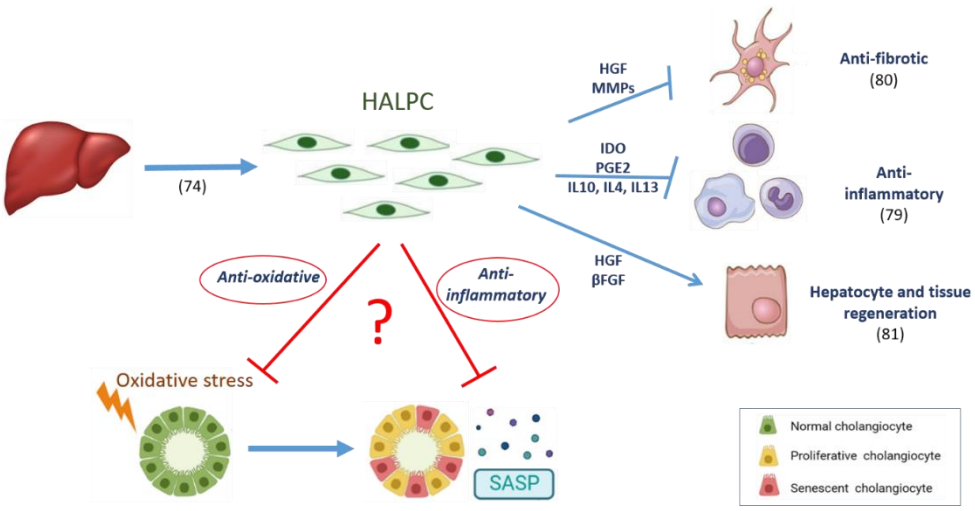

Figure 5. Human allogenic liver-derived progenitor cells (HALPC) properties. SASP: senescence-associated secretory phenotype. Created with Biorender.com.

Research question and objectives

Cholestatic liver diseases – and especially BA – are the first cause of liver transplantation in the pediatric population (1). Supportive therapies are available, but there are no curative treatments and liver transplantation remains the only therapeutic option when chronic cholestasis evolves to end-stage liver disease (1). Although the outcome of liver transplantation improved in the last decades, there is still important mortality and morbidity related to this heavy procedure, generating a need for alternative therapies (3).

Premature senescence has emerged as an important feature of adult chronic hepatobiliary diseases since this phenomenon was associated to disease severity and adverse outcomes through deleterious effects on liver tissue remodeling and hepatic function (18, 19, 84). Numerous preclinical experiments demonstrated that liver disease improves when senescence decreases (15, 26-28, 30). A few studies also suggested the presence of liver senescence in BA, but the possibility of using anti-senescence therapies was never explored in pediatric biliary cirrhosis (40, 41).

In this context and since there is a need for new therapies to avoid or postpone liver transplantation in pediatric biliary cirrhosis, the aim of our work was to deeply investigate premature senescence in BA and to assess translatable senotherapies in a preclinical model of biliary cirrhosis.

Main methods

Senescence characterization

Since the gold standard to assess senescence is to quantify various senescence-associated parameters, we developed several methods that allowed us to characterize senescence through multiple markers and techniques on both human and rat liver (5). Those methods include senescence-associated β-gal (SA-β-gal) activity, p16 and p21 gene and protein expression, γ-H2AX protein expression and SASP-related gene expression. SA-β-gal activity is a widely used biomarker of cellular senescence in fresh tissue sections (85). In order to allow multiple testing on the same samples and to facilitate the research, we developed an optimized SA-β-gal activity protocol that allowed us to extend the use of the SA-β-gal activity assay to cryopreserved tissue (see Chapter 2) (86). To investigate the cellular localization of senescence, we developed multiple immunofluorescence (IF) staining of senescence/DNA-damage (p21 or γ-H2AX), cholangiocytes (CK19) and hepatocytes (HNF4α). We also designed a histological co-staining of SA-β-gal activity and CK19 IHC. Finally, to deeply characterize senescence in diseased human livers with regard to the affected cell type, we performed the first digital spatial profiling whole transcriptome analysis ever reported in BA livers.

Choice of senotherapies that could be translated to clinical applications

Numerous senotherapeutics were tested in preclinical studies, but very few have the potential of reaching clinical application. Since MSC already demonstrated to have anti-senescence properties *in vivo*, we first decided to test HALPC, a population of liver-specific MSC that was already approved for clinical applications (58-61, 75, 76). To have a positive control, we also decided to use the very well described combination of the pro-apoptotic drugs D+Q that was already tested in

clinical trials in diabetic kidney disease or idiopathic pulmonary fibrosis amongst others (87, 88).

Choice of a preclinical model of biliary cirrhosis and senescence

We needed a preclinical model of biliary cirrhosis and senescence in which we could test the selected senotherapeutics. Bile duct ligation (BDL) in young rats is classically described as a model of biliary cirrhosis rather than BA, even if it was also reported as a BA model in mice (89). This model allows rapid and constant progression to biliary fibrosis and cirrhosis with a very high survival rate, unlike the classical RRV BA model (90, 91). In addition, liver senescence was previously reported in the BDL model, increasing the chances of developing a robust model of biliary senescence (92-94). The reassortant RRV mice model of BA was considered as an alternative (90). In this improved version of the original RRV model, the reassortant virus (RRV(VP2,VP4)-TUCH) injected to newborn mice allowed to lower the mortality rate and increase fibrosis development. Reassortant RRV mice displayed a 38% survival rate at 30 days of age and 63% demonstrated to have advanced liver fibrosis at 28 days. However, the low survival rate at 14 days (less than 50%) and the lack of systematic fibrotic evolution would have made the assessment of liver senescence and disease evolution very challenging. Moreover, senescence was never investigated in this model. Finally, we considered the BDL model in three-weeks-old rats as it would potentially better mimic the neonatal conditions of BA, but technical considerations convinced us to proceed with the same model in young (two-months-old) – but not neonate – rats (95).

Thesis layout

In Chapter 2 we provide an optimized SA-β-gal activity protocol that allowed us to extend the use of the SA-β-gal activity assay to cryopreserved liver tissue. The main results of the project are reported in Chapter 3, which contains an extensive description of liver senescence in BA and in the BDL rat model. This chapter also provides the results of HALPC and D+Q administrations that were tested in rats once we confirmed that BDL was an appropriate model of biliary cirrhosis and senescence. Since we obtained promising results with HALPC in the short-term experiment reported in Chapter 3, we next performed a long-term experiment with HALPC and D+Q repeated administrations, of which the results are presented in Chapter 4. Finally, Chapter 5 contains a brief description of liver senescence in ALGS, another leading cause of biliary cirrhosis in children. All the above-mentioned results are discussed in Chapter 6, which provides a general discussion as well as conclusions and perspectives of the project.

References

1. Feldman AG, Sokol RJ. Neonatal cholestasis: emerging molecular diagnostics and potential novel therapeutics. Nat Rev Gastroenterol Hepatol. 2019;16(6):346-60. Epub 2019/03/25. doi: 10.1038/s41575-019-0132-z. PubMed PMID: 30903105.
2. Elisofon SA, Magee JC, Ng VL, Horslen SP, Fioravanti V, Economides J, et al. Society of pediatric liver transplantation: Current registry status 2011-2018. Pediatr Transplant. 2020;24(1):e13605. Epub 2019/11/05. doi: 10.1111/petr.13605. PubMed PMID: 31680409.
3. Tran LT, Carullo PC, Banh DPT, Vitu C, Davis PJ. Pediatric Liver Transplantation: Then and Now. J Cardiothorac Vasc Anesth. 2020;34(8):2028-35. Epub 2020/04/04. doi: 10.1053/j.jvca.2020.02.019. PubMed PMID: 32241678.
4. Campisi J. From cells to organisms: can we learn about aging from cells in culture? Exp Gerontol. 2001;36(4-6):607-18. Epub 2001/04/11. PubMed PMID: 11295503.
5. Gorgoulis V, Adams PD, Alimonti A, Bennett DC, Bischof O, Bishop C, et al. Cellular Senescence: Defining a Path Forward. Cell. 2019;179(4):813-27. Epub 2019/11/02. doi: 10.1016/j.cell.2019.10.005. PubMed PMID: 31675495.

6. Di Micco R, Krizhanovsky V, Baker D, d'Adda di Fagagna F. Cellular senescence in ageing: from mechanisms to therapeutic opportunities. Nat Rev Mol Cell Biol. 2021;22(2):75-95. Epub 2020/12/18. doi: 10.1038/s41580-020-00314-w. PubMed PMID: 33328614; PubMed Central PMCID: PMCPMC8344376.
7. Gonzalez-Gualda E, Baker AG, Fruk L, Munoz-Espin D. A guide to assessing cellular senescence in vitro and in vivo. FEBS J. 2021;288(1):56-80. Epub 2020/09/23. doi: 10.1111/febs.15570. PubMed PMID: 32961620.
8. Kurz DJ, Decary S, Hong Y, Erusalimsky JD. Senescence-associated (beta)-galactosidase reflects an increase in lysosomal mass during replicative ageing of human endothelial cells. J Cell Sci. 2000;113 (Pt 20):3613-22. Epub 2000/10/06. PubMed PMID: 11017877.
9. Aravinthan AD, Alexander GJM. Senescence in chronic liver disease: Is the future in aging? J Hepatol. 2016;65(4):825-34. doi: 10.1016/j.jhep.2016.05.030. PubMed PMID: 27245432.
10. Hoare M, Das T, Alexander G. Ageing, telomeres, senescence, and liver injury. J Hepatol. 2010;53(5):950-61. doi: 10.1016/j.jhep.2010.06.009. PubMed PMID: 20739078.
11. Coppe JP, Desprez PY, Krtolica A, Campisi J. The senescence-associated secretory phenotype: the dark side of tumor suppression. Annu Rev Pathol. 2010;5:99-118. doi: 10.1146/annurev-pathol-121808-102144. PubMed PMID: 20078217; PubMed Central PMCID: PMCPMC4166495.
12. Basisty N, Kale A, Jeon OH, Kuehnemann C, Payne T, Rao C, et al. A proteomic atlas of senescence-associated secretomes for aging biomarker development. PLoS Biol. 2020;18(1):e3000599. Epub 2020/01/17. doi: 10.1371/journal.pbio.3000599. PubMed PMID: 31945054; PubMed Central PMCID: PMCPMC6964821 following competing interests: JC is a founder and shareholder of Unity Biotechnology, which develops senolytic drugs. All other authors have declared no competing interests.
13. Hernandez-Segura A, de Jong TV, Melov S, Guryev V, Campisi J, Demaria M. Unmasking Transcriptional Heterogeneity in Senescent Cells. Curr Biol. 2017;27(17):2652-60 e4. Epub 2017/08/29. doi: 10.1016/j.cub.2017.07.033. PubMed PMID: 28844647; PubMed Central PMCID: PMCPMC5788810.
14. Aravinthan A, Shannon N, Heaney J, Hoare M, Marshall A, Alexander GJ. The senescent hepatocyte gene signature in chronic liver disease. Exp Gerontol. 2014;60:37-45. doi: 10.1016/j.exger.2014.09.011. PubMed PMID: 25240687.
15. Ferreira-Gonzalez S, Lu WY, Raven A, Dwyer B, Man TY, O'Duibhir E, et al. Paracrine cellular senescence exacerbates biliary injury and impairs regeneration. Nat Commun. 2018;9(1):1020. Epub 2018/03/11. doi: 10.1038/s41467-018-03299-5. PubMed PMID: 29523787; PubMed Central PMCID: PMCPMC5844882.
16. Childs BG, Durik M, Baker DJ, van Deursen JM. Cellular senescence in aging and age-related disease: from mechanisms to therapy. Nat Med. 2015;21(12):1424-35. doi: 10.1038/nm.4000. PubMed PMID: 26646499; PubMed Central PMCID: PMCPMC4748967.
17. Wiemann SU, Satyanarayana A, Tsahuridu M, Tillmann HL, Zender L, Klempnauer J, et al. Hepatocyte telomere shortening and senescence are general markers of human liver cirrhosis. FASEB J. 2002;16(9):935-42. doi: 10.1096/fj.01-0977com. PubMed PMID: 12087054.

18. Cazzagon N, Sarcognato S, Floreani A, Corra G, De Martin S, Guzzardo V, et al. Cholangiocyte senescence in primary sclerosing cholangitis is associated with disease severity and prognosis. JHEP Rep. 2021;3(3):100286. Epub 2021/05/28. doi: 10.1016/j.jhepr.2021.100286. PubMed PMID: 34041468; PubMed Central PMCID: PMCPMC8141934.
19. Nakanuma Y, Sasaki M, Harada K. Autophagy and senescence in fibrosing cholangiopathies. J Hepatol. 2015;62(4):934-45. Epub 2014/12/02. doi: 10.1016/j.jhep.2014.11.027. PubMed PMID: 25435435.
20. Aravinthan A, Scarpini C, Tachtatzis P, Verma S, Penrhyn-Lowe S, Harvey R, et al. Hepatocyte senescence predicts progression in non-alcohol-related fatty liver disease. J Hepatol. 2013;58(3):549-56. doi: 10.1016/j.jhep.2012.10.031. PubMed PMID: 23142622.
21. Sasaki M, Sato Y, Nakanuma Y. Increased p16(INK4a)-expressing senescent bile ductular cells are associated with inadequate response to ursodeoxycholic acid in primary biliary cholangitis. J Autoimmun. 2020;107:102377. Epub 2019/12/10. doi: 10.1016/j.jaut.2019.102377. PubMed PMID: 31812332.
22. Sasaki M, Miyakoshi M, Sato Y, Nakanuma Y. Modulation of the microenvironment by senescent biliary epithelial cells may be involved in the pathogenesis of primary biliary cirrhosis. J Hepatol. 2010;53(2):318-25. Epub 2010/06/24. doi: 10.1016/j.jhep.2010.03.008. PubMed PMID: 20570384.
23. Ferreira-Gonzalez S, Rodrigo-Torres D, Gadd VL, Forbes SJ. Cellular Senescence in Liver Disease and Regeneration. Semin Liver Dis. 2021;41(1):50-66. Epub 2021/03/26. doi: 10.1055/s-0040-1722262. PubMed PMID: 33764485.
24. Banales JM, Huebert RC, Karlsen T, Strazzabosco M, LaRusso NF, Gores GJ. Cholangiocyte pathobiology. Nat Rev Gastroenterol Hepatol. 2019;16(5):269-81. Epub 2019/03/10. doi: 10.1038/s41575-019-0125-y. PubMed PMID: 30850822; PubMed Central PMCID: PMCPMC6563606.
25. Meadows V, Baiocchi L, Kundu D, Sato K, Fuentes Y, Wu C, et al. Biliary Epithelial Senescence in Liver Disease: There Will Be SASP. Front Mol Biosci. 2021;8:803098. Epub 2022/01/08. doi: 10.3389/fmolb.2021.803098. PubMed PMID: 34993234; PubMed Central PMCID: PMCPMC8724525.
26. Rudolph KL, Chang S, Millard M, Schreiber-Agus N, DePinho RA. Inhibition of experimental liver cirrhosis in mice by telomerase gene delivery. Science. 2000;287(5456):1253-8. PubMed PMID: 10678830.
27. Ogrodnik M, Miwa S, Tchkonia T, Tiniakos D, Wilson CL, Lahat A, et al. Cellular senescence drives age-dependent hepatic steatosis. Nat Commun. 2017;8:15691. doi: 10.1038/ncomms15691. PubMed PMID: 28608850; PubMed Central PMCID: PMCPMC5474745.
28. Amor C, Feucht J, Leibold J, Ho YJ, Zhu C, Alonso-Curbelo D, et al. Senolytic CAR T cells reverse senescence-associated pathologies. Nature. 2020;583(7814):127-32. Epub 2020/06/20. doi: 10.1038/s41586-020-2403-9. PubMed PMID: 32555459.
29. Bird TG, Muller M, Boulter L, Vincent DF, Ridgway RA, Lopez-Guadamillas E, et al. TGFbeta inhibition restores a regenerative response in acute liver injury by suppressing paracrine senescence. Sci Transl Med. 2018;10(454). doi: 10.1126/scitranslmed.aan1230. PubMed PMID: 30111642.

30. Alsuraih M, O'Hara SP, Woodrum JE, Pirius NE, LaRusso NF. Genetic or pharmacological reduction of cholangiocyte senescence improves inflammation and fibrosis in the Mdr2 (-/-) mouse. JHEP Rep. 2021;3(3):100250. Epub 2021/04/20. doi: 10.1016/j.jhepr.2021.100250. PubMed PMID: 33870156; PubMed Central PMCID: PMCPMC8044431.
31. Krizhanovsky V, Yon M, Dickins RA, Hearn S, Simon J, Miething C, et al. Senescence of activated stellate cells limits liver fibrosis. Cell. 2008;134(4):657-67. doi: 10.1016/j.cell.2008.06.049. PubMed PMID: 18724938; PubMed Central PMCID: PMCPMC3073300.
32. Cheng N, Kim KH, Lau LF. Senescent hepatic stellate cells promote liver regeneration through IL-6 and ligands of CXCR2. JCI Insight. 2022;7(14). Epub 2022/06/17. doi: 10.1172/jci.insight.158207. PubMed PMID: 35708907; PubMed Central PMCID: PMCPMC9431681.
33. Grosse L, Wagner N, Emelyanov A, Molina C, Lacas-Gervais S, Wagner KD, et al. Defined p16(High) Senescent Cell Types Are Indispensable for Mouse Healthspan. Cell Metab. 2020;32(1):87-99 e6. Epub 2020/06/03. doi: 10.1016/j.cmet.2020.05.002. PubMed PMID: 32485135.
34. Bezerra JA, Wells RG, Mack CL, Karpen SJ, Hoofnagle JH, Doo E, et al. Biliary Atresia: Clinical and Research Challenges for the Twenty-First Century. Hepatology. 2018;68(3):1163-73. Epub 2018/04/01. doi: 10.1002/hep.29905. PubMed PMID: 29604222; PubMed Central PMCID: PMCPMC6167205.
35. Gurevich M, Guy-Viterbo V, Janssen M, Stephenne X, Smets F, Sokal E, et al. Living Donor Liver Transplantation in Children: Surgical and Immunological Results in 250 Recipients at Universite Catholique de Louvain. Ann Surg. 2015;262(6):1141-9. Epub 2015/01/08. doi: 10.1097/SLA.0000000000001094. PubMed PMID: 25563870.
36. Lendahl U, Lui VCH, Chung PHY, Tam PKH. Biliary Atresia - emerging diagnostic and therapy opportunities. EBioMedicine. 2021;74:103689. Epub 2021/11/16. doi: 10.1016/j.ebiom.2021.103689. PubMed PMID: 34781099; PubMed Central PMCID: PMCPMC8604670.
37. Davenport M. Biliary atresia: clinical aspects. Semin Pediatr Surg. 2012;21(3):175-84. Epub 2012/07/18. doi: 10.1053/j.sempedsurg.2012.05.010. PubMed PMID: 22800970.
38. Wang W, Donnelly B, Bondoc A, Mohanty SK, McNeal M, Ward R, et al. The rhesus rotavirus gene encoding VP4 is a major determinant in the pathogenesis of biliary atresia in newborn mice. J Virol. 2011;85(17):9069-77. Epub 2011/06/24. doi: 10.1128/JVI.02436-10. PubMed PMID: 21697466; PubMed Central PMCID: PMCPMC3165802.
39. Hellen DJ, Bennett A, Malla S, Klindt C, Rao A, Dawson PA, et al. Liver-restricted deletion of the biliary atresia candidate gene Pkd1l1 causes bile duct dysmorphogenesis and ciliopathy. Hepatology. 2023. Epub 2023/01/17. doi: 10.1097/HEP.0000000000000029. PubMed PMID: 36645229.
40. Gutierrez-Reyes G, del Carmen Garcia de Leon M, Varela-Fascinetto G, Valencia P, Perez Tamayo R, Rosado CG, et al. Cellular senescence in livers from children with end stage liver disease. PLoS One. 2010;5(4):e10231. doi: 10.1371/journal.pone.0010231. PubMed PMID: 20422055; PubMed Central PMCID: PMCPMC2858078.
41. Sasaki M, Kuo FY, Huang CC, Swanson PE, Chen CL, Chuang JH, et al. Increased expression of senescence-associated cell cycle regulators in the progression of biliary

atresia: an immunohistochemical study. Histopathology. 2018;72(7):1164-71. doi: 10.1111/his.13476. PubMed PMID: 29392752.
42. Sanada Y, Aida J, Kawano Y, Nakamura K, Shimomura N, Ishikawa N, et al. Hepatocellular telomere length in biliary atresia measured by Q-FISH. World J Surg. 2012;36(4):908-16. Epub 2012/02/09. doi: 10.1007/s00268-012-1453-z. PubMed PMID: 22311140.
43. Chen L, Goryachev A, Sun J, Kim P, Zhang H, Phillips MJ, et al. Altered expression of genes involved in hepatic morphogenesis and fibrogenesis are identified by cDNA microarray analysis in biliary atresia. Hepatology. 2003;38(3):567-76. Epub 2003/08/27. doi: 10.1053/jhep.2003.50363. PubMed PMID: 12939583.
44. Wajapeyee N, Serra RW, Zhu X, Mahalingam M, Green MR. Oncogenic BRAF induces senescence and apoptosis through pathways mediated by the secreted protein IGFBP7. Cell. 2008;132(3):363-74. Epub 2008/02/13. doi: 10.1016/j.cell.2007.12.032. PubMed PMID: 18267069; PubMed Central PMCID: PMCPMC2266096.
45. Suzuki H, Igarashi S, Nojima M, Maruyama R, Yamamoto E, Kai M, et al. IGFBP7 is a p53-responsive gene specifically silenced in colorectal cancer with CpG island methylator phenotype. Carcinogenesis. 2010;31(3):342-9. Epub 2009/07/30. doi: 10.1093/carcin/bgp179. PubMed PMID: 19638426.
46. Morsli S, Doherty GJ, Munoz-Espin D. Activatable senoprobes and senolytics: Novel strategies to detect and target senescent cells. Mech Ageing Dev. 2022;202:111618. Epub 2022/01/07. doi: 10.1016/j.mad.2021.111618. PubMed PMID: 34990647.
47. Gasek NS, Kuchel GA, Kirkland JL, Xu M. Strategies for Targeting Senescent Cells in Human Disease. Nat Aging. 2021;1(10):870-9. Epub 2021/11/30. doi: 10.1038/s43587-021-00121-8. PubMed PMID: 34841261; PubMed Central PMCID: PMCPMC8612694.
48. Baker DJ, Wijshake T, Tchkonia T, LeBrasseur NK, Childs BG, van de Sluis B, et al. Clearance of p16Ink4a-positive senescent cells delays ageing-associated disorders. Nature. 2011;479(7372):232-6. Epub 2011/11/04. doi: 10.1038/nature10600. PubMed PMID: 22048312; PubMed Central PMCID: PMCPMC3468323.
49. Birch J, Gil J. Senescence and the SASP: many therapeutic avenues. Genes Dev. 2020;34(23-24):1565-76. Epub 2020/12/03. doi: 10.1101/gad.343129.120. PubMed PMID: 33262144; PubMed Central PMCID: PMCPMC7706700.
50. Zhu Y, Tchkonia T, Pirtskhalava T, Gower AC, Ding H, Giorgadze N, et al. The Achilles' heel of senescent cells: from transcriptome to senolytic drugs. Aging Cell. 2015;14(4):644-58. doi: 10.1111/acel.12344. PubMed PMID: 25754370; PubMed Central PMCID: PMCPMC4531078.
51. Zhu Y, Tchkonia T, Fuhrmann-Stroissnigg H, Dai HM, Ling YY, Stout MB, et al. Identification of a novel senolytic agent, navitoclax, targeting the Bcl-2 family of anti-apoptotic factors. Aging Cell. 2016;15(3):428-35. Epub 2015/12/30. doi: 10.1111/acel.12445. PubMed PMID: 26711051; PubMed Central PMCID: PMCPMC4854923.
52. Zhu Y, Doornebal EJ, Pirtskhalava T, Giorgadze N, Wentworth M, Fuhrmann-Stroissnigg H, et al. New agents that target senescent cells: the flavone, fisetin, and the BCL-XL inhibitors, A1331852 and A1155463. Aging (Albany NY). 2017;9(3):955-63. Epub 2017/03/09. doi: 10.18632/aging.101202. PubMed PMID: 28273655; PubMed Central PMCID: PMCPMC5391241.

53. Ekpenyong-Akiba AE, Poblocka M, Althubiti M, Rada M, Jurk D, Germano S, et al. Amelioration of age-related brain function decline by Bruton's tyrosine kinase inhibition. Aging Cell. 2020;19(1):e13079. Epub 2019/11/19. doi: 10.1111/acel.13079. PubMed PMID: 31736210; PubMed Central PMCID: PMCPMC6974713.
54. Povedano JM, Martinez P, Serrano R, Tejera A, Gomez-Lopez G, Bobadilla M, et al. Therapeutic effects of telomerase in mice with pulmonary fibrosis induced by damage to the lungs and short telomeres. Elife. 2018;7. Epub 2018/01/31. doi: 10.7554/eLife.31299. PubMed PMID: 29378675; PubMed Central PMCID: PMCPMC5818250.
55. Lapasset L, Milhavet O, Prieur A, Besnard E, Babled A, Ait-Hamou N, et al. Rejuvenating senescent and centenarian human cells by reprogramming through the pluripotent state. Genes Dev. 2011;25(21):2248-53. Epub 2011/11/08. doi: 10.1101/gad.173922.111. PubMed PMID: 22056670; PubMed Central PMCID: PMCPMC3219229.
56. Reyes NS, Krasilnikov M, Allen NC, Lee JY, Hyams B, Zhou M, et al. Sentinel p16(INK4a+) cells in the basement membrane form a reparative niche in the lung. Science. 2022;378(6616):192-201. Epub 2022/10/14. doi: 10.1126/science.abf3326. PubMed PMID: 36227993.
57. Ikehara S, Li M. Stem cell transplantation improves aging-related diseases. Front Cell Dev Biol. 2014;2:16. Epub 2014/11/05. doi: 10.3389/fcell.2014.00016. PubMed PMID: 25364723; PubMed Central PMCID: PMCPMC4206983.
58. Lai X, Huang S, Lin S, Pu L, Wang Y, Lin Y, et al. Mesenchymal stromal cells attenuate alveolar type 2 cells senescence through regulating NAMPT-mediated NAD metabolism. Stem Cell Res Ther. 2022;13(1):12. Epub 2022/01/12. doi: 10.1186/s13287-021-02688-w. PubMed PMID: 35012648; PubMed Central PMCID: PMCPMC8751376.
59. Zhang M, Liu D, Li S, Chang L, Zhang Y, Liu R, et al. Bone marrow mesenchymal stem cell transplantation retards the natural senescence of rat hearts. Stem Cells Transl Med. 2015;4(5):494-502. doi: 10.5966/sctm.2014-0206. PubMed PMID: 25855590; PubMed Central PMCID: PMCPMC4414220.
60. Rodrigues CE, Capcha JM, de Braganca AC, Sanches TR, Gouveia PQ, de Oliveira PA, et al. Human umbilical cord-derived mesenchymal stromal cells protect against premature renal senescence resulting from oxidative stress in rats with acute kidney injury. Stem Cell Res Ther. 2017;8(1):19. Epub 2017/01/29. doi: 10.1186/s13287-017-0475-8. PubMed PMID: 28129785; PubMed Central PMCID: PMCPMC5273809.
61. Wu Q, He S, Zhu Y, Pu S, Zhou Z. Antiobesity Effects of Adipose-Derived Stromal/Stem Cells in a Naturally Aged Mouse Model. Obesity (Silver Spring). 2021;29(1):133-42. Epub 2020/11/14. doi: 10.1002/oby.23036. PubMed PMID: 33185001.
62. Zhang S, Dong Z, Peng Z, Lu F. Anti-aging effect of adipose-derived stem cells in a mouse model of skin aging induced by D-galactose. PLoS One. 2014;9(5):e97573. Epub 2014/05/17. doi: 10.1371/journal.pone.0097573. PubMed PMID: 24831697; PubMed Central PMCID: PMCPMC4022592.
63. Xu P, Xin Y, Zhang Z, Zou X, Xue K, Zhang H, et al. Extracellular vesicles from adipose-derived stem cells ameliorate ultraviolet B-induced skin photoaging by attenuating reactive oxygen species production and inflammation. Stem Cell Res Ther. 2020;11(1):264. Epub 2020/07/03. doi: 10.1186/s13287-020-01777-6. PubMed PMID: 32611371; PubMed Central PMCID: PMCPMC7329484.

64. Dorronsoro A, Santiago FE, Grassi D, Zhang T, Lai RC, McGowan SJ, et al. Mesenchymal stem cell-derived extracellular vesicles reduce senescence and extend health span in mouse models of aging. Aging Cell. 2021;20(4):e13337. Epub 2021/03/18. doi: 10.1111/acel.13337. PubMed PMID: 33728821; PubMed Central PMCID: PMCPMC8045949.
65. Cheng T, Ding S, Liu S, Li Y, Sun L. Human umbilical cord-derived mesenchymal stem cell therapy ameliorates lupus through increasing CD4+ T cell senescence via MiR-199a-5p/Sirt1/p53 axis. Theranostics. 2021;11(2):893-905. Epub 2021/01/05. doi: 10.7150/thno.48080. PubMed PMID: 33391511; PubMed Central PMCID: PMCPMC7738872.
66. Brunet A, Goodell MA, Rando TA. Ageing and rejuvenation of tissue stem cells and their niches. Nat Rev Mol Cell Biol. 2023;24(1):45-62. Epub 2022/07/22. doi: 10.1038/s41580-022-00510-w. PubMed PMID: 35859206; PubMed Central PMCID: PMCPMC9879573.
67. Scheers I, Maerckx C, Khuu DN, Marcelle S, Decottignies A, Najimi M, et al. Adult-derived human liver progenitor cells in long-term culture maintain appropriate gatekeeper mechanisms against transformation. Cell Transplant. 2012;21(10):2241-55. doi: 10.3727/096368912X639026. PubMed PMID: 22525602.
68. Ezquer F, Bahamonde J, Huang YL, Ezquer M. Administration of multipotent mesenchymal stromal cells restores liver regeneration and improves liver function in obese mice with hepatic steatosis after partial hepatectomy. Stem Cell Res Ther. 2017;8(1):20. doi: 10.1186/s13287-016-0469-y. PubMed PMID: 28129776; PubMed Central PMCID: PMCPMC5273822.
69. Yovchev MI, Xue Y, Shafritz DA, Locker J, Oertel M. Repopulation of the fibrotic/cirrhotic rat liver by transplanted hepatic stem/progenitor cells and mature hepatocytes. Hepatology. 2014;59(1):284-95. doi: 10.1002/hep.26615. PubMed PMID: 23840008; PubMed Central PMCID: PMCPMC4091900.
70. Moore JK, Stutchfield BM, Forbes SJ. Systematic review: the effects of autologous stem cell therapy for patients with liver disease. Aliment Pharmacol Ther. 2014;39(7):673-85. doi: 10.1111/apt.12645. PubMed PMID: 24528093.
71. Berardis S, Dwisthi Sattwika P, Najimi M, Sokal EM. Use of mesenchymal stem cells to treat liver fibrosis: current situation and future prospects. World J Gastroenterol. 2015;21(3):742-58. doi: 10.3748/wjg.v21.i3.742. PubMed PMID: 25624709; PubMed Central PMCID: PMCPMC4299328.
72. Chen W, Zhu J, Lin F, Xu Y, Feng B, Feng X, et al. Human placenta mesenchymal stem cell-derived exosomes delay H2O2-induced aging in mouse cholangioids. Stem Cell Res Ther. 2021;12(1):201. Epub 2021/03/24. doi: 10.1186/s13287-021-02271-3. PubMed PMID: 33752720; PubMed Central PMCID: PMCPMC7983269.
73. Fang J, Liang W. ASCs -derived exosomes loaded with vitamin A and quercetin inhibit rapid senescence-like response after acute liver injury. Biochem Biophys Res Commun. 2021;572:125-30. Epub 2021/08/08. doi: 10.1016/j.bbrc.2021.07.059. PubMed PMID: 34364291.
74. Najimi M, Khuu DN, Lysy PA, Jazouli N, Abarca J, Sempoux C, et al. Adult-derived human liver mesenchymal-like cells as a potential progenitor reservoir of hepatocytes? Cell Transplant. 2007;16(7):717-28. PubMed PMID: 18019361.

75. Smets F, Dobbelaere D, McKiernan P, Dionisi-Vici C, Broue P, Jacquemin E, et al. Phase I/II Trial of Liver-derived Mesenchymal Stem Cells in Pediatric Liver-based Metabolic Disorders: A Prospective, Open Label, Multicenter, Partially Randomized, Safety Study of One Cycle of Heterologous Human Adult Liver-derived Progenitor Cells (HepaStem) in Urea Cycle Disorders and Crigler-Najjar Syndrome Patients. Transplantation. 2019;103(9):1903-15. Epub 2019/02/26. doi: 10.1097/TP.0000000000002605. PubMed PMID: 30801523.
76. Nevens F, Gustot T, Laterre PF, Lasser LL, Haralampiev LE, Vargas V, et al. A phase II study of human allogeneic liver-derived progenitor cell therapy for acute-on-chronic liver failure and acute decompensation. JHEP Rep. 2021;3(4):100291. Epub 2021/06/26. doi: 10.1016/j.jhepr.2021.100291. PubMed PMID: 34169246; PubMed Central PMCID: PMCPMC8207211.
77. Khuu DN, Scheers I, Ehnert S, Jazouli N, Nyabi O, Buc-Calderon P, et al. In vitro differentiated adult human liver progenitor cells display mature hepatic metabolic functions: a potential tool for in vitro pharmacotoxicological testing. Cell Transplant. 2011;20(2):287-302. doi: 10.3727/096368910X516655. PubMed PMID: 20719066.
78. Berardis S, Lombard C, Evraerts J, El Taghdouini A, Rosseels V, Sancho-Bru P, et al. Gene expression profiling and secretome analysis differentiate adult-derived human liver stem/progenitor cells and human hepatic stellate cells. PLoS One. 2014;9(1):e86137. doi: 10.1371/journal.pone.0086137. PubMed PMID: 24516514; PubMed Central PMCID: PMCPMC3906387.
79. Sana G, Lombard C, Vosters O, Jazouli N, Andre F, Stephenne X, et al. Adult human hepatocytes promote CD4(+) T-cell hyporesponsiveness via interleukin-10-producing allogeneic dendritic cells. Cell Transplant. 2014;23(9):1127-42. doi: 10.3727/096368913X666421. PubMed PMID: 23582182.
80. Najimi M, Berardis S, El-Kehdy H, Rosseels V, Evraerts J, Lombard C, et al. Human liver mesenchymal stem/progenitor cells inhibit hepatic stellate cell activation: in vitro and in vivo evaluation. Stem Cell Res Ther. 2017;8(1):131. doi: 10.1186/s13287-017-0575-5. PubMed PMID: 28583205; PubMed Central PMCID: PMCPMC5460523.
81. Herrero A, Prigent J, Lombard C, Rosseels V, Daujat-Chavanieu M, Breckpot K, et al. Adult-Derived Human Liver Stem/Progenitor Cells Infused 3 Days Postsurgery Improve Liver Regeneration in a Mouse Model of Extended Hepatectomy. Cell Transplant. 2017;26(2):351-64. doi: 10.3727/096368916X692960. PubMed PMID: 27657746; PubMed Central PMCID: PMCPMC5657763.
82. Maerckx C, Tondreau T, Berardis S, van Pelt J, Najimi M, Sokal E. Human liver stem/progenitor cells decrease serum bilirubin in hyperbilirubinemic Gunn rat. World J Gastroenterol. 2014;20(30):10553-63. doi: 10.3748/wjg.v20.i30.10553. PubMed PMID: 25132775; PubMed Central PMCID: PMCPMC4130866.
83. Senturk S, Mumcuoglu M, Gursoy-Yuzugullu O, Cingoz B, Akcali KC, Ozturk M. Transforming growth factor-beta induces senescence in hepatocellular carcinoma cells and inhibits tumor growth. Hepatology. 2010;52(3):966-74. doi: 10.1002/hep.23769. PubMed PMID: 20583212.
84. Meng L, Quezada M, Levine P, Han Y, McDaniel K, Zhou T, et al. Functional role of cellular senescence in biliary injury. Am J Pathol. 2015;185(3):602-9. Epub 2015/01/27. doi: 10.1016/j.ajpath.2014.10.027. PubMed PMID: 25619959; PubMed Central PMCID: PMCPMC4348464.

85. Debacq-Chainiaux F, Erusalimsky JD, Campisi J, Toussaint O. Protocols to detect senescence-associated beta-galactosidase (SA-betagal) activity, a biomarker of senescent cells in culture and in vivo. Nat Protoc. 2009;4(12):1798-806. doi: 10.1038/nprot.2009.191. PubMed PMID: 20010931.
86. Jannone G, Rozzi M, Najimi M, Decottignies A, Sokal EM. An Optimized Protocol for Histochemical Detection of Senescence-associated Beta-galactosidase Activity in Cryopreserved Liver Tissue. J Histochem Cytochem. 2020:22155420913534. Epub 2020/03/11. doi: 10.1369/0022155420913534. PubMed PMID: 32154749.
87. Justice JN, Nambiar AM, Tchkonia T, LeBrasseur NK, Pascual R, Hashmi SK, et al. Senolytics in idiopathic pulmonary fibrosis: Results from a first-in-human, open-label, pilot study. EBioMedicine. 2019;40:554-63. Epub 2019/01/09. doi: 10.1016/j.ebiom.2018.12.052. PubMed PMID: 30616998; PubMed Central PMCID: PMCPMC6412088.
88. Hickson LJ, Langhi Prata LGP, Bobart SA, Evans TK, Giorgadze N, Hashmi SK, et al. Senolytics decrease senescent cells in humans: Preliminary report from a clinical trial of Dasatinib plus Quercetin in individuals with diabetic kidney disease. EBioMedicine. 2019;47:446-56. Epub 2019/09/23. doi: 10.1016/j.ebiom.2019.08.069. PubMed PMID: 31542391.
89. Lee S, Kim S, Le HD, Meisel J, Strijbosch RA, Nose V, et al. Reduction of hepatocellular injury after common bile duct ligation using omega-3 fatty acids. J Pediatr Surg. 2008;43(11):2010-5. Epub 2008/10/31. doi: 10.1016/j.jpedsurg.2008.05.030. PubMed PMID: 18970933.
90. Mohanty SK, Lobeck I, Donnelly B, Dupree P, Walther A, Mowery S, et al. Rotavirus Reassortant-Induced Murine Model of Liver Fibrosis Parallels Human Biliary Atresia. Hepatology. 2020;71(4):1316-30. Epub 2019/08/24. doi: 10.1002/hep.30907. PubMed PMID: 31442322; PubMed Central PMCID: PMCPMC7384231.
91. Kountouras J, Billing BH, Scheuer PJ. Prolonged bile duct obstruction: a new experimental model for cirrhosis in the rat. Br J Exp Pathol. 1984;65(3):305-11. Epub 1984/06/01. PubMed PMID: 6743531; PubMed Central PMCID: PMCPMC2040968.
92. McDaniel K, Meng F, Wu N, Sato K, Venter J, Bernuzzi F, et al. Forkhead box A2 regulates biliary heterogeneity and senescence during cholestatic liver injury in micedouble dagger. Hepatology. 2017;65(2):544-59. doi: 10.1002/hep.28831. PubMed PMID: 27639079; PubMed Central PMCID: PMCPMC5258713.
93. Wan Y, Meng F, Wu N, Zhou T, Venter J, Francis H, et al. Substance P increases liver fibrosis by differential changes in senescence of cholangiocytes and hepatic stellate cells. Hepatology. 2017;66(2):528-41. doi: 10.1002/hep.29138. PubMed PMID: 28256736; PubMed Central PMCID: PMCPMC5519428.
94. Kim KH, Chen CC, Monzon RI, Lau LF. Matricellular protein CCN1 promotes regression of liver fibrosis through induction of cellular senescence in hepatic myofibroblasts. Mol Cell Biol. 2013;33(10):2078-90. Epub 2013/03/20. doi: 10.1128/MCB.00049-13. PubMed PMID: 23508104; PubMed Central PMCID: PMCPMC3647960.
95. Garrido M, Escobar C, Zamora C, Rejas C, Varas J, Parraga M, et al. Bile duct ligature in young rats: A revisited animal model for biliary atresia. Eur J Histochem. 2017;61(3):2803.

Epub 2017/10/20. doi: 10.4081/ejh.2017.2803. PubMed PMID: 29046057; PubMed Central PMCID: PMCPMC5607851.

Chapter 2: an optimized protocol for histochemical detection of senescence-associated beta-galactosidase activity in cryopreserved liver tissue

Giulia Jannone[1], Milena Rozzi[1], Mustapha Najimi[1], Anabelle Decottignies[2] and Etienne M Sokal[1]

[1]Laboratory of Pediatric Hepatology and Cell Therapy, Institut de Recherche Expérimentale et Clinique, Université Catholique de Louvain, 1200 Brussels, Belgium
[2]Genetic and Epigenetic Alterations of Genomes group, de Duve Institute, Université Catholique de Louvain, 1200 Brussels, Belgium

J Histochem Cytochem. 2020 Apr;68(4):269-278.

Summary

The senescence-associated beta-galactosidase (SA-β-gal) activity assay is commonly used to evaluate the increased β-gal activity in senescent cells related to enhanced lysosomal activity. Although the optimal pH for β-gal is 4.0, this enzymatic activity has been most commonly investigated at a suboptimal pH by using histochemical reaction on fresh tissue material.

In the current study, we optimized a SA-β-gal activity histochemistry protocol that can also be applied on cryopreserved hepatic tissue. This protocol was developed on livers obtained from control rats and after bile duct resection (BDR). A significant increase in β-gal liver activity was observed in BDR rats versus controls after two

hours staining at physiological pH 4.0 (6.98 ± 1.19 % of stained/total area versus 0.38 ± 0.22; $p<0.01$) and after overnight staining at pH 5.8 (24.09 ± 6.88 versus 0.12 ± 0.08; $p<0.01$). Although we noticed that β-gal activity staining decreased with cryopreservation time (from 4 to 12 months storage at -80°C; $p<0.05$), the enhanced staining observed in BDR compared to controls remained detectable after up to 12 months post-cryopreservation ($p<0.01$).

In conclusion, we provide an optimized protocol for SA-β-gal activity histochemical detection at physiological pH 4.0 on long term cryopreserved liver tissue.

Introduction

Senescence-associated β-galactosidase (SA-β-gal) activity is a widely used biomarker of cellular senescence both in cultured cells and in tissue sections, using histochemical staining. SA-β-gal activity results from an increased expression of *GLB-1*, the gene encoding the lysosomal β-gal (1). The increase in *GLB-1* mRNA and protein levels results from an elevation of the number and activity of lysosomes, which is probably due to the accumulation of damaged macromolecules in senescent cells (2). Even if β-gal optimal pH of reaction is 4.0, the enzymatic activity has been most commonly analyzed at pH 6.0 in senescent cells, due to its increased lysosomal production related to senescent conditions. Hence, SA-β-gal activity was originally defined as the β-galactosidase activity detected at pH 6.0 (3). Subsequently, to increase the sensitivity of the assay, SA-β-gal activity was sometimes measured at slightly lower pH values (5.5 to 5.8) according to cell type (4, 5).

Interestingly, patients with GM1-gangliosidosis (defective β-gal) do not show any SA-β-gal activity when their cells reach replicative senescence, suggesting that the SA-β-gal activity is not itself required for cell senescence (1). Still, SA-β-gal activity is present in most senescent cell types, making it a very useful tool to monitor this

feature. Over the years, this test has been used in a large variety of cell cultures and tissues in rodents and humans, and especially in human fibroblasts (2, 4, 6). Although several studies briefly mentioned SA-β-gal activity tests on liver tissue, no proper and detailed protocol is currently available. Experimental parameters including freezing and fixation methods, as well as the thickness of the slides and the pH of the solution were not consistently described (Supplementary Table 1) (5, 7-19). Cryopreservation techniques were not detailed, and slide thickness could vary between 4 µm and 7 µm when mentioned. Fixation methods varied widely, with 0.2-0.5% glutaraldehyde and/or 3-4% (para)formaldehyde for 1 minute to 4 hours, before or after freezing, and at RT (room temperature) or 4C. The pH of the solution ranged between 5.5 and 6.0, as suggested in other cellular types (4, 5).

The aim of this study was to deeply optimize a protocol that measures β-gal activity and its kinetics in normal and diseased liver tissue, based on the previously documented methodologies (20, 21). To develop and evaluate the usefulness of our protocol, we used the murine bile duct resection (BDR) model of biliary cirrhosis, in which SA-β-gal activity has previously been described on fresh liver tissue (22, 23). By optimizing the histochemical reaction conditions, we aimed at extending the use of the SA-β-gal activity assay to cryopreserved tissue in order to facilitate future research.

Materials and methods

Rat liver samples and bile duct resection

Liver tissue was obtained from wild type male Wistar rats. Biliary cirrhosis was induced in 2 months old rats (n=6) with the extra-hepatic BDR surgical procedure as previously described (24). Animals were sacrificed 2 or 4 weeks after the surgical procedure, and they all presented with histological biliary cirrhosis at the time of sacrifice. Controls (n=4) underwent sham procedure (bile duct dissection without

resection) at the same age and were sacrificed at the same timepoints. Healthy 2 months old male Wistar rats (n=4) were used for specific tests. This project was approved by the Ethical Committee for Animal Experimentation of Université Catholique de Louvain, Brussels (2018/UCL/MD/43).

β-galactosidase activity on cryopreserved liver tissue protocol

The final β-gal activity protocol that we developed and applied on cryopreserved liver samples is the following:

1. Briefly rinse fresh tissue with NaCl 0.9% to remove excessive residual blood.
2. Immediately embed the tissue in OCT compound (Tissue-Tek) and flash freeze in liquid nitrogen containing isopentane (Fisher Scientific, CAS no. 78-78-4):
    a. Fill a metal beaker in with 2/3 isopentane and place it in enough liquid nitrogen to come up to about 1/3 of the container (prepare at least 10 minutes before freezing).
    b. Freeze the sample in the clear portion of isopentane without fully submerging.
    c. Avoid block cracking by removing the sample from isopentane when there is still a small drop size of unfrozen OCT. Transfer sample to dry ice while continuing on to other samples.
3. Immediately section the frozen tissue in -20C cryostat (15 µm sections), or store the samples at -80C for up to twelve months. The sections must remain in the cryostat chamber during the procedure to avoid tissue thawing.
4. Fixation with 0.2% glutaraldehyde (Merck, CAS no. 111-30-8) in PBS for 10 minutes at RT.
5. Remove the fixative and wash in PBS (enough to cover the slides) for one minute three times at RT.
6. Add freshly prepared staining solution (2): 40 mM citric acid monohydrate/sodium dihydrogen phosphate monohydrate buffer at pH 4.0 or pH

5.8 as needed (Merck, CAS no. 5949-29-1 and 10049-21-5), 5 mM potassium hexacyano-ferrate (II) trihydrate (Merck, CAS no. 14459-95-1), 5 mM potassium hexacyano-ferrate (III) (Merck, CAS no. 13746-66-2), 150 mM sodium chloride (Merck, CAS no. 7647-14-5), 2 mM magnesium chloride hexahydrate (Merck, CAS no. 7791-18-6) and 1 mg/ml (pH 5.8) or 0.5 mg/ml (pH 4.0) 5-bromo-4-chloro-3-indolyl-β-D-galactopyranoside (X-gal) (Merck, CAS no. 7240-90-6) in distilled water. Incubate a control section in the absence of X-gal to verify the specificity of the enzyme reaction.

Note: 200µl of solution per section is enough if a hydrophobic pen is used to surround the tissue (Dako Pen, Agilent). Otherwise, the slides must be fully immersed in the solution. Additional details concerning the preparation of the solutions are available in the protocol of Debacq-Chainiaux et al (2).

7. Incubate overnight at 37C without CO2 (or shorter period for pH 4.0 manipulations); wash twice in PBS.

8. Counterstain one minute in hematoxylin if indicated; wash twice in PBS.

Note: counterstaining helps identifying tissue architecture, but can make a weak staining harder to detect.

Quantification of β-galactosidase activity staining in whole tissue sections

Stained slides were digitalized using a SCN400 slide scanner (Leica Biosystems, Wetzlar, Germany) at x20 magnification (x40 for illustrations). Scanned slides were then analyzed using the image analysis tool Author version 2017.2 (Visiopharm, Hørsholm, Denmark) for β-gal activity staining digital quantification. Using a first Analysis Protocol Package (APP), tissue was automatically delineated at a low digital magnification (x4) (Fig. 1a). Large empty spaces (vessels, damaged tissue) were automatically discarded. This first delineation operation was visually checked and manually corrected if required. Histological artifacts were manually discarded.

Within the final selected regions, β-gal staining was detected at high resolution (x20) in a second APP with a thresholding classification relying on the RGB-R matrix of the software, which was tested and optimized manually (Fig. 1b). Results were expressed as [(stained area/total tissue area) x 100] to obtain a percentage of stained area. The parameters of the designed APPs were kept constant for all sections.

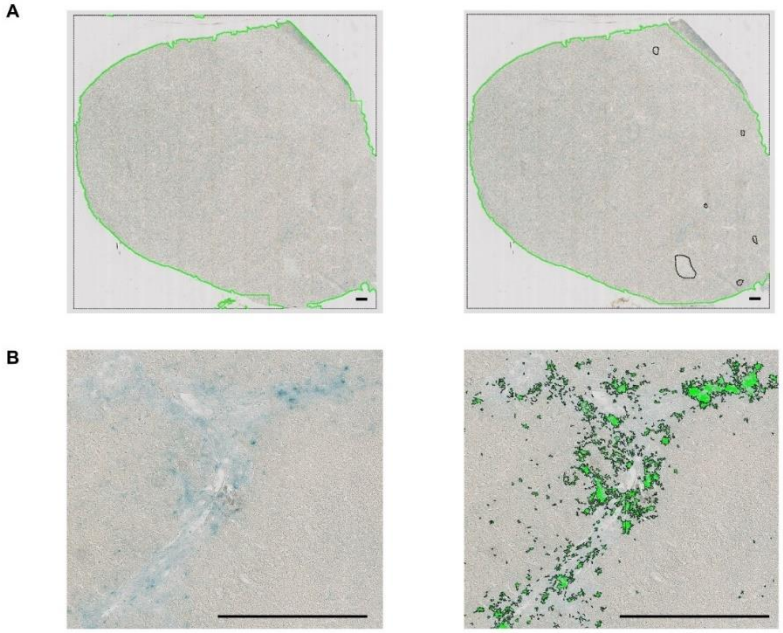

Figure 1. Quantification of β-gal staining with the Visiopharm software. (A) Left image shows the automatic tissue delineation obtained with the first Analysis Protocol Package (APP) (green line). Right image shows the final delineation after manual correction and exclusion of histological artifacts (surrounded by a black circle); (B) Left image shows the pathological liver tissue with histochemical β-gal activity staining before digital staining detection (positive blue staining). Right image shows the digital β-gal staining detection obtained with the second APP (positive green staining). Scale bars = 500µm.

Statistical analysis

Statistical analysis was conducted using Graphpad Prism 5.0 (GraphPad Software, La Jolla, CA, USA). Continuous variables were presented as mean ± standard error of the mean (SEM). The Mann-Whitney *U*-test was used to compare continuous variables between subgroups. The Student's paired t-test was used when specified in the text, to compare repeated measures. A two-tailed p-value ≤ 0.05 was considered to indicate statistical significance for all analyses.

Results

Optimization of β-galactosidase activity assay

Different reaction parameters were tested on 2 months old healthy Wistar rat livers (n=4) at physiological pH 4.0 (Fig. 2). Fixation with 0.2% glutaraldehyde for 10 minutes at RT provided a higher β-gal staining (9.79 ± 2.17 % of stained/total area) as compared to 1% formaldehyde for 1 minute at RT (0.09 ± 0.04; $p<0.05$) or to the absence of fixation (0.08 ± 0.04; $p<0.05$) (Fig. 2a).

Increasing substrate (Xgal) concentration from 1 mg/ml to 2 mg/ml did not enhance the intensity of β-gal staining (9.79 ± 2.17 % of stained/total area versus 2.99 ± 0.74; $p=0.34$) (Fig. 2b). Furthermore, decreasing Xgal concentration from 1 mg/ml to 0.5 mg/ml did not decrease the staining (9.79 ± 2.17 % of stained/total area versus 10.72 ± 2.59; $p=0.49$). β-gal staining increased for sections thickness of 10 µm and 15 µm as compared to 5 µm (9.79 ± 2.17 and 27.39 ± 5.9 % of stained/total area versus 0.57 ± 0.31; $p<0.05$) (Fig. 2c).

No difference in β-gal staining was noticed when we compared the following cryopreservation methods: freezing OCT-embed specimens in liquid nitrogen containing isopentane versus snap freezing in liquid nitrogen before OCT-embedding (9.79 ± 2.17 % of stained/total area versus 3.58 ± 1.83; $p=0.06$). However, the isopentane method showed a better preservation of the tissue

quality as compared to snap freezing (Fig. 2d). Finally, while the pH 4.0 solution left overnight allowed physiological β-gal activity staining in healthy rats, β-gal staining overnight at pH 5.8 remained negative (9.79 ± 2.17 % of stained/total area versus 0.04 ± 0.01; $p<0.05$) (Fig. 2e).

Altogether, the following conditions were selected to obtain an optimal β-gal staining signal for the further experiments: freezing of OCT-embedded fresh specimens in liquid nitrogen containing isopentane, slicing the liver at 15 µm thickness sections and 10 minutes fixation with 0.2% glutaraldehyde at RT (see Materials and Methods for detailed protocol). The use of 0.5 mg/ml X-gal was selected for the final β-gal activity staining protocol at pH 4.0. A reduction of the X-gal concentration was not attempted for β-gal staining at pH 5.8 since we considered this pH as already being a suboptimal reaction condition.

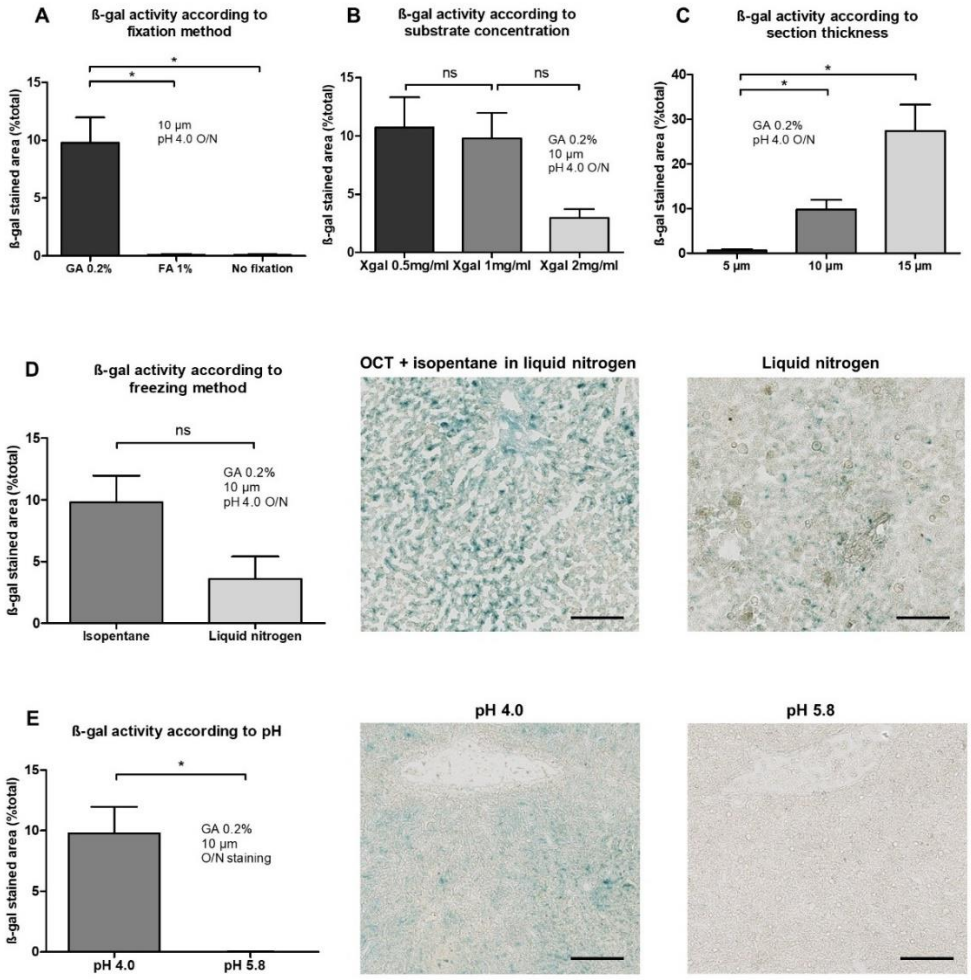

Figure 2. Optimisation of experimental conditions for the detection of β-gal activity in healthy rat liver tissue. (A) 10 minutes glutaraldehyde (GA) 0.2% versus 1 minute formaldehyde (FA) 1% versus no fixation; (B) Usual (1 mg/ml) versus doubled (2 mg/ml) or reduced (0.5 mg/ml) X-gal concentration; (C) Sections thickness of 5 µm versus 10 µm versus 15 µm; (D) OCT-embed specimens frozen in liquid nitrogen containing isopentane versus flash-freezing in liquid nitrogen followed by OCT embedding; (E) Testing physiological pH (pH 4.0) versus SA-β-gal activity pH (pH 5.8). Data is presented as mean ± SEM (n=4). Scale bars = 100 µm. O/N: overnight.

β-galactosidase activity at pH 4.0 on cryopreserved liver tissue

β-gal activity staining at pH 4.0 was tested after different reaction durations in BDR (biliary cirrhosis) rats (n=4) versus controls (n=2) (Fig. 3a). Cirrhotic rats seemed to have a higher percentage of β-gal staining (% of stained/total area) at pH 4.0 when compared to controls from early time points. To confirm this observation, we compared β-gal staining at pH 4.0 after two hours of reaction in BDR rats (n=6) versus controls (n=4). Three liver cryosections obtained after 3 to 12 months of cryopreservation were stained per rat. For each of the three staining, all sections were obtained at the same cryopreservation timepoint. The mean of those triplicates is presented for each rat in Fig. 3b. The staining after two hours of reaction at pH 4.0 was higher in BDR rats versus controls (6.98 ± 2.92 versus 0.38 ± 0.22; $p<0.01$) (Figs. 3b & 3c). When each replicate was considered separately, a significant difference in β-gal staining after 2 hours at pH 4.0 was evidenced between BDR and controls after 3 months, 4 months and 12 months of -80C storage ($p<0.01$) (data not shown). All controls remained negative after two hours of reaction at pH 4.0 for up to 12 months post-cryopreservation. The impact of cryopreservation duration was investigated by comparing β-gal staining at pH 4.0 (two hours) between the replicates mentioned above, obtained from the same rat after different -80C freezing intervals (Fig. 3d). β-gal activity staining (% of stained/total area) in BDR rats was lower after 12 months as compared to 4 months post-cryopreservation (2.23 ± 0.61 versus 7.58 ± 1.8, $p<0.05$; Student's paired t-test, n=6).

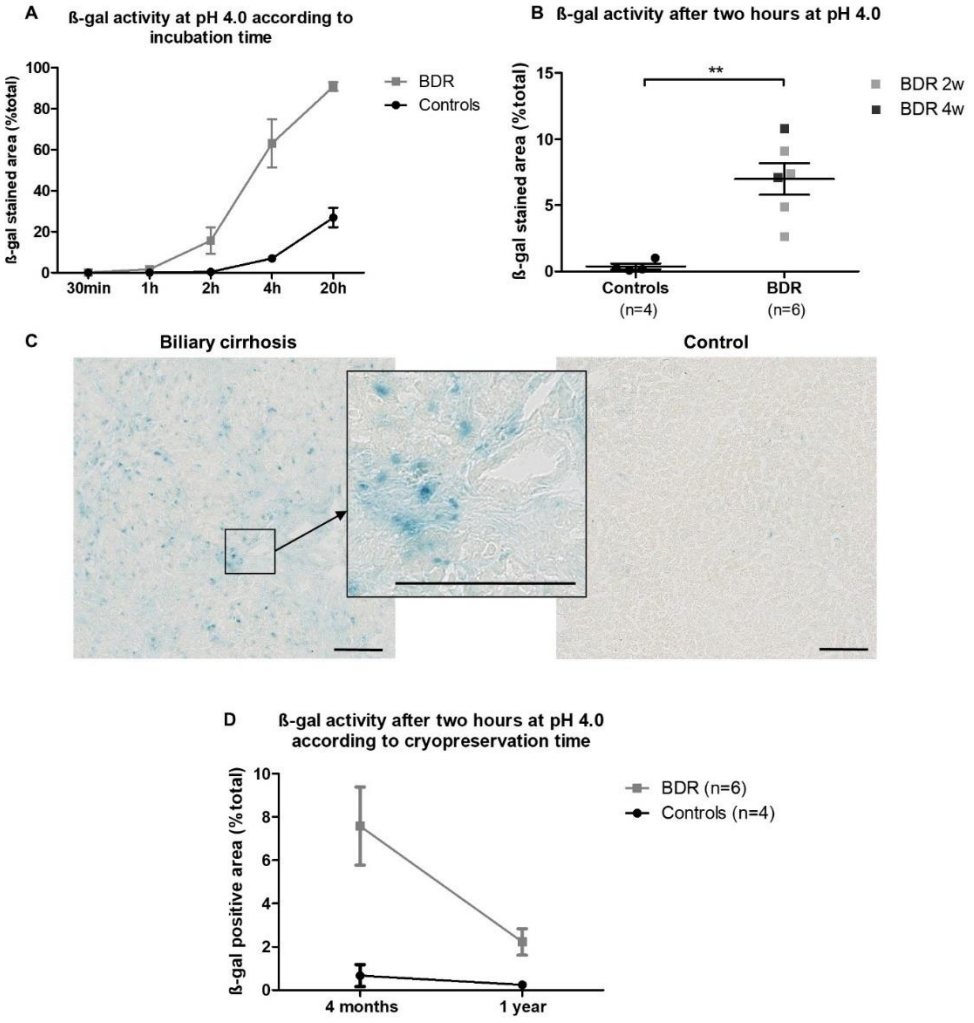

Figure 3. Analysis of β-gal activity at pH 4.0 in the livers of rats with biliary cirrhosis. (A) β-gal activity (pH 4.0) after different incubation times in rats which underwent bile duct resection (BDR, n=4) (sacrificed 2 weeks [n=2] and 4 weeks [n=2] post-surgery) versus controls (sham procedure, n=2); (B) β-gal staining comparison between biliary cirrhosis rats (BDR, n=6) and controls (sham procedure, n=4) after two hours of reaction at pH 4.0. Each point is the mean of three replicates for the same animal, from liver samples obtained after 3 to 12 months of cryopreservation. **p<0.01; (C) Images of biliary cirrhosis (BDR 2w) versus control after two hours of staining at pH 4.0 (liver tissue cryopreserved for 4 months); (D) Variations of β-gal activity staining after two hours of reaction at pH 4.0 between replicates of the same animals according to cryopreservation time. Data is presented as mean ± SEM.

Scale bars = 100 µm. BDR 2w: BDR rats sacrificed 2 weeks post-surgery; BDR 4w: BDR rats sacrificed 4 weeks post-surgery.

β-galactosidase activity at pH 5.8 on cryopreserved liver tissue

β-gal activity staining was also tested after different times of reaction at pH 5.8 in BDR (biliary cirrhosis) rats (n=4) versus control samples (n=2) (Fig. 4a). Cirrhotic rats did not show any β-gal activity staining at early time points at pH 5.8, while controls did not show any activity even after overnight incubation. After twenty hours of reaction at pH 5.8, β-gal activity staining (% of stained/total area) was significantly higher in BDR rats (n=6) versus controls (n=4) (24.09 ± 6.88 versus 0.12 ± 0.08; $p<0.01$) (Figs. 4b & 4c). Three liver cryosections obtained after 4 to 12 months of cryopreservation were stained per rat. For each of the three staining, all sections were obtained at the same cryopreservation timepoint. The mean of those triplicates is presented for each rat in Fig. 4b. When each replicate was considered separately, a significant difference in β-gal staining after twenty hours at pH 5.8 was evidenced between BDR and controls after 4 months, 6 months and 12 months of -80C storage ($p<0.01$) (data not shown). All controls remained negative after twenty hours of reaction at pH 5.8 after up to 12 months post-cryopreservation. The impact of cryopreservation duration was investigated by comparing β-gal staining at pH 5.8 (overnight) between replicates obtained from the same rat after different -80C freezing intervals (Fig. 4d). There was a decrease in β-gal activity staining (% of stained/total area) in BDR rats after 12 months post-cryopreservation versus 4 months (10.22 ± 5.11 versus 34.06 ± 9.94, $p<0.01$; Student's paired t-tests, n=6).

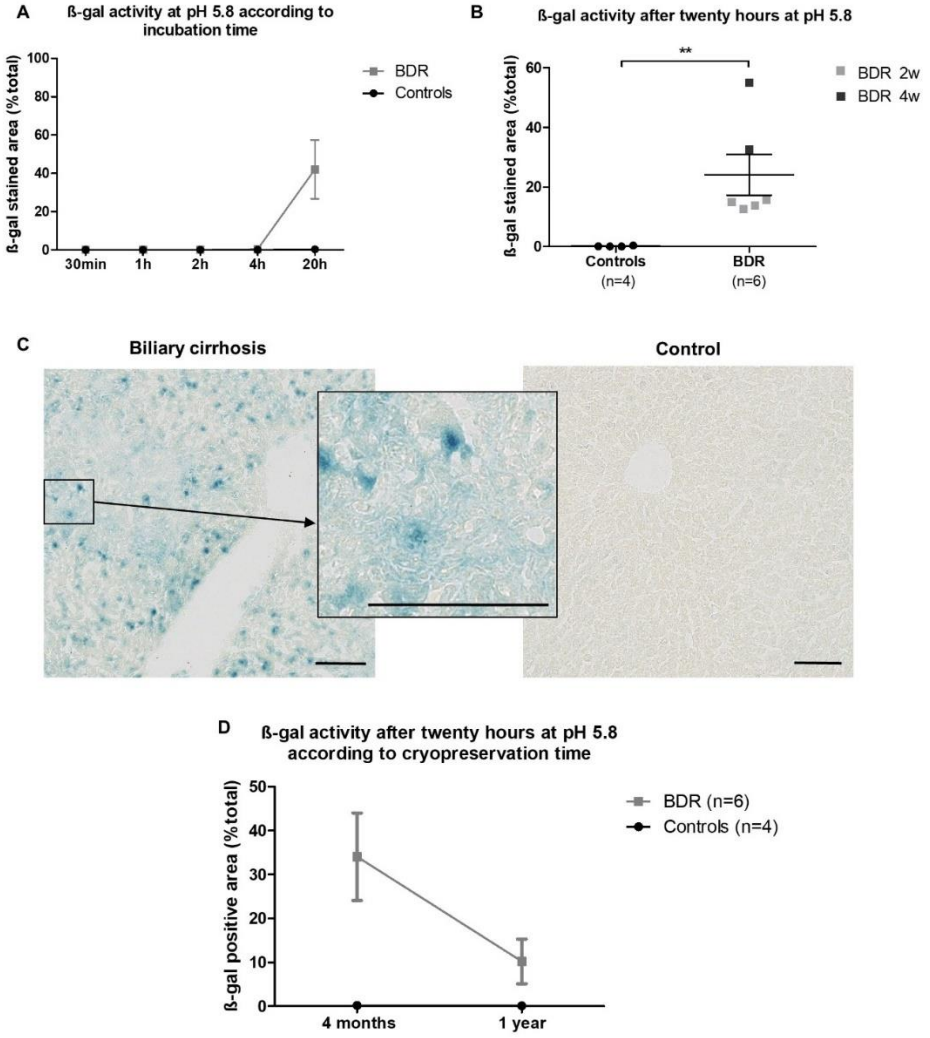

Figure 4. Analysis of β-gal activity at pH 5.8 in the livers of rats with biliary cirrhosis. (A) β-gal activity (pH 5.8) after different incubation times in rats which underwent bile duct resection (BDR, n=4) (sacrificed 2 weeks [n=2] and 4 weeks [n=2] post-surgery) versus controls (sham procedure, n=2); (B) β-gal staining comparison between biliary cirrhosis rats (bile duct resection, n=6) and controls (sham procedure, n=4) after twenty hours of reaction at pH 5.8. Each point is the mean of three replicates for the same animal, from liver samples obtained after 4 to 12 months of cryopreservation. **p<0.01; (C) Images of biliary cirrhosis (BDR 2w) versus control after twenty hours of staining at pH 5.8 (liver tissue cryopreserved for 4 months); (D) Variations of β-gal activity staining after twenty hours of reaction at pH 5.8 between replicates of the same animals according to cryopreservation time. Data is

presented as mean ± SEM. Scale bars = 100 µm. BDR 2w: BDR rats sacrificed 2 weeks post-surgery; BDR 4w: BDR rats sacrificed 4 weeks post-surgery.

Discussion

The SA-β-gal histochemical staining protocol proposed here is a significant improvement of existing protocols. By performing the histochemical reaction at optimal assay conditions, it allows a more sensitive detection of the enzyme activity and a semi-quantitative assessment of this activity in different zones of the liver tissue. It also allows to detect activity in cryopreserved tissue, which was not the case for previously reported protocols. The structural quality of tissue was better preserved when isopentane was used for freezing as compared to snap freezing in liquid nitrogen, which is in line with our previous histochemistry protocols on cryopreserved human and rodent liver tissue (20, 21, 25). This was probably caused by the unpredictable freezing pattern of liquid nitrogen related to the vapor barrier, which can cause important freezing artefacts (26). The fixative choice was a second crucial part of the protocol, since only glutaraldehyde allowed to preserve sufficient β-gal activity detectable via histochemical analysis. The absence of fixative probably caused a leak of the enzyme from the tissue, while β-gal activity might have been lost upon formaldehyde treatment due to protein denaturation (27, 28). Indeed, it is known that enzymes react differently to fixation conditions (29). The β-gal staining increased with sections of thickness superior to 5 µm, as expected with higher enzyme content. We did not test sections thicker than 15 µm since a delay in substrate penetration can be observed for those sections (30). A pH 4.0 solution used overnight allowed physiological staining of healthy liver tissue (positive control). No staining was observed at pH 5.8 overnight in healthy 2 months old Wistar rats, confirming that a pH slightly lower than 6.0 can improve sensitivity without impairing specificity as compared to pH 6.0. Increasing the substrate (X-gal) concentration did not improve the intensity of β-gal staining, probably because

of a saturation of the reaction sites. At the optimal pH 4.0 of reaction, it was even possible to lower down X-gal concentration without impairing the β-gal staining intensity

The study of β-gal kinetics at pH 4.0 allowed us to evidence a noticeable SA-β-gal activity staining at early times of incubation as seen in rats with biliary cirrhosis (BDR model). A significant difference in β-gal staining between BDR rats and controls was already revealed after two hours of pH 4.0 reaction. Conversely, SA-β-gal activity at early times of incubation was nearly undetectable at pH 5.8 in BDR rats. After overnight incubation at pH 5.8, there was a significant difference in β-gal activity staining between BDR and control rats. Our results show that SA-β-gal activity can be evidenced at early time points at pH 4.0, as well as at late time points at pH 5.8. Close monitoring of the negative controls is mandatory at pH 4.0, because all tissues will eventually stain positive for β-gal activity due to low concentration of the enzyme also in normal tissue. Still, senescent tissues have earlier and more intense staining at pH 4.0 compared to non-senescent ones. The state of the art in histochemistry is to test enzymatic activity at the optimum pH of the enzyme, because even small variations of pH can drastically affect the results (20, 31). On this basis, optimizing SA-β-gal activity assay to pH 4.0 should allow the detection of senescence at earlier stages as compared to the suboptimal pH 5.8. Further demonstration on mildly senescent tissues will have to be conducted to confirm this hypothesis. Identifying the type of liver senescent cells with specific markers should contribute to a better understanding of the BDR model in the future.

Enzyme activity can be affected by cryopreservation to a different extent according to the type of enzyme and to storage conditions (32). When we investigated the impact of -80C cryopreservation on our liver tissue samples, it appeared that the β-gal staining tended to decrease with freezing time. This result might be related to the loss of the enzyme activity caused by cryopreservation (32). However, a significant difference in β-gal staining between BDR and controls was still observed

after 12 months post-cryopreservation. Cryopreservation can also potentially lead to an increase in the enzyme activity detected, due to lysosomal membrane leakage caused by cryopreservation (32). Still, all controls remained negative at pH 4.0 (two hours) or pH 5.8 (overnight) for up to 12 months post-cryopreservation. According to our results, the SA-β-gal activity assay remains a specific test despite several months of tissue cryopreservation, as long as all specimens (senescent tissues and controls) are analyzed after the same storage duration. This observation is of major importance since no study so far has evaluated the impact of cryopreservation on β-gal activity staining. Being able to use cryopreserved tissue allows multiple testing on the same samples, and should facilitate further research involving SA-β-gal activity assay. However, we observed a noticeable inter-experimental variability, which could be explained by a variability in sections location and/or by a difference in tissue senescence intensity between animals. Due to the inter-experimental variations that we observed, negative controls are mandatory to corroborate results on cryopreserved tissue.

In conclusion, our results provide the first detailed optimized protocol for SA-β-gal activity staining on rat liver tissue cryopreserved for up to 12 months. We demonstrated that SA-β-gal activity can be evidenced in cryopreserved tissue after two hours of reaction at physiological pH 4.0, as well as after overnight staining at pH 5.8.

References

1. Lee BY, Han JA, Im JS, Morrone A, Johung K, Goodwin EC, Kleijer WJ, DiMaio D, Hwang ES. Senescence-associated beta-galactosidase is lysosomal beta-galactosidase. Aging Cell. 2006;5(2):187-95. Epub 2006/04/22. doi: 10.1111/j.1474-9726.2006.00199.x. PubMed PMID: 16626397.
2. Debacq-Chainiaux F, Erusalimsky JD, Campisi J, Toussaint O. Protocols to detect senescence-associated beta-galactosidase (SA-betagal) activity, a biomarker of senescent cells in culture and in vivo. Nat Protoc. 2009;4(12):1798-806. doi: 10.1038/nprot.2009.191. PubMed PMID: 20010931.
3. Dimri GP, Lee X, Basile G, Acosta M, Scott G, Roskelley C, Medrano EE, Linskens M, Rubelj I, Pereira-Smith O, et al. A biomarker that identifies senescent human cells in culture and in aging skin in vivo. Proc Natl Acad Sci U S A. 1995;92(20):9363-7. PubMed PMID: 7568133; PubMed Central PMCID: PMCPMC40985.
4. Itahana K, Campisi J, Dimri GP. Methods to detect biomarkers of cellular senescence: the senescence-associated beta-galactosidase assay. Methods Mol Biol. 2007;371:21-31. Epub 2007/07/20. PubMed PMID: 17634571.
5. Zhao J, Fuhrmann-Stroissnigg H, Gurkar AU, Flores RR, Dorronsoro A, Stolz DB, St Croix CM, Niedernhofer LJ, Robbins PD. Quantitative Analysis of Cellular Senescence in Culture and In Vivo. Curr Protoc Cytom. 2017;79:9 51 1-9 25. Epub 2017/01/06. doi: 10.1002/cpcy.16. PubMed PMID: 28055114.
6. Noren Hooten N, Evans MK. Techniques to Induce and Quantify Cellular Senescence. J Vis Exp. 2017(123). Epub 2017/05/19. doi: 10.3791/55533. PubMed PMID: 28518126; PubMed Central PMCID: PMCPMC5565152.
7. Wiemann SU, Satyanarayana A, Tsahuridu M, Tillmann HL, Zender L, Klempnauer J, Flemming P, Franco S, Blasco MA, Manns MP, Rudolph KL. Hepatocyte telomere shortening and senescence are general markers of human liver cirrhosis. FASEB J. 2002;16(9):935-42. doi: 10.1096/fj.01-0977com. PubMed PMID: 12087054.
8. Paradis V, Youssef N, Dargere D, Ba N, Bonvoust F, Deschatrette J, Bedossa P. Replicative senescence in normal liver, chronic hepatitis C, and hepatocellular carcinomas. Hum Pathol. 2001;32(3):327-32. Epub 2001/03/29. doi: 10.1053/hupa.2001.22747. PubMed PMID: 11274643.
9. Sigal SH, Rajvanshi P, Gorla GR, Sokhi RP, Saxena R, Gebhard DR, Jr., Reid LM, Gupta S. Partial hepatectomy-induced polyploidy attenuates hepatocyte replication and activates cell aging events. Am J Physiol. 1999;276(5 Pt 1):G1260-72. Epub 1999/05/18. PubMed PMID: 10330018.
10. Pacheco-Rivera R, Fattel-Fazenda S, Arellanes-Robledo J, Silva-Olivares A, Aleman-Lazarini L, Rodriguez-Segura M, Perez-Carreon J, Villa-Trevino S, Shibayama M, Serrano-Luna J. Double staining of beta-galactosidase with fibrosis and cancer markers reveals the chronological appearance of senescence in liver carcinogenesis induced by diethylnitrosamine. Toxicol Lett. 2016;241:19-31. Epub 2015/11/22. doi: 10.1016/j.toxlet.2015.11.011. PubMed PMID: 26589970.

11. Serra MP, Marongiu F, Sini M, Laconi E. Hepatocyte senescence in vivo following preconditioning for liver repopulation. Hepatology. 2012;56(2):760-8. doi: 10.1002/hep.25698. PubMed PMID: 22392699.
12. Ogrodnik M, Miwa S, Tchkonia T, Tiniakos D, Wilson CL, Lahat A, Day CP, Burt A, Palmer A, Anstee QM, Grellscheid SN, Hoeijmakers JHJ, Barnhoorn S, Mann DA, Bird TG, Vermeij WP, Kirkland JL, Passos JF, von Zglinicki T, Jurk D. Cellular senescence drives age-dependent hepatic steatosis. Nat Commun. 2017;8:15691. doi: 10.1038/ncomms15691. PubMed PMID: 28608850; PubMed Central PMCID: PMCPMC5474745.
13. Wang MJ, Chen F, Li JX, Liu CC, Zhang HB, Xia Y, Yu B, You P, Xiang D, Lu L, Yao H, Borjigin U, Yang GS, Wangensteen KJ, He ZY, Wang X, Hu YP. Reversal of hepatocyte senescence after continuous in vivo cell proliferation. Hepatology. 2014;60(1):349-61. doi: 10.1002/hep.27094. PubMed PMID: 24711261.
14. Krizhanovsky V, Yon M, Dickins RA, Hearn S, Simon J, Miething C, Yee H, Zender L, Lowe SW. Senescence of activated stellate cells limits liver fibrosis. Cell. 2008;134(4):657-67. doi: 10.1016/j.cell.2008.06.049. PubMed PMID: 18724938; PubMed Central PMCID: PMCPMC3073300.
15. Nishizawa H, Iguchi G, Fukuoka H, Takahashi M, Suda K, Bando H, Matsumoto R, Yoshida K, Odake Y, Ogawa W, Takahashi Y. IGF-I induces senescence of hepatic stellate cells and limits fibrosis in a p53-dependent manner. Sci Rep. 2016;6:34605. doi: 10.1038/srep34605. PubMed PMID: 27721459; PubMed Central PMCID: PMCPMC5056388.
16. Ueberham E, Glockner P, Gohler C, Straub BK, Teupser D, Schonig K, Braeuning A, Hohn AK, Jerchow B, Birchmeier W, Gaunitz F, Arendt T, Sansom O, Gebhardt R, Ueberham U. Global increase of p16INK4a in APC-deficient mouse liver drives clonal growth of p16INK4a-negative tumors. Mol Cancer Res. 2015;13(2):239-49. Epub 2014/10/02. doi: 10.1158/1541-7786.MCR-14-0278-T. PubMed PMID: 25270420.
17. Abu-Tair L, Axelrod JH, Doron S, Ovadya Y, Krizhanovsky V, Galun E, Amer J, Safadi R. Natural killer cell-dependent anti-fibrotic pathway in liver injury via Toll-like receptor-9. PLoS One. 2013;8(12):e82571. Epub 2013/12/18. doi: 10.1371/journal.pone.0082571. PubMed PMID: 24340043; PubMed Central PMCID: PMCPMC3858328.
18. Gutierrez-Reyes G, del Carmen Garcia de Leon M, Varela-Fascinetto G, Valencia P, Perez Tamayo R, Rosado CG, Labonne BF, Rochilin NM, Garcia RM, Valadez JA, Latour GT, Corona DL, Diaz GR, Zlotnik A, Kershenobich D. Cellular senescence in livers from children with end stage liver disease. PLoS One. 2010;5(4):e10231. doi: 10.1371/journal.pone.0010231. PubMed PMID: 20422055; PubMed Central PMCID: PMCPMC2858078.
19. Sasaki M, Ikeda H, Haga H, Manabe T, Nakanuma Y. Frequent cellular senescence in small bile ducts in primary biliary cirrhosis: a possible role in bile duct loss. J Pathol. 2005;205(4):451-9. Epub 2005/02/03. doi: 10.1002/path.1729. PubMed PMID: 15685690.
20. Sokal EM, Trivedi P, Cheeseman P, Portmann B, Mowat AP. The application of quantitative cytochemistry to study the acinar distribution of enzymatic activities in human liver biopsy sections. J Hepatol. 1989;9(1):42-8. Epub 1989/07/01. PubMed PMID: 2549121.
21. Sokal EM, Trivedi P, Portmann B, Mowat AP. Adaptative changes of metabolic zonation during the development of cirrhosis in growing rats. Gastroenterology. 1990;99(3):785-92. Epub 1990/09/01. doi: 10.1016/0016-5085(90)90969-8. PubMed PMID: 2165952.

22. Wan Y, Meng F, Wu N, Zhou T, Venter J, Francis H, Kennedy L, Glaser T, Bernuzzi F, Invernizzi P, Glaser S, Huang Q, Alpini G. Substance P increases liver fibrosis by differential changes in senescence of cholangiocytes and hepatic stellate cells. Hepatology. 2017;66(2):528-41. doi: 10.1002/hep.29138. PubMed PMID: 28256736; PubMed Central PMCID: PMCPMC5519428.
23. McDaniel K, Meng F, Wu N, Sato K, Venter J, Bernuzzi F, Invernizzi P, Zhou T, Kyritsi K, Wan Y, Huang Q, Onori P, Francis H, Gaudio E, Glaser S, Alpini G. Forkhead box A2 regulates biliary heterogeneity and senescence during cholestatic liver injury in micedouble dagger. Hepatology. 2017;65(2):544-59. doi: 10.1002/hep.28831. PubMed PMID: 27639079; PubMed Central PMCID: PMCPMC5258713.
24. Sokal EM, Mostin J, Buts JP. Liver metabolic zonation in rat biliary cirrhosis: distribution is reverse of that in toxic cirrhosis. Hepatology. 1992;15(5):904-8. PubMed PMID: 1314772.
25. Sokal EM, Trivedi P, Portmann B, Mowat AP. Developmental changes in the intra-acinar distribution of succinate dehydrogenase, glutamate dehydrogenase, glucose-6-phosphatase, and NADPH dehydrogenase in the rat liver. J Pediatr Gastroenterol Nutr. 1989;8(4):522-7. Epub 1989/05/01. PubMed PMID: 2542510.
26. Scouten C, Cunningham M. Freezing Biological Samples. Microscopy today. 2006;14(1):48.
27. Lojda Z. Indigogenic methods for glycosidases. I. An improved method for beta-D-glucosidase and its application to localization studies on intestinal and renal enzymes. Histochemie. 1970;22(4):347-61. Epub 1970/01/01. PubMed PMID: 4194240.
28. Takahashi M, Hakamata Y, Takeuchi K, Kobayashi E. Effects of different fixatives on beta-galactosidase activity. J Histochem Cytochem. 2003;51(4):553-4. Epub 2003/04/25. doi: 10.1177/002215540305100419. PubMed PMID: 12710460.
29. Hopwood D. Some aspects of fixation with glutaraldehyde. A biochemical and histochemical comparison of the effects of formaldehyde and glutaraldehyde fixation on various enzymes and glycogen, with a note on penetration of glutaraldehyde into liver. J Anat. 1967;101(Pt 1):83-92. Epub 1967/01/01. PubMed PMID: 6047703; PubMed Central PMCID: PMCPMC1270860.
30. Sokal EM. Adaptive changes of metabolic zonation in liver cirrhosis. Brussels: Université Catholique de Louvain; 1993.
31. Pearse AGE. Histochemistry Theoretical and Applied. 3. Fourth ed. Edinburgh: Churchill Livingstone; 1991.
32. Bode C, Meinel A. The effect of storage at - 80 degrees C on the activities of cytoplasmic, mitochondrial and microsomal enzymes in rat liver. J Clin Chem Clin Biochem. 1982;20(1):9-13. Epub 1982/01/01. PubMed PMID: 7069380.

Chapter 3: senescence and senotherapies in biliary atresia and biliary cirrhosis

Giulia Jannone[1*], Eliano Bonaccorsi Riani[2], Catherine de Magnée[3], Roberto Tambucci[3], Jonathan Evraerts[1], Joachim Ravau[1], Pamela Baldin[4], Caroline Bouzin[5], Axelle Loriot[6], Laurent Gatto[6], Anabelle Decottignies[7], Mustapha Najimi[1], Etienne Marc Sokal[1]

[1]Pediatric Hepatology and Cell Therapy Unit, Institut de Recherche Expérimentale et Clinique, UCLouvain, Brussels, Belgium
[2]Abdominal Transplantation Unit, Department of Surgery, Cliniques Universitaires Saint-Luc, UCLouvain, Brussels, Belgium
[3]Pediatric Surgery and Transplantation Unit, Department of Surgery, Cliniques Universitaires Saint-Luc, UCLouvain, Brussels, Belgium
[4]Department of Anatomopathology, Cliniques Universitaires Saint-Luc, UCLouvain, Brussels, Belgium
[5]IREC Imaging Platform (2IP), Institut de Recherche Expérimentale et Clinique, UCLouvain, Brussels, Belgium
[6]Computational Biology and Bioinformatics Unit, de Duve Institute, UCLouvain, Brussels, Belgium
[7]Genetic and Epigenetic Alterations of Genomes Group, de Duve Institute, UCLouvain, Brussels, Belgium

This work was submitted for publication

Summary

Background: Premature senescence occurs in adult hepatobiliary diseases and worsens the prognosis through deleterious liver remodeling and hepatic dysfunction. Senescence might also arises in biliary atresia (BA), the first cause of pediatric liver transplantation. Since alternatives to transplantation are needed, our aim was to investigate premature senescence in BA and to assess senotherapies in a preclinical model of biliary cirrhosis.

Methods: BA liver tissues were prospectively obtained at hepatoportoenterostomy (n=5) and liver transplantation (n=30) and compared to controls (n=10). Senescence was investigated through spatial whole transcriptome analysis, SA-β-gal activity, p16 and p21 expression, γ-H2AX and senescence-associated secretory phenotype (SASP). Human allogenic liver-derived progenitor cells (HALPC) or dasatinib and quercetin (D+Q) were administrated to two-month-old Wistar rats after bile duct ligation (BDL).

Results: Advanced premature senescence was evidenced in BA livers from early stage and continued to progress until liver transplantation. Senescence and SASP were predominant in cholangiocytes, but also present in surrounding hepatocytes. HALPC but not D+Q reduced the early marker of senescence p21 in BDL rats and improved biliary injury (serum γGT and *Sox9* expression) and hepatocytes mass loss (*Hnf4a*).

Conclusions: BA livers displayed advanced cellular senescence at diagnosis that continued to progress until liver transplantation. HALPC reduced early senescence and improved liver disease in a preclinical model of BA, providing encouraging preliminary results regarding the use of senotherapies in pediatric biliary cirrhosis. However, efficacy of cell-type specific senotherapeutics on established senescence and liver disease will have to be demonstrated before considering to translate senotherapies to pediatric biliary cirrhosis.

Introduction

Senescence is a process of cellular ageing, resulting in metabolic modifications and in an irreversible cell cycle arrest (1). Various cellular changes reflect this complex phenomenon, including upregulation of cell cycle inhibitors (e.g. p21 and p16) and

anti-apoptotic pathways, increased lysosomal protein content and senescence-associated beta-galactosidase (SA-β-gal) activity, accumulation of DNA damage foci (e.g. γ-H2AX and/or 53BP1-positive foci), and a senescence-associated secretory phenotype (SASP). Because there are no completely specific senescence features, the gold standard is to assess cellular senescence through the evaluation of multiple markers (2).

Accelerated senescence occurs in numerous chronic adult hepatobiliary diseases and has been associated to disease severity and cirrhosis (3-5). The initial biliary damage in cholangiopathies induces premature senescence in cholangiocytes, and senescence subsequently spreads due to autocrine and paracrine transmission through the SASP (6-8). Senescence progression worsens the disease prognosis as the SASP directly participates in the deleterious tissue remodeling and leads to liver dysfunction by inducing senescence in surrounding hepatocytes (9). Furthermore, clearance of senescent cells or inhibition of the paracrine transmission of senescence improves liver function, histological fibrosis or steatosis in mouse models of hepatobiliary diseases (9-13). Existing data demonstrate that liver disease improves when senescence decreases, thus supporting the development of senotherapeutics that could be translated to clinical applications.

Biliary atresia (BA) is a severe pediatric disease caused by the progressive fibro-inflammatory obliteration of extrahepatic bile ducts, leading to biliary cirrhosis and end-stage liver disease (14). Despite the fact that BA is the first cause of liver transplantation in children, its underlying mechanisms are still not completely elucidated (14, 15). A hepatoportoenterostomy procedure can be attempted in case of early diagnosis, but liver transplantation remains the only curative treatment in about two thirds of the cases (16). A few studies described premature senescence in BA by using single technical approaches, but the possibility of using anti-senescence therapies was never explored in pediatric biliary cirrhosis (17-20).

In brief, premature senescence worsens the prognosis of adult chronic hepatobiliary diseases and some evidence suggests that this phenomenon could also occur in BA, which is the leading cause of liver transplantation in children. As there is a need for new therapies to avoid or delay liver transplantation in pediatric biliary cirrhosis, the aim of our work was to investigate premature senescence in BA through a multi-technical approach and to assess senotherapies in a preclinical model of biliary cirrhosis.

Results

Premature senescence is present at diagnosis in BA and progresses until liver transplantation

Liver tissue samples were obtained from thirty BA patients undergoing liver transplantation (BA late group) and five patients during hepatoportoenterostomy procedure (BA early group), the latter procedure being performed very shortly after the diagnosis. All BA patients were pediatric, while the ten control livers were obtained from pediatric and adult individuals (four adults aged 28 – 41 years old). General characteristics of the study population are summarized in Supplementary Table 1. As expected, fibrosis and biliary proliferation increased in BA livers as COL1A1 gene expression was already elevated in early stage BA, while histological fibrosis and CK19 gene expression increased in late stage BA (Supplementary Figure 1).

Senescence was evidenced in BA through multiple markers and techniques, including SA-β-gal activity, p16 protein and gene expression, γH2AX protein expression and SASP markers gene expression elevation (IL-8 and TGF-β1) (Figures 1a-1d & Supplementary Figure 2b). Of note, p16 and IL-8 gene expression

significantly increased only in late stage BA (Figures 1c & 1d). Advanced premature senescence was already present in the BA early group, as suggested by an increased protein expression of p16 but not p21, p16 being described as a late marker of senescence (Figure 1b & Supplementary Figure 2a) (21). However, there was still a clear progression of senescence between the time of diagnosis and liver transplantation (Figures 1c & 1e). Interestingly, senescence development was correlated to disease progression (Supplementary Figures 1b & 1c). Senescence was predominant in cholangiocytes and also present in surrounding perinodular hepatocytes (Figures 1a, 1b & 1e, Figure 2). When we investigated the telomeric DNA damages in late stage BA, γH2AX-positive DNA damage foci were evenly distributed in the whole DNA sequence without any specific accumulation in telomeres (Supplementary Figure 2c). However, the absolute increase in the number of telomere damage foci might per se induce senescence in the affected cells (2).

Our results show that premature senescence was already advanced at diagnosis in BA and continued to progress until liver transplantation. Senescence was predominant in cholangiocytes and perinodular hepatocytes, corroborating the hypothesis of a paracrine transmission of senescence through elevated SASP markers.

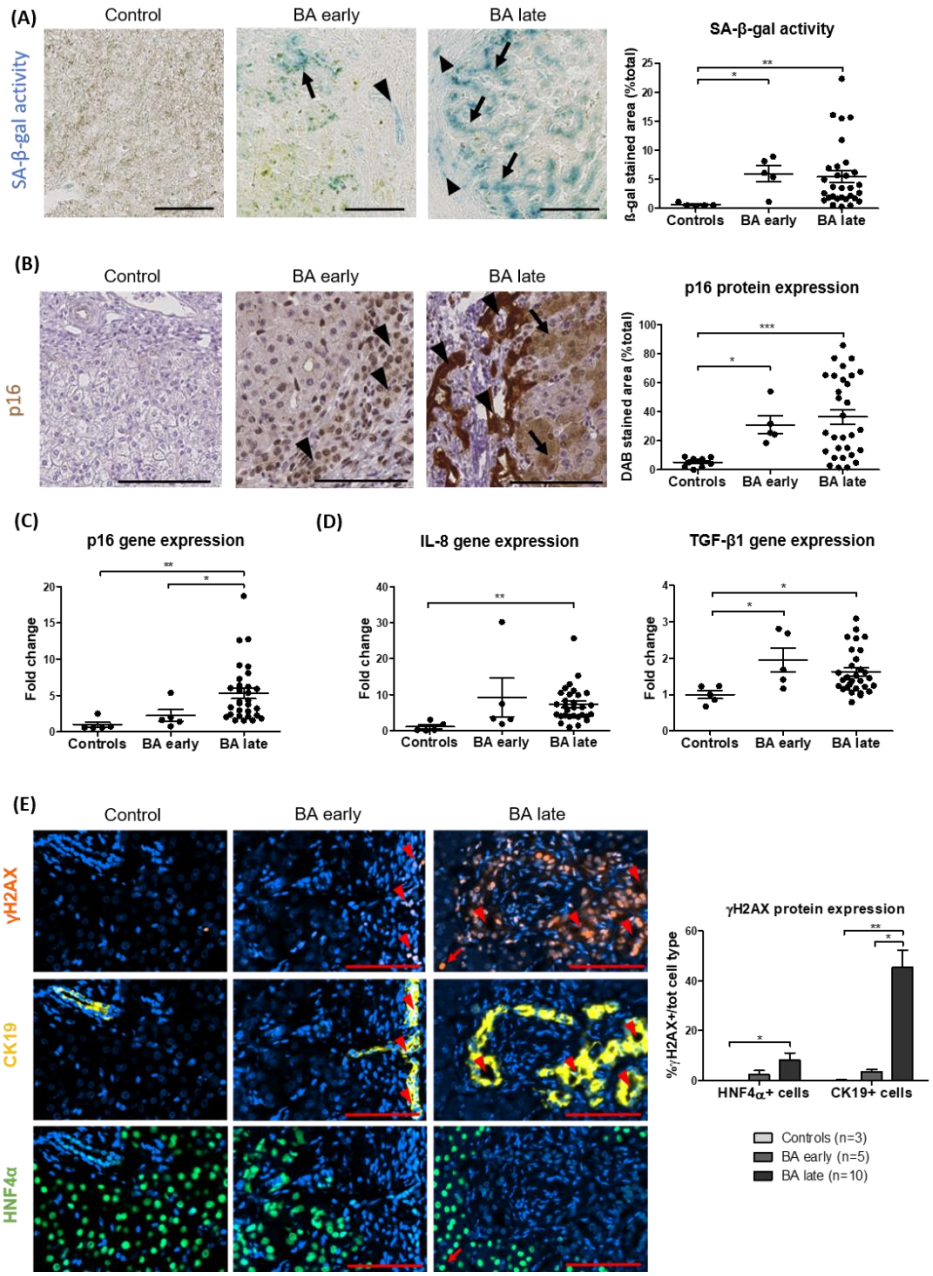

Figure 1. Senescence increases in BA livers and predominates in cholangiocytes and perinodular hepatocytes. (A): SA-β-gal activity increases in cholangiocytes (arrowheads) and surrounding perinodular hepatocytes (arrows) in BA livers. (B): p16 protein expression also

increases in cholangiocytes (arrowheads) and surrounding perinodular hepatocytes (arrows) in BA livers. (C): Gene expression of p16 progresses until liver transplantation in BA. (D): Gene expression of SASP markers IL-8 and TGF-β1 increase in BA livers versus controls. (E): DNA damage γH2AX-positive foci increase in both hepatocytes and cholangiocytes in BA livers and progress until liver transplantation in cholangiocytes. BA: biliary atresia; DAB: 3,3'-diaminobenzidine; SA-β-gal: senescence-associated beta-galactosidase; Data is presented as mean ± SEM; *p≤0.05, **p<0.01, ***p<0.001. Scale bars = 100 µm.

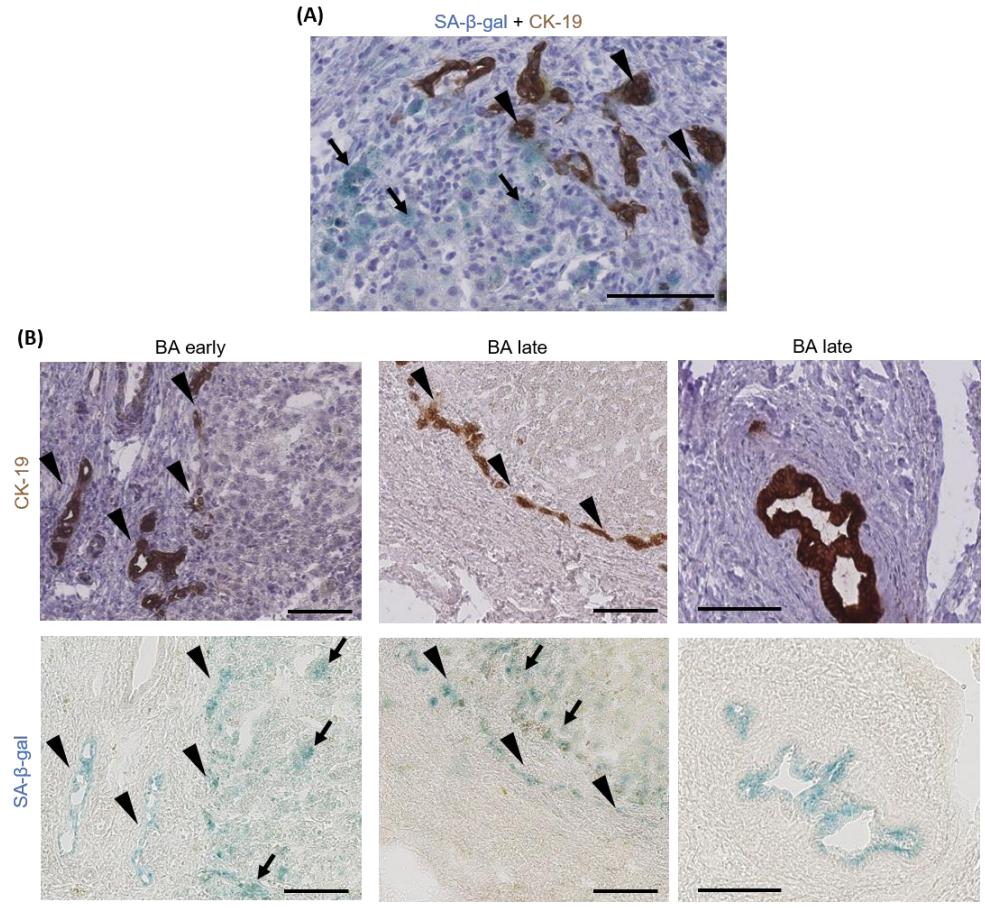

Figure 2. Cholangiocytes and perinodular hepatocytes display cellular senescence in BA livers. (A): Co-staining of SA-β-gal activity and CK-19 IHC on BA livers: some bile ductules cholangiocytes show staining co-localization (arrowheads) while perinodular hepatocytes are only positive for SA-β-gal (arrows); (B): Serial staining of SA-β-gal activity and CK-19 IHC on BA livers cryosections. Left and middle images: bile ductules (arrowheads) and

perinodular hepatocytes (arrows) are positive for SA-β-gal in both early and late stage BA. Right images: remaining large septal bile duct display SA-β-gal activity. BA: biliary atresia; IHC: immunohistochemistry; SA-β-gal: senescence-associated beta-galactosidase. Scale bars = 100 µm.

Digital spatial transcriptomic analysis in BA livers confirms that senescence and SASP predominate in cholangiocytes and progress with disease stage

To further assess the localization and progression of cellular senescence, we performed a digital spatial whole transcriptomic analysis on BA and control liver samples. Both cholangiocytes and hepatocytes regions of interest (ROI) were selected in BA early, BA late and control livers (Figure 3a). Principal component analysis (PCA) revealed that the transcriptomes differed according to cell type (cholangiocytes versus hepatocytes) and disease stage (Figure 3b). Early and late stage BA transcriptomes were clustered together and differed from controls for each cell type. Differential expression analysis was performed between disease stages subgroups for each cell type and data is available for the main differentially expressed genes in Supplementary figure 3. Gene ontology (GO) enrichment analysis of biological processes (MSigDB Collection: C5 GO BP) and hallmark gene sets enrichment analysis (MSigDB Collection: H) were also performed on our dataset (Supplementary Figure 4). GO terms that appeared to be the most significant when comparing genes differentially expressed between diseased cholangiocytes versus controls corresponded to “supramolecular fiber organization”, “cell adhesion” and “ion transport” categories, in line with the disruption of apical-basal polarization described in BA cholangiocytes (22).

Enrichment analysis of senescence gene lists available in the literature was then performed in our dataset (Figure 3c). A geneset corresponding to genes that were upregulated in senescent HepG2 cells as well as in both senescent HepG2 and

diseased human adult livers was significantly enriched in diseased cholangiocytes (BA early and late stages) as compared to controls, supporting the presence of senescence in BA cholangiocytes (23). The same gene lists as well as two other datasets obtained from senescent HepG2 cells and from an organ-independent literature-based senescence signature database were significantly enriched in BA late stage cholangiocytes as compared to BA early stage, underlying the progression of senescence until liver transplantation in BA cholangiocytes (24, 25). Volcano plots and detailed results are available in Supplementary Figure 5 for the leading edge genes of the enrichment analysis. In contrast, a core transcriptome database obtained from senescent human fibroblasts, melanocytes, keratinocytes and astrocytes was not significantly enriched in our diseased cholangiocytes, underlying that the transcriptome of senescent cells is highly heterogeneous depending on the senescent organ (26). None of those publically available senescence datasets were enriched in our diseased hepatocytes. Various SASP genes obtained from two published datasets were differentially expressed in both diseased cholangiocytes and hepatocytes in our cohort (Figure 3d) (26, 27). The two most overexpressed SASP factors in diseased cholangiocytes as compared to controls were IL-32 and CCL2 (log2 fold change > 2.5; p-adj < 1x10-20). IL-32 is a pro-inflammatory cytokine that was evidenced before in BA livers, while CCL2 has been associated to the paracrine transmission of senescence in cholangiopathy (28, 29). A publically available SASP gene list obtained from senescent HepG2 cells was significantly enriched in BA late stage cholangiocytes as compared to BA early stage (NES 1.6; p-adj 0.007), and in diseased cholangiocytes as compared to hepatocytes (NES 1.47; p-adj 0.04) (27). Altogether, those results confirm the progressive development of senescence and SASP in cholangiocytes until liver transplantation and highlight the predominance of senescence in BA cholangiocytes as compared to hepatocytes.

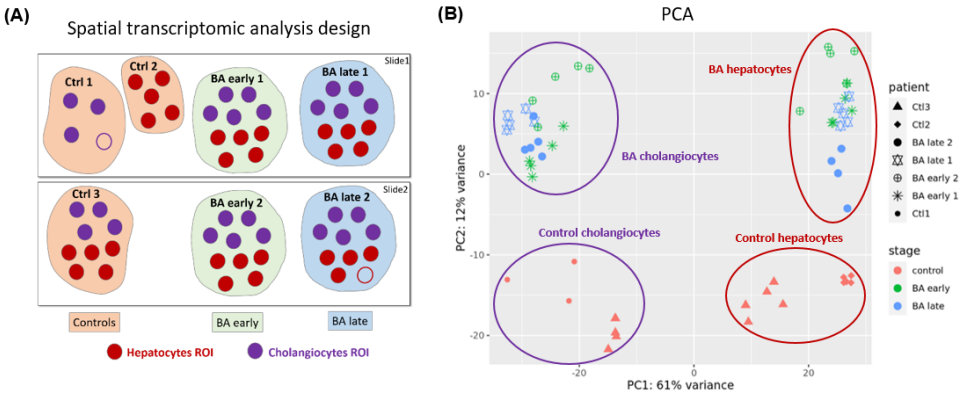

(C)

Senescence gene list reference	Type(s) of senescent cells/tissue	N° detected genes/total	Cholangiocytes BA early vs controls	Cholangiocytes BA late vs controls	Cholangiocytes BA late vs BA early
Aravinthan *et al* 2014 (37)	Senescent HepG2 (H2O2-induced senescence)	196/353	NES 1.25 *p*-adj 0.01	NES 1.45 *p*-adj 4.87e-06	NES 1.46 *p*-adj 4.32e-07
Aravinthan *et al* 2014 (37)	Senescent HepG2 crossed with data from NASH, ASH & HCV liver samples	31/40	NES 1.43 *p*-adj 0.03	NES 1.78 *p*-adj 2.11e-05	NES 1.54 *p*-adj 5.93e-03
Nagano *et al* 2016 (38)	Senescent HepG2 (etoposide-induced senescence)	11/26	Ns	Ns	NES 1.67 *p*-adj 7.14e-03
Zhao *et al* 2016 (39)	Literature-based senescence gene list (all human cell types/organs)	275/489	Ns	Ns	NES 1.2 *p*-adj 8.74e-03
Hernandez *et al* 2017 (40)	Core transcriptome shared by senescent fibroblasts, melanocytes, keratinocytes and astrocytes	39/55	Ns	Ns	Ns

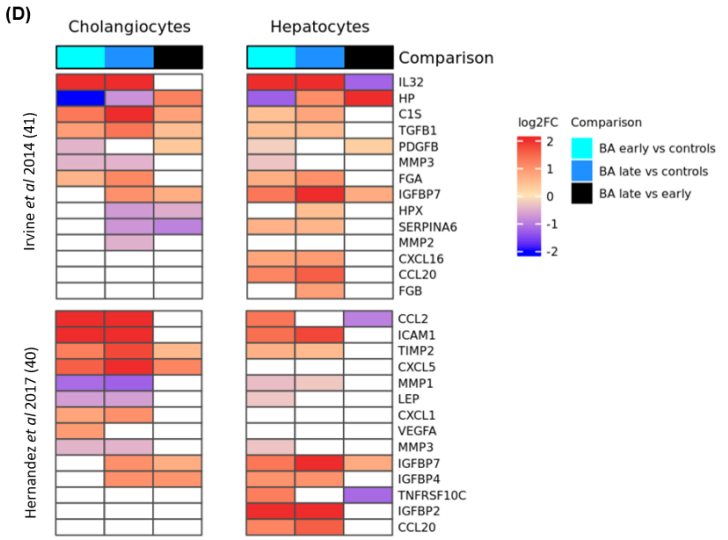

Figure 3. Digital spatial whole transcriptomic analysis in BA livers. (A) Design of the analysis. (B) PCA of the dataset. (C) Enrichment analysis of published senescence gene lists between

cholangiocytes subgroups. (D) Heatmaps of SASP genes obtained from two different published datasets in cholangiocytes and hepatocytes subgroups. BA: biliary atresia; Ctrl: control; FC: fold change; NES: normalized enrichment score; p-adj: adjusted p-value; PCA: principal component analysis; ROI: region of interest; SASP: senescence-associated secretory phenotype.

Senescence progresses from cholangiocytes to hepatocytes after BDL surgery in rats

Bile duct ligation (BDL) was performed in two-months-old rats to generate a model of biliary senescence in which we could test senotherapeutics. The operated rats developed progressive cholestasis, biliary proliferation, loss of hepatocytes mass and liver fibrosis as expected (Supplementary Figure 6). Senescence progression was confirmed in the animal model as demonstrated by an increased SA-β-gal activity, p21 protein and gene expression, p16 gene expression and SASP-related genes expression (Figure 4). Biliary proliferation and liver fibrosis significantly correlated with senescence development (Supplementary Figures 6a & 6b). As expected, the earliest marker of senescence was p21 as it was significantly increased in whole liver homogenates from 1 week after the surgery (Figure 4b). The percentage of senescent p21-positive cholangiocytes was already maximal after 48 hours and subsequently decreased, while senescence progressively increased in hepatocytes of the parenchyma (Figure 4b).

Our results confirm that BDL is a robust model of biliary senescence. Studying early post-surgical stages allowed us to demonstrate that senescence developed first in cholangiocytes and subsequently in hepatocytes during biliary injury.

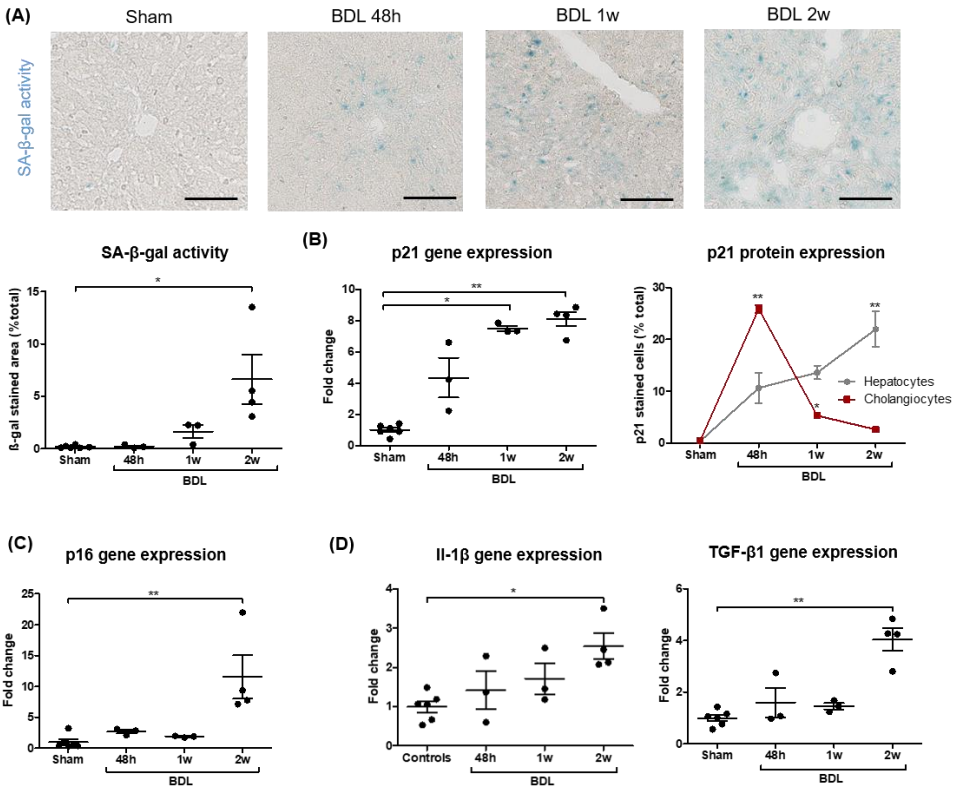

Figure 4. Senescence progressively develops in BDL rats and appears in cholangiocytes before hepatocytes. (A) SA-β-gal activity increases after the surgery. (B) p21 gene expression progressively increase in BDL livers as compared to controls. Senescence (p21-positive cell percentage) is maximal in cholangiocytes 48 hours post-BDL, while hepatocytes senescence increases progressively to become significant only two weeks after the surgery. The percentages of p21-positive cells at different timepoints are compared to the correspondent cellular type of control rats. (C) p16 gene expression increases in diseased rats two weeks post-surgery. (D) Gene expression of SASP markers Il-1β and TGF-β1 increase in BDL livers as compared to controls. BDL: bile duct ligation; SA-β-gal: senescence-associated β-galactosidase; SASP: senescence-associated secretory phenotype; 48h – 1w – 2w : rats sacrificed 48 hours (n=3) – 1 week (n=3) – 2 weeks (n=4) after BDL surgery. Data is presented as mean ± SEM; *p≤0.05; **p<0.01. Scale bars = 100µm.

HALPC but not D+Q decrease early senescence and liver disease in the BDL model

Once we demonstrated that biliary senescence occurs in the BDL model, we evaluated the efficacy of human allogenic liver-derived progenitor cells (HALPC) or dasatinib (D) + quercetin (Q) in the operated animals. Both therapies were administered 48 hours after the surgery and the animals were compared to vehicle-treated controls (Figure 5a and Supplementary Figure 7a). Since the low dose and the high dose of cells provided comparable results, all the animals injected with HALPC were grouped for further analyses. Intravenous HALPC injection reduced the gene expression of the early marker of senescence p21, while no significant effect was observed regarding SA-β-gal activity nor p16 gene expression (Figure 5b). HALPC improved biliary injury (serum γGT levels) and proliferation (transcription factor SOX-9 – *Sox9* – expression) (Figure 5c). The cells had no effect on the hepatocytes injury (serum AST), but slightly improved the hepatocytes mass loss (hepatocyte nuclear factor 4-alpha - *Hnf4a* – expression) (Figure 5d). No effect was observed on liver histological fibrosis (Figure 5e). The anti-oxidative properties of HALPC were investigated through the gene expression of glutathione peroxidase 1 (*Gpx1*) in liver homogenates and we observed a decrease of *Gpx1* expression in the group that received the cells as compared to the vehicle (Figure 5f). Unexpectedly, the very well described combination of D+Q had no effect on senescence nor liver disease progression as compared to the vehicle and on the opposite appeared to aggravate the hepatocytes mass loss (Supplementary Figure 7).

Our results suggest that HALPC but not D+Q improve early senescence and liver injury in the BDL model of biliary cirrhosis.

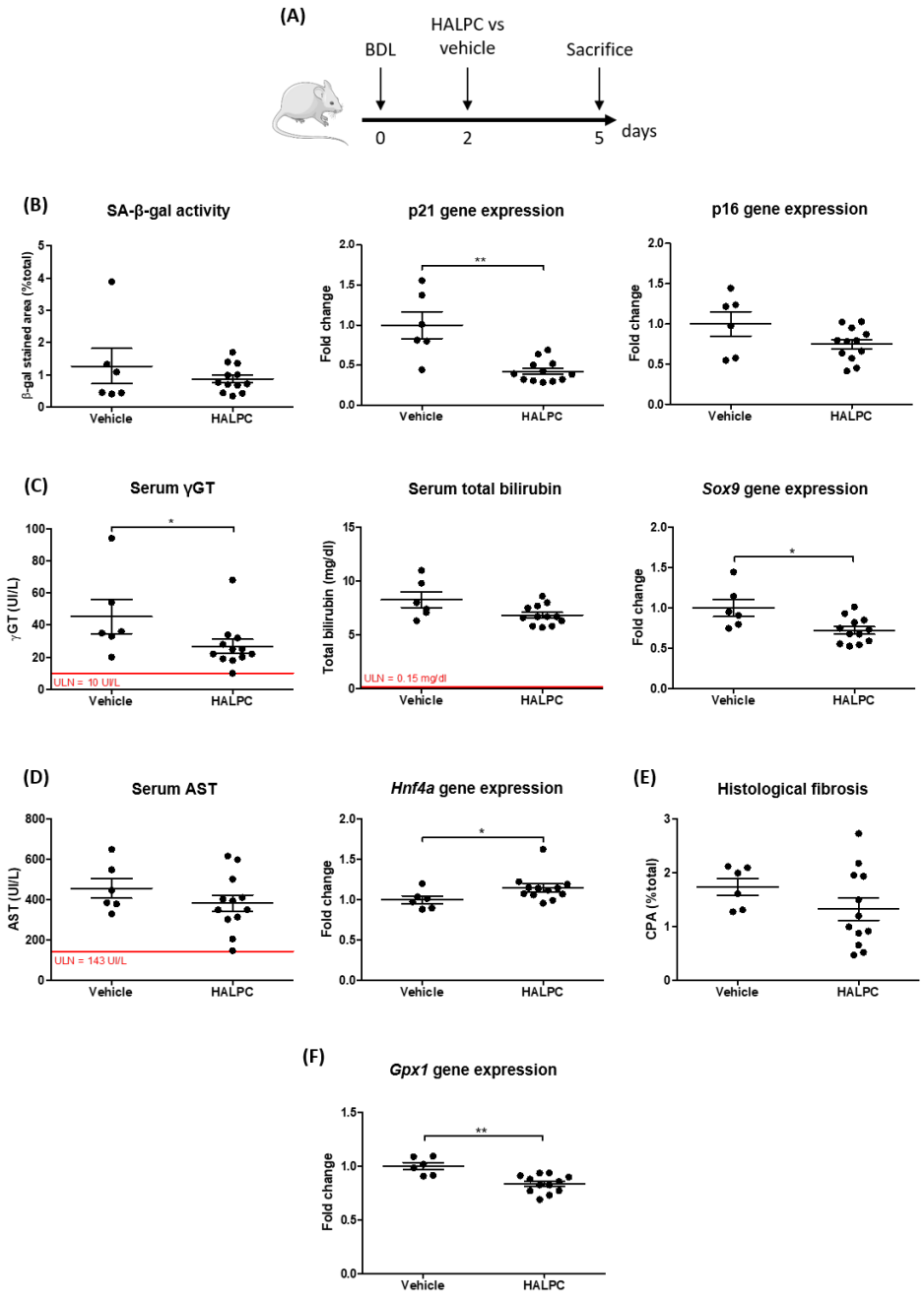

Figure 5. HALPC administration in BDL rats. (A) Operated rats received HALPC (n=12) through peripheral vein injection 48 hours after BDL and were compared to vehicle-treated controls (n=6). (B) HALPC decreased the early marker of senescence p21 gene expression,

but no significant effect was observed on later markers (SA-β-gal activity and p16 gene expression). (C) HALPC decreased cholangiocytes injury (serum γGT) and biliary proliferation (*Sox9*), but had no significant effect on biochemical cholestasis (serum total bilirubin). (D-E) HALPC slightly reduced the hepatocytes mass loss (*Hnf4α*) while having no significant effect on serum AST nor on liver histological fibrosis. (F) HALPC reduced *Gpx1* expression. BDL: bile duct ligation; HALPC: human allogenic liver-derived progenitor cells; SA-β-gal: senescence-associated β-galactosidase; ULN: upper limit of normal. Data is presented as mean ± SEM; *p≤0.05; **p<0.01.

Discussion

Our data provide the first integrative report about premature senescence in pediatric BA and demonstrate that liver senescence and SASP are already present from early stage in BA but continue to progress until liver transplantation, supporting the potential benefit of senotherapeutic interventions following hepatoportoenterostomy. Senescence and SASP were predominant in cholangiocytes as compared to hepatocytes in BA, and senescence progressively developed from cholangiocytes to hepatocytes in the BDL preclinical model of biliary cirrhosis. Furthermore, CCL2 and TGF-β1 – two SASP components that are widely incriminated in the paracrine transmission of senescence – were elevated in our BA livers (9, 29, 30). Our data corroborate the likelihood of a paracrine transmission of senescence from cholangiocytes to surrounding hepatocytes through the SASP in cholangiopathies, further supporting the use of senotherapies to limit the deleterious effects of the SASP on senescence expansion, tissue remodeling and liver dysfunction (8, 9, 31).

Since we evidenced advanced senescence in BA, the next step was to test senotherapeutics that could be translated to pediatric biliary cirrhosis in the BDL model of biliary cirrhosis. We first demonstrated that the progression of disease and senescence in the liver of operated young rats was in many aspects comparable

to BA, before administrating the animals with HALPC or D+Q. We chose to test HALPC – a population of mesenchymal stem cells (MSC) obtained from healthy human liver – in our preclinical model because those cells are already approved for clinical application and because various MSC types already demonstrated to have anti-senescence properties *in vivo* through antioxidant and anti-inflammatory effects (32-35). However, since HALPC anti-senescence properties remained to be demonstrated, we chose to compare their effect with the very well described combination of the pro-apoptotic drugs D and Q, which was already tested in clinical trials in age-related diseases such as diabetic kidney disease or idiopathic pulmonary fibrosis (36, 37).

HALPC transplantation in BDL young rats improved the early marker of senescence p21, as well as biliary injury and hepatocytes loss, providing encouraging preliminary results regarding the use of senotherapeutics in biliary cirrhosis. HALPC also demonstrated to reduce Gpx1 expression in our BDL model, possibly due to a cell-mediated reduction of the oxidative stress that could explain a beneficial effect on liver senescence (38). However, further studies will be needed to truly consider HALPC as senotherapeutics since we observed an improvement of early senescence only with no effect of the cells on the markers of established senescence p16 and SA-β-gal activity nor on liver fibrosis in our short-time experiment. In addition, HALPC are known to secrete numerous bioactive factors with paracrine activity, including anti-inflammatory, anti-fibrotic and regenerative effects (39-43). We hypothesized that the disease improvement observed in BDL rats was related to the reduction of early senescence by the cells, but other HALPC paracrine properties might also have contributed to this improvement. Proof of efficacy regarding therapeutic interventions that act specifically on senescence and thereby improve liver disease will be needed before translating senotherapies to pediatric biliary cirrhosis.

Unexpectedly, the combination of senolytics D+Q had no effect on senescence nor liver disease progression in our model. Senolytics are – by definition – able to selectively or preferentially kill senescent cells (44). D+Q induce the selective apoptosis of senescent cells and were shown to decrease hepatocytes senescence and liver steatosis in a preclinical model of non-alcoholic fatty liver disease (NAFLD) (11). However, a more recent publication showed no effect of D+Q on senescence, liver steatosis nor fibrosis in a model of NAFLD-induced hepatocellular carcinoma (45). D+Q even seemed to display a pro-tumorigenic effect in this model. In line with this observation, the apoptosis of senescent liver sinusoidal endothelial cells induced perivascular liver fibrosis and health deterioration in aged mice (46). Also, senescent hepatic stellate cells can limit liver fibrosis and promote liver regeneration in preclinical models (47, 48). Caution should thereby be advised regarding the use of senolytic therapies in liver disease as consequences could differ according to the removed senescent cell type.

In conclusion, BA livers displayed advanced senescence at diagnosis and senescence and SASP continued to progress until liver transplantation. HALPC but not D+Q reduced early senescence and improved liver disease in a preclinical model of biliary cirrhosis, providing encouraging preliminary results. However, the development of therapeutic agents that target selected senescent cell-types through clearly identified mechanisms and thereby improve established senescence and liver disease will be needed before considering to translate senotherapies to pediatric biliary cirrhosis.

Materials and methods

Human samples

Patients who underwent hepatoportoenterostomy procedure (n = 5) or liver transplantation (n = 30) for BA were prospectively recruited in the Pediatric Gastroenterology and Hepatology Unit of Cliniques Universitaires Saint-Luc between 2018 and 2022. A liver biopsy or a fragment of the explanted liver was collected for each patient and obtained from the Cliniques Universitaires Saint-Luc Hepatic Biobank. Biochemical data were obtained the day before the procedure. Control livers (n=10) were obtained from the Cliniques Universitaires Saint-Luc biobank when consent for research purposes was given. Cryopreserved material was available for 5/10 controls. This project was approved by the Ethics Committee of Cliniques Universitaires Saint-Luc (registration number B403201938739). Written informed consent was obtained for all study participants.

Animal model and senotherapeutics administration

Biliary cirrhosis was induced in 2-month-old wild-type male Wistar rats by performing the extrahepatic bile duct ligation-resection surgical procedure as previously described (49). Controls underwent sham procedure (bile duct dissection without resection) at the same age and were sacrificed at the same time points. Cryopreserved HALPC were obtained from the Hepatic Biobank of Cliniques Universitaires Saint-Luc. The cells were originally derived from the liver of a male donor aged 4 months as previously described and cultured on Corning CellBIND flasks (Merck, Kenilworth, NJ, USA) (50). For our experiments, cells cryopreserved at P4 were thawed and re-suspended in PBS supplemented with heparin 60UI/106 cells. Cells were subsequently injected to the animals at high dose (12.5x106 cells/kg, n=6) and low dose (1.25x106 cells/kg, n=6) through the penile vein 48

hours after BDL procedure. D (5 mg/kg; Merck) and Q (50 mg/kg; Merck) were diluted in 50% PEG400 and administered by oral gavage 48 hours after BDL surgery (n=5). Controls underwent BDL as well and were either injected with the cell vehicle (n=6) or received 50% PEG400 by oral gavage (n=5) at the same timepoints. All animals were sacrificed three days after the treatment. This project was approved by the Ethical Committee for Animal Experimentation of UCLouvain, Brussels (2018/UCL/MD/43).

Senescence-associated β-galactosidase activity assay

SA-β-gal activity assay was performed on cryopreserved liver tissue as previously described (51). The reaction was performed at pH 4 and the staining solution was removed after one hour (for human liver) or two hours (for rat liver) of incubation at 37C. Stained sections were washed with PBS before subsequent immunohistochemical staining when indicated.

Immunohistochemistry – immunofluorescence

Five µm formalin-fixed paraffin-embedded (FFPE) liver sections were deparaffinized and rehydrated in xylene and graded alcohol series. Antigen retrieval was performed with Tris-EDTA buffer (Merck) or with citrate buffer (Dako Target Retrieval Solution, Agilent, Santa Clara, CA, USA) (Supplementary Table 2). Non-specific immuno-staining was prevented by 1 hour incubation in PBS containing 5% Bovine Serum Albumin (Merck) ± 5% Normal Goat Serum (Thermo Fisher Scientific, Waltham, MA, USA). Thereafter, sections were incubated with primary antibody for 1 hour at 37C (Supplementary Table 2). After washing, sections were incubated with species-specific secondary antibodies (Dako EnVision+ System HRP, Agilent). Immunohistochemical detection was performed with liquid 3,3'-diaminobenzidine (DAB) chromogen and substrate buffer (Dako,

Agilent), and was followed by Mayer's hematoxylin counterstaining. For immunofluorescence staining, tyramide-fluorophore amplification was performed sequentially with different fluorochromes (Alexa-488, 555, 594 or 647, Atto-425, Thermo Fisher Scientific or Invitrogen, Waltham, MA, USA) for each antibody as previously described (52). Sections were mounted with DAPI containing media or counterstained with Hoechst (Merck) and mounted with Dako fluorescence mounting medium (Dako).

Imaging and quantification of staining in whole tissue sections

Quantification of staining was assessed as previously described (51). Briefly, stained slides were digitalized using a SCN400 slide scanner (Leica Biosystems, Wetzlar, Germany) or Axio Scan.Z1 scanner for immunofluorescence (Zeiss, Oberkochen, Germany) (x20 magnification). For selected experiments, high magnification images (x100) with z-stack imaging were obtained through spinning disk confocal microscopy (Zeiss). Scanned slides were then analyzed using the image analysis tool Author version 2017.2 (Visiopharm, Hørsholm, Denmark) for computer-assisted quantification of histological staining. Results were expressed as (stained area/total tissue area) x 100 to obtain a percentage of stained area or as (stained cells/total number of cells) x 100 to obtain a percentage of stained cells. The parameters of the designed Visiopharm APPs were kept constant for all sections.

Reverse transcription quantitative polymerase chain reaction (RT-qPCR)

Liver homogenates were obtained with the FastPrep-24 Classic Instrument (MP Biomedicals, Irvine, CA, USA) from liver biopsies cryopreserved in Lysing Matrix D tubes (MP Biomedicals) filled with Tripure isolation reagent (Roche, Basel, Switzerland). Total RNA was extracted from liver homogenates using Tripure

isolation reagent (Roche), according to the manufacturer's instructions. Genomic DNA was digested by DNase I (Invitrogen). RNA was retro-transcribed using the high-capacity cDNA reverse transcription kit (Applied Biosystems, Waltham, CA, USA). RT-qPCR was carried out in duplicate using TaqMan universal MasterMix (Applied Biosystems) and pre-designed TaqMan probes obtained from Thermo Fisher Scientific or Integrated DNA Technologies (IDT; Coralville, IA, USA) on a StepOnePlus real-time PCR machine (Applied Biosystems) (Supplementary Table 3). Relative gene expression was determined with the ΔΔCt method using *TBP* and *PPIA* as housekeeping genes for human experiments and *Gapdh* and *B2m* for rat experiments (53).

Digital spatial whole transcriptome of BA livers

Digital spatial profiling (DSP) GeoMx slide preparation and analysis were performed by the Utrecht Sequencing Facility (USEQ) team (Utrecht, Netherlands). FFPE samples of BA late (n=2), BA early (n=2) and control (n=3) livers were processed and prepared according to the RNA FFPE Manual Slide Preparation Protocol section of the GeoMx NGS Slide Preparation User Manual (MAN-10115-05) by NanoString Technologies (Seattle, WA, USA). Briefly, FFPE slides were baked at 60C for 30 minutes immediately before deparaffinization and rehydration. The slides were then incubated in 100C Tris-EDTA for 15 min to achieve target retrieval. RNA targets were exposed through incubation with Proteinase K at 37C for 15min and a post-fixation step was performed to preserve the samples. The slides were hybridized overnight with GeoMx Human Whole Transcriptome Atlas Human RNA probe mix for Illumina Systems (NanoString Technologies). Stringent washes were performed to remove off-target probes and samples were blocked with Buffer W (NanoString Technologies). Prepared slides were then stained for one hour with immunofluorescent antibodies to allow the identification of tissue morphology and

the detection of specific cell types during the ROI selection step. The morphological markers used were pan-cytokeratin (2 µg/ml; NBP2-33200AF532, Novus Biologicals, Centennial, CO, USA), alpha smooth muscle actin (1.25 µg/ml; ab202368, Abcam, Cambridge, UK) and Syto13 (S7575, Thermo Fisher Scientific). Slides were then washed and loaded into the GeoMx DSP machine for scanning (x20 magnification) and ROI selection. Selection of 4-5 ROI for hepatocytes and 4-5 ROI for cholangiocytes was manually performed in each sample. Only the cell type of interest was digitally selected in each ROI thanks to the pan-cytokeratin immunofluorescent staining (high intensity staining for cholangiocytes and low intensity staining for hepatocytes). ROI were validated only if containing at least 100 targeted cells in order to allow sufficient signal for subsequent detection. GeoMx Human Whole Transcriptome Atlas RNA assay contains in situ hybridization probes conjugated to unique DNA oligonucleotides (DSP barcodes) via a UV-photocleavable linker. After ROI selection, the DSP barcodes were tagged according to their ROI location and then UV-cleaved and collected to be sequenced on an Illumina sequencer (San Diego, CA, USA). Sequenced oligonucleotides were processed and then imported back into the GeoMx DSP analysis software for integration with the ROI selection information and generation of spatially- and cell type-resolved transcriptomic data.

Analysis of DSP whole transcriptome data

Two low-performing ROI segments with less than 10% of the genes detected were removed from the analysis (genes were considered as detected when their counts were higher than the LOQ value, defined as the negative probes geometric means + 2 standard deviations). Genes lowly detected across the dataset (in less than 10% of the segments) were removed, leaving 9146 genes for the differential expression analyses. Raw counts were normalized by the Q3 normalization method.

Differential expression analyses were performed with DESeq2 Bioconductor package v1.32.0 (54). Gene set enrichment analyses were done using clusterProfiler v4.0.5 (55).

Statistical analysis

Statistical analysis was conducted using Graphpad Prism 5.0 (GraphPad Software, La Jolla, CA, USA). Continuous variables were presented as mean ± standard error of the mean (SEM) or median (range) and categorical variables as numbers and percentages. The non-parametric Mann-Whitney U test was used to compare continuous variables between subgroups. When more than two groups were included in the analysis, a non-parametric Kruskal-Wallis One-Way ANOVA with Dunn's post-hoc test was performed. A two-tailed p-value ≤ 0.05 was considered to indicate statistical significance for all analyses.

Acknowledgements

All our thanks to Florence Chainiaux for her expert advice and to Jean-Paul Dehoux for his help. We also thank the IREC 2IP and the de Duve Institute imaging platforms for the use of laboratory facilities, and especially Aurélie Daumerie, Michele de Beukelaer, Guillaume Courtois, Manon Mahieu and Patrick Van Der Smissen for their valuable assistance and advice. Giulia Jannone, Catherine de Magnée, Roberto Tambucci and Etienne Sokal are members of the European Reference Networks Rare-Liver and/or TransplantChild.

References

1. Campisi J. From cells to organisms: can we learn about aging from cells in culture? Exp Gerontol. 2001; 36: 607-18.
2. Gorgoulis V, Adams PD, Alimonti A, Bennett DC, Bischof O, Bishop C, Campisi J, Collado M, Evangelou K, Ferbeyre G, Gil J, Hara E, Krizhanovsky V, et al. Cellular Senescence: Defining a Path Forward. Cell. 2019; 179: 813-27.
3. Wiemann SU, Satyanarayana A, Tsahuridu M, Tillmann HL, Zender L, Klempnauer J, Flemming P, Franco S, Blasco MA, Manns MP, Rudolph KL. Hepatocyte telomere shortening and senescence are general markers of human liver cirrhosis. FASEB J. 2002; 16: 935-42.
4. Cazzagon N, Sarcognato S, Floreani A, Corra G, De Martin S, Guzzardo V, Russo FP, Guido M. Cholangiocyte senescence in primary sclerosing cholangitis is associated with disease severity and prognosis. JHEP Rep. 2021; 3: 100286.
5. Nakanuma Y, Sasaki M, Harada K. Autophagy and senescence in fibrosing cholangiopathies. J Hepatol. 2015; 62: 934-45.
6. Ferreira-Gonzalez S, Rodrigo-Torres D, Gadd VL, Forbes SJ. Cellular Senescence in Liver Disease and Regeneration. Semin Liver Dis. 2021; 41: 50-66.
7. Banales JM, Huebert RC, Karlsen T, Strazzabosco M, LaRusso NF, Gores GJ. Cholangiocyte pathobiology. Nat Rev Gastroenterol Hepatol. 2019; 16: 269-81.
8. Meadows V, Baiocchi L, Kundu D, Sato K, Fuentes Y, Wu C, Chakraborty S, Glaser S, Alpini G, Kennedy L, Francis H. Biliary Epithelial Senescence in Liver Disease: There Will Be SASP. Front Mol Biosci. 2021; 8: 803098.
9. Ferreira-Gonzalez S, Lu WY, Raven A, Dwyer B, Man TY, O'Duibhir E, Lewis PJS, Campana L, Kendall TJ, Bird TG, Tarrats N, Acosta JC, Boulter L, et al. Paracrine cellular senescence exacerbates biliary injury and impairs regeneration. Nat Commun. 2018; 9: 1020.
10. Rudolph KL, Chang S, Millard M, Schreiber-Agus N, DePinho RA. Inhibition of experimental liver cirrhosis in mice by telomerase gene delivery. Science. 2000; 287: 1253-8.
11. Ogrodnik M, Miwa S, Tchkonia T, Tiniakos D, Wilson CL, Lahat A, Day CP, Burt A, Palmer A, Anstee QM, Grellscheid SN, Hoeijmakers JHJ, Barnhoorn S, et al. Cellular senescence drives age-dependent hepatic steatosis. Nat Commun. 2017; 8: 15691.
12. Alsuraih M, O'Hara SP, Woodrum JE, Pirius NE, LaRusso NF. Genetic or pharmacological reduction of cholangiocyte senescence improves inflammation and fibrosis in the Mdr2 (-/-) mouse. JHEP Rep. 2021; 3: 100250.
13. Amor C, Feucht J, Leibold J, Ho YJ, Zhu C, Alonso-Curbelo D, Mansilla-Soto J, Boyer JA, Li X, Giavridis T, Kulick A, Houlihan S, Peerschke E, et al. Senolytic CAR T cells reverse senescence-associated pathologies. Nature. 2020; 583: 127-32.
14. Bezerra JA, Wells RG, Mack CL, Karpen SJ, Hoofnagle JH, Doo E, Sokol RJ. Biliary Atresia: Clinical and Research Challenges for the Twenty-First Century. Hepatology. 2018; 68: 1163-73.
15. Gurevich M, Guy-Viterbo V, Janssen M, Stephenne X, Smets F, Sokal E, Lefebvre C, Balligand JL, Pirotte T, Veyckemans F, Clapuyt P, Menten R, Dumitriu D, et al. Living Donor

Liver Transplantation in Children: Surgical and Immunological Results in 250 Recipients at Universite Catholique de Louvain. Ann Surg. 2015; 262: 1141-9.
16. Chardot C, Buet C, Serinet MO, Golmard JL, Lachaux A, Roquelaure B, Gottrand F, Broue P, Dabadie A, Gauthier F, Jacquemin E. Improving outcomes of biliary atresia: French national series 1986-2009. J Hepatol. 2013; 58: 1209-17.
17. Nakajima Y, Yamazaki Y, Gao X, Hashimoto M, Nio M, Wada M, Fujishima F, Sasano H. Association between mitochondrial and nuclear DNA damages and cellular senescence in the patients with biliary atresia undergoing Kasai portoenterostomy and liver transplantation. Med Mol Morphol. 2022; 55: 131-45.
18. Gutierrez-Reyes G, del Carmen Garcia de Leon M, Varela-Fascinetto G, Valencia P, Perez Tamayo R, Rosado CG, Labonne BF, Rochilin NM, Garcia RM, Valadez JA, Latour GT, Corona DL, Diaz GR, et al. Cellular senescence in livers from children with end stage liver disease. PLoS One. 2010; 5: e10231.
19. Sanada Y, Aida J, Kawano Y, Nakamura K, Shimomura N, Ishikawa N, Arai T, Poon SS, Yamada N, Okada N, Wakiya T, Hayashida M, Saito T, et al. Hepatocellular telomere length in biliary atresia measured by Q-FISH. World J Surg. 2012; 36: 908-16.
20. Sasaki M, Kuo FY, Huang CC, Swanson PE, Chen CL, Chuang JH, Yeh MM. Increased expression of senescence-associated cell cycle regulators in the progression of biliary atresia: an immunohistochemical study. Histopathology. 2018; 72: 1164-71.
21. Stein GH, Drullinger LF, Soulard A, Dulic V. Differential roles for cyclin-dependent kinase inhibitors p21 and p16 in the mechanisms of senescence and differentiation in human fibroblasts. Mol Cell Biol. 1999; 19: 2109-17.
22. Lendahl U, Lui VCH, Chung PHY, Tam PKH. Biliary Atresia - emerging diagnostic and therapy opportunities. EBioMedicine. 2021; 74: 103689.
23. Aravinthan A, Shannon N, Heaney J, Hoare M, Marshall A, Alexander GJ. The senescent hepatocyte gene signature in chronic liver disease. Exp Gerontol. 2014; 60: 37-45.
24. Nagano T, Nakano M, Nakashima A, Onishi K, Yamao S, Enari M, Kikkawa U, Kamada S. Identification of cellular senescence-specific genes by comparative transcriptomics. Sci Rep. 2016; 6: 31758.
25. Zhao M, Chen L, Qu H. CSGene: a literature-based database for cell senescence genes and its application to identify critical cell aging pathways and associated diseases. Cell Death Dis. 2016; 7: e2053.
26. Hernandez-Segura A, de Jong TV, Melov S, Guryev V, Campisi J, Demaria M. Unmasking Transcriptional Heterogeneity in Senescent Cells. Curr Biol. 2017; 27: 2652-60 e4.
27. Irvine KM, Skoien R, Bokil NJ, Melino M, Thomas GP, Loo D, Gabrielli B, Hill MM, Sweet MJ, Clouston AD, Powell EE. Senescent human hepatocytes express a unique secretory phenotype and promote macrophage migration. World J Gastroenterol. 2014; 20: 17851-62.
28. Okamura A, Harada K, Nio M, Nakanuma Y. Interleukin-32 production associated with biliary innate immunity and proinflammatory cytokines contributes to the pathogenesis of cholangitis in biliary atresia. Clin Exp Immunol. 2013; 173: 268-75.

29. Sasaki M, Miyakoshi M, Sato Y, Nakanuma Y. Modulation of the microenvironment by senescent biliary epithelial cells may be involved in the pathogenesis of primary biliary cirrhosis. J Hepatol. 2010; 53: 318-25.
30. Acosta JC, Banito A, Wuestefeld T, Georgilis A, Janich P, Morton JP, Athineos D, Kang TW, Lasitschka F, Andrulis M, Pascual G, Morris KJ, Khan S, et al. A complex secretory program orchestrated by the inflammasome controls paracrine senescence. Nat Cell Biol. 2013; 15: 978-90.
31. Tabibian JH, O'Hara SP, Splinter PL, Trussoni CE, LaRusso NF. Cholangiocyte senescence by way of N-ras activation is a characteristic of primary sclerosing cholangitis. Hepatology. 2014; 59: 2263-75.
32. Nevens F, Gustot T, Laterre PF, Lasser LL, Haralampiev LE, Vargas V, Lyubomirova D, Albillos A, Najimi M, Michel S, Stoykov I, Gordillo N, Vainilovich Y, et al. A phase II study of human allogeneic liver-derived progenitor cell therapy for acute-on-chronic liver failure and acute decompensation. JHEP Rep. 2021; 3: 100291.
33. Zhang M, Liu D, Li S, Chang L, Zhang Y, Liu R, Sun F, Duan W, Du W, Wu Y, Zhao T, Xu C, Lu Y. Bone marrow mesenchymal stem cell transplantation retards the natural senescence of rat hearts. Stem Cells Transl Med. 2015; 4: 494-502.
34. Lai X, Huang S, Lin S, Pu L, Wang Y, Lin Y, Huang W, Wang Z. Mesenchymal stromal cells attenuate alveolar type 2 cells senescence through regulating NAMPT-mediated NAD metabolism. Stem Cell Res Ther. 2022; 13: 12.
35. Rodrigues CE, Capcha JM, de Braganca AC, Sanches TR, Gouveia PQ, de Oliveira PA, Malheiros DM, Volpini RA, Santinho MA, Santana BA, Calado RD, Noronha IL, Andrade L. Human umbilical cord-derived mesenchymal stromal cells protect against premature renal senescence resulting from oxidative stress in rats with acute kidney injury. Stem Cell Res Ther. 2017; 8: 19.
36. Justice JN, Nambiar AM, Tchkonia T, LeBrasseur NK, Pascual R, Hashmi SK, Prata L, Masternak MM, Kritchevsky SB, Musi N, Kirkland JL. Senolytics in idiopathic pulmonary fibrosis: Results from a first-in-human, open-label, pilot study. EBioMedicine. 2019; 40: 554-63.
37. Hickson LJ, Langhi Prata LGP, Bobart SA, Evans TK, Giorgadze N, Hashmi SK, Herrmann SM, Jensen MD, Jia Q, Jordan KL, Kellogg TA, Khosla S, Koerber DM, et al. Senolytics decrease senescent cells in humans: Preliminary report from a clinical trial of Dasatinib plus Quercetin in individuals with diabetic kidney disease. EBioMedicine. 2019; 47: 446-56.
38. Iskusnykh IY, Popova TN, Agarkov AA, Pinheiro de Carvalho MA, Rjevskiy SG. Expression of Glutathione Peroxidase and Glutathione Reductase and Level of Free Radical Processes under Toxic Hepatitis in Rats. J Toxicol. 2013; 2013: 870628.
39. Khuu DN, Scheers I, Ehnert S, Jazouli N, Nyabi O, Buc-Calderon P, Meulemans A, Nussler A, Sokal E, Najimi M. In vitro differentiated adult human liver progenitor cells display mature hepatic metabolic functions: a potential tool for in vitro pharmacotoxicological testing. Cell Transplant. 2011; 20: 287-302.
40. Berardis S, Lombard C, Evraerts J, El Taghdouini A, Rosseels V, Sancho-Bru P, Lozano JJ, van Grunsven L, Sokal E, Najimi M. Gene expression profiling and secretome analysis differentiate adult-derived human liver stem/progenitor cells and human hepatic stellate cells. PLoS One. 2014; 9: e86137.

41. Sana G, Lombard C, Vosters O, Jazouli N, Andre F, Stephenne X, Smets F, Najimi M, Sokal EM. Adult human hepatocytes promote CD4(+) T-cell hyporesponsiveness via interleukin-10-producing allogeneic dendritic cells. Cell Transplant. 2014; 23: 1127-42.
42. Najimi M, Berardis S, El-Kehdy H, Rosseels V, Evraerts J, Lombard C, El Taghdouini A, Henriet P, van Grunsven L, Sokal EM. Human liver mesenchymal stem/progenitor cells inhibit hepatic stellate cell activation: in vitro and in vivo evaluation. Stem Cell Res Ther. 2017; 8: 131.
43. Herrero A, Prigent J, Lombard C, Rosseels V, Daujat-Chavanieu M, Breckpot K, Najimi M, Deblandre G, Sokal EM. Adult-Derived Human Liver Stem/Progenitor Cells Infused 3 Days Postsurgery Improve Liver Regeneration in a Mouse Model of Extended Hepatectomy. Cell Transplant. 2017; 26: 351-64.
44. Morsli S, Doherty GJ, Munoz-Espin D. Activatable senoprobes and senolytics: Novel strategies to detect and target senescent cells. Mech Ageing Dev. 2022; 202: 111618.
45. Raffaele M, Kovacovicova K, Frohlich J, Lo Re O, Giallongo S, Oben JA, Faldyna M, Leva L, Giannone AG, Cabibi D, Vinciguerra M. Mild exacerbation of obesity- and age-dependent liver disease progression by senolytic cocktail dasatinib + quercetin. Cell Commun Signal. 2021; 19: 44.
46. Grosse L, Wagner N, Emelyanov A, Molina C, Lacas-Gervais S, Wagner KD, Bulavin DV. Defined p16(High) Senescent Cell Types Are Indispensable for Mouse Healthspan. Cell Metab. 2020; 32: 87-99 e6.
47. Cheng N, Kim KH, Lau LF. Senescent hepatic stellate cells promote liver regeneration through IL-6 and ligands of CXCR2. JCI Insight. 2022; 7.
48. Krizhanovsky V, Yon M, Dickins RA, Hearn S, Simon J, Miething C, Yee H, Zender L, Lowe SW. Senescence of activated stellate cells limits liver fibrosis. Cell. 2008; 134: 657-67.
49. Sokal EM, Mostin J, Buts JP. Liver metabolic zonation in rat biliary cirrhosis: distribution is reverse of that in toxic cirrhosis. Hepatology. 1992; 15: 904-8.
50. Najimi M, Khuu DN, Lysy PA, Jazouli N, Abarca J, Sempoux C, Sokal EM. Adult-derived human liver mesenchymal-like cells as a potential progenitor reservoir of hepatocytes? Cell Transplant. 2007; 16: 717-28.
51. Jannone G, Rozzi M, Najimi M, Decottignies A, Sokal EM. An Optimized Protocol for Histochemical Detection of Senescence-associated Beta-galactosidase Activity in Cryopreserved Liver Tissue. J Histochem Cytochem. 2020: 22155420913534.
52. Aboubakar Nana F, Hoton D, Ambroise J, Lecocq M, Vanderputten M, Sibille Y, Vanaudenaerde B, Pilette C, Bouzin C, Ocak S. Increased Expression and Activation of FAK in Small-Cell Lung Cancer Compared to Non-Small-Cell Lung Cancer. Cancers (Basel). 2019; 11.
53. Livak KJ, Schmittgen TD. Analysis of relative gene expression data using real-time quantitative PCR and the 2(-Delta Delta C(T)) Method. Methods. 2001; 25: 402-8.
54. Love MI, Huber W, Anders S. Moderated estimation of fold change and dispersion for RNA-seq data with DESeq2. Genome Biol. 2014; 15: 550.
55. Yu G, Wang LG, Han Y, He QY. clusterProfiler: an R package for comparing biological themes among gene clusters. OMICS. 2012; 16: 284-7.

Supplementary tables

	Controls (n=10)	**BA early (n=5)**	**BA late (n=30)**
Median age	9.5 y (3 d - 41 y)	7 w (17 d - 2 m)	12 m (6 m - 15 y)
Gender (M/F)	5 (50%) / 5	3 (60%) / 2	15 (50%) / 15
AST (UI/L) (< 80)	NA	232 ± 78	228 ± 19
ALT (UI/L) (< 35)	NA	155 ± 57	123 ± 11
γGT (UI/L) (< 40)	NA	455 ± 78	221 ± 30
Total bilirubin (mg/dL) (< 1.2)	NA	9.1 ± 1.7	17.5 ± 1.7
INR (0.8-1.2)	NA	1 ± 0.04	1.5 ± 0.1
Histological fibrosis (Metavir):			
F0	10 (100%)	1 (20%)	0
F1	0	0	0
F2	0	1 (20%)	0
F3	0	1 (20%)	0
F4	0	2 (40%)	30 (100%)

Supplementary Table 1. Description of the study population. In the first column, standard values are indicated for all biochemical parameters. Continuous data is presented as median (range) or mean ± SEM. D: days; m: months; NA: not available; y: years.

Primary antibody (target)	Company	Cat. No	Species	Ag retrieval	Dilution
p21 WAF1/Cip1 (H)	Agilent	M7202	M mAb	T 1 hour 98C	IHC 1/400
p21 WAF1/Cip1 (R)	Agilent	M7202	M mAb	T 900W 4 min - 90W 15 min - 900W 1.5 min - T Retriever 2100	IHC 1/50 IF 1/50
p16 INK4a (H)	Abcam	ab108349	Rb mAb	T 1 hour 98C	IHC 1/1000
gamma H2A.X (Ser139) (H)	Abcam	ab81299	Rb mAb	C 35 min 98C C Retriever 2100	IHC 1/500 IF 1/500
gamma H2A.X (Ser139) (H)	Merck	05-636	M mAb	C 5 min 450W	IF 1/1000
TRF2 (H)	Novus	NB110-57130	Rb pAb	C 5 min 450W	IF 1/2000
HNF4α (H-R)	R&D	PP-H1415	M mAb	C Retriever 2100	IF 1/400
CK19 (H)	Dako	M0888	M mAb	C 35 min 98C C Retriever 2100	IHC 1/100 IF 1/100
CK19 (R)	Abcam	ab220193	M mAb	C Retriever 2100	IF 1/200

Supplementary Table 2. Primary antibodies. Ag: antigen; C: citrate; H: human; IF: immunofluorescence; IHC: immunohistochemistry; M: Mouse; mAb: monoclonal antibody; pAb: polyclonal antibody; R: rat; Rb: rabbit; T: Tris-EDTA.

Gene of interest (specie)	Company	Reference
CDKN1A (H)	Thermo Fisher Scientific	Hs00355782_m1
CDKN2A (H)	Thermo Fisher Scientific	Hs00923894_m1
CXCL8 (H)	IDT	Hs.PT.58.38869678.g
TGFB1 (H)	IDT	Hs.PT.58.39813975
COL1A1 (H)	Thermo Fisher Scientific	Hs00164004_m1
KRT19 (H)	Thermo Fisher Scientific	Hs00761767_s1
HNF4A (H)	Thermo Fisher Scientific	Hs00230853_m1
TBP (H)	Thermo Fisher Scientific	Hs99999910_m1
PPIA (H)	Thermo Fisher Scientific	Hs99999904_m1
Cdkn1a (R)	IDT	Rn.PT.58.12154239
Cdkn2a (R)	Thermo Fisher Scientific	Rn00580664_m1
Il1b (R)	IDT	Rn.PT.58.38028824
Tgfb1 (R)	IDT	Rn.PT.58.6690138
Col1a1 (R)	IDT	Rn.PT.58.7562513
Sox9 (R)	IDT	Rn.PT.58.29440750
Hnf4a (R)	IDT	Rn.PT.58.34229621.g
Gpx1 (R)	IDT	Rn.PT.58.7204268.g
Gapdh (R)	Thermo Fisher Scientific	Rn01775763_g1
B2m (R)	Thermo Fisher Scientific	Rn00560865_m1

Supplementary Table 3. Pre-designed TaqMan probes used for reverse transcription quantitative polymerase chain reaction.

Supplementary figures

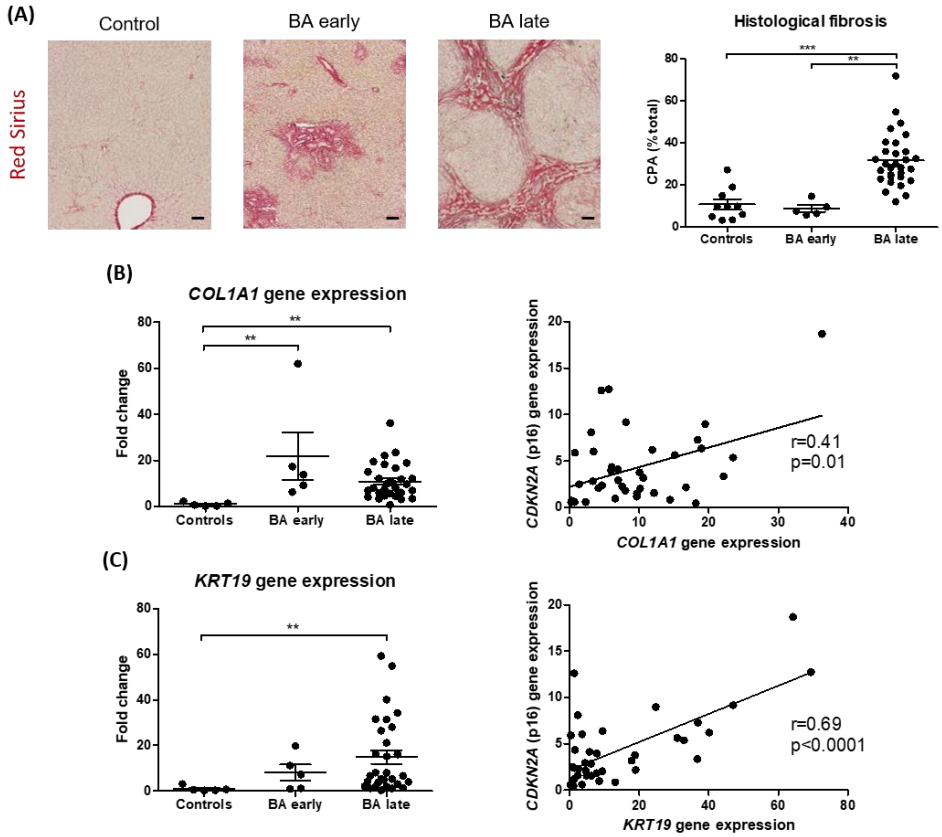

Supplementary Figure 1. Fibrosis and bile ducts mass in BA livers versus controls. (A) Histological fibrosis increases in late BA patients compared to controls and to early stage BA; (B) Myofibroblasts activation (*COL1A1* expression) increases in BA patients compared to controls and weakly correlates with senescence development; (C): Bile ducts mass (*KRT19* expression) increases in BA patients compared to controls and correlates with senescence development. BA: biliary atresia; CPA: collagen proportionate area. Data is presented as mean ± SEM; **p<0.01; ***p<0.001. Scale bars = 100 µm.

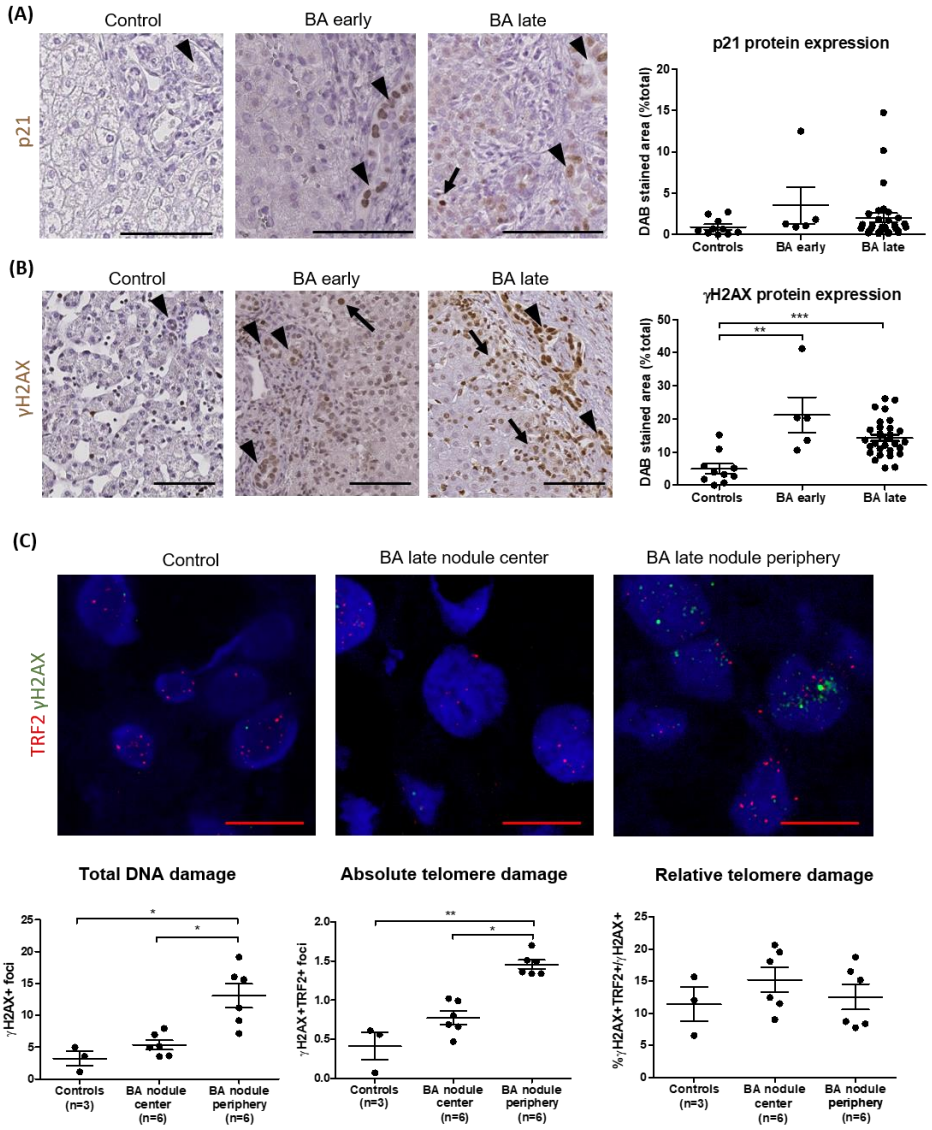

Supplementary Figure 2. DNA and telomere damages increase in BA. (A) BA livers do not display an increased p21 protein expression. (B): γH2AX protein expression increases in BA and predominates in cholangiocytes (arrowheads) and perinodular hepatocytes (arrows). (C): Late stage BA livers display increased DNA damage foci (γH2AX staining) and telomere damage foci (co-localization γH2AX-TRF2) in the periphery of the BA nodules (n=6) as compared to the center of the nodules (n=6) and to controls (n=3). Relative telomere damage (co-localization of γH2AX and TRF2 reported to total DNA damage) do not increase in late BA livers. BA: biliary atresia; DAB: 3,3′-diaminobenzidine. Data is presented as mean ± SEM; *p≤0.05, **p<0.01, ***p<0.001. Black scale bars = 100 µm; red scale bars = 10 µm.

Cholangiocytes: BA early vs controls

gene	log2FC	padj
UBD	3.81	5.69e-77
SLC3A1	-3.02	3.33e-61
SCGB3A1	-2.87	5.51e-46
TFF3	-3.11	5.66e-46
IL32	3.44	3.17e-45
KCNJ15	-2.60	1.37e-38
PRMT8	-1.99	2.64e-37
MUC1	-2.75	2.95e-37
ACE2	-2.37	5.30e-36
MPP6	-1.91	6.69e-36

451 DE genes (padj < 0.05 and |log2FC| > 1)

Hepatocytes: BA early vs controls

gene	log2FC	padj
UBD	3.04	1.96e-111
PPP2R1B	2.12	4.05e-94
IL32	3.27	6.40e-87
TGFBI	2.79	5.16e-77
IGF2	6.52	2.61e-73
GPC3	4.10	6.90e-73
HSD11B1	-2.53	3.80e-72
ACSL4	3.82	4.76e-63
SPP2	2.34	6.60e-60
CFB	2.33	1.89e-56

347 DE genes (padj < 0.05 and |log2FC| > 1)

Cholangiocytes: BA late vs controls

gene	log2FC	padj
SLC3A1	-3.00	1.11e-58
UBD	3.34	1.17e-58
MCAM	3.03	5.08e-58
BACE2	2.53	5.36e-57
MPP6	-2.49	8.47e-55
TFF3	-3.38	8.36e-53
KCNJ15	-3.15	1.17e-50
CXCL6	3.99	4.58e-48
SCGB3A1	-2.79	1.47e-43
ACE2	-2.64	8.97e-42

518 DE genes (padj < 0.05 and |log2FC| > 1)

Hepatocytes: BA late vs controls

gene	log2FC	padj
LEPR	3.11	9.00e-100
MFSD2A	2.12	4.25e-59
CFB	2.24	6.25e-49
ABCB4	2.34	1.01e-46
A1BG	2.05	2.07e-46
TNFSF14	1.81	1.06e-45
RNASE4	1.42	8.10e-40
PPP2R1B	1.43	1.13e-39
C8G	1.37	1.58e-39
ITIH3	2.74	8.55e-39

228 DE genes (padj < 0.05 and |log2FC| > 1)

Cholangiocytes: BA late vs BA early

gene	log2FC	padj
TNC	2.35	2.03e-70
BACE2	1.61	2.03e-70
KRT23	2.35	2.37e-29
MCAM	1.25	9.20e-29
KRT81	1.87	9.20e-29
CCND2	1.40	1.88e-24
PPP1R12B	1.11	1.07e-22
CLU	-2.09	6.92e-22
GDA	1.46	2.36e-20
IGF2	-3.43	1.13e-18

90 DE genes (padj < 0.05 and |log2FC| > 1)

Hepatocytes: BA late vs BA early

gene	log2FC	padj
MFSD2A	2.89	1.29e-101
HSD11B1	2.41	3.97e-62
SLC1A1	1.72	1.41e-57
GPC3	-3.56	3.35e-53
UBD	-2.01	1.27e-50
ZNF771	-1.25	1.27e-43
NNMT	4.39	2.22e-41
TNFRSF10C	-1.19	3.58e-37
PLIN2	2.64	7.47e-34
ADAM15	-1.00	6.78e-30

145 DE genes (padj < 0.05 and |log2FC| > 1)

Supplementary Figure 3. Differential expression analysis between subgroups in BA spatial WTA dataset. Total number of differentially expressed genes (padj < 0.05 and |log2FC| > 1) is mentioned for each subgroup comparison. Detailed data are listed for the top 10 main significantly modified genes in each subgroup comparison. BA: biliary atresia; DE: differentially expressed; FC: fold change; padj: adjusted p-value; WTA: whole transcriptome analysis.

Supplementary Figure 4. GSEA between subgroups in BA spatial WTA dataset. The ten most significantly enriched GO terms (A) or hallmark gene lists (B) are represented for each subgroup comparison. BA: biliary atresia; GO: gene ontology; GSEA: gene set enrichment analysis; NES: normalized enrichment score; WTA: whole transcriptome analysis.

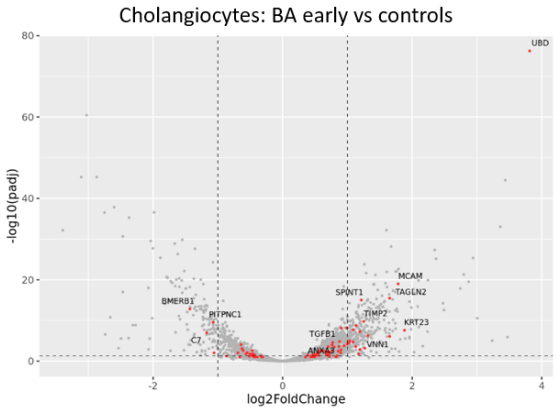

Gene	Log2FC	padj
UBD	3,81	5,69E-77
MCAM	1,78	1,01E-19
TAGLN2	1,65	3,23E-16
SPINT1	1,21	9,26E-16
BMERB1	-1,43	1,46E-13
TIMP2	1,25	1,74E-10
PITPNC1	-1,07	2,82E-10
RHOC	1,13	1,68E-9
S100A11	0,99	6,26E-9
TAX1BP3	0,90	7,20E-9
HSPG2	1,09	1,97E-8
KRT23	1,88	2,49E-8
DTNA	1,19	5,65E-8
C7	-1,17	1,08E-7
C1S	1,32	5,37E-7
VNN1	1,65	8,22E-7
PLK2	1,03	1,02E-5
TGFB1	0,88	1,52E-5
LAPTM5	1,09	1,90E-5

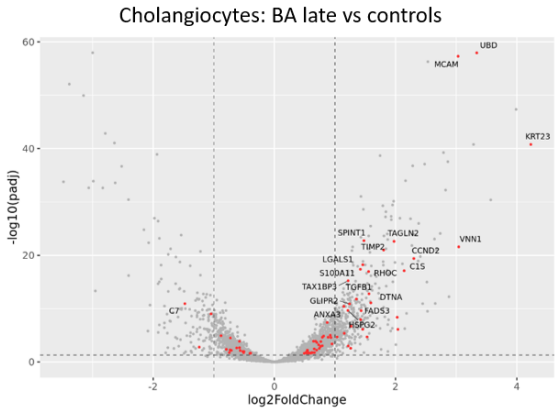

Gene	Log2FC	padj
UBD	3,34	1,17E-58
MCAM	3,03	5,08E-58
KRT23	4,23	1,69E-41
SPINT1	1,48	1,82E-23
TAGLN2	1,98	2,47E-23
VNN1	3,04	2,66E-22
TIMP2	1,80	1,04E-21
CCND2	2,30	4,11E-20
LGALS1	1,46	5,96E-19
S100A11	1,42	4,19E-18
C1S	2,14	8,06E-18
RHOC	1,55	1,13E-17
TAX1BP3	1,22	6,08E-16
DTNA	1,56	1,67E-13
TGFB1	1,35	1,6E-12
FADS3	1,59	8,38E-12
C7	-1,48	1,18E-11
GLIPR2	1,24	1,31E-11
ANXA3	1,15	3,82E-11
HSPG2	1,21	2,17E-10

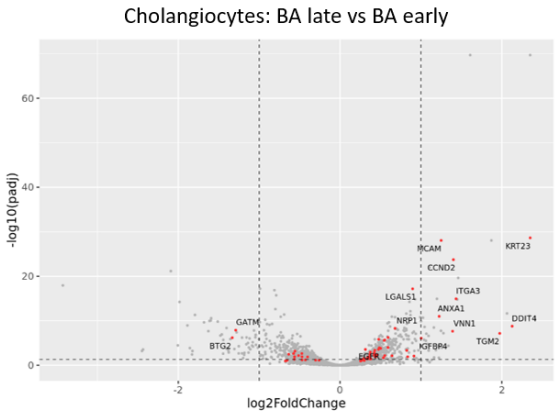

Gene	Log2FC	padj
KRT23	2,35	2,36E-29
MCAM	1,25	9,20E-29
CCND2	1,40	1,88E-24
LGALS1	0,90	6,57E-18
ITGA3	1,43	1,16E-15
ANXA1	1,23	1,02E-11
DDIT4	2,13	1,68E-9
NRP1	0,68	5,27E-9
GATM	-1,29	1,30E-8
VNN1	1,39	2,26E-8
TGM2	1,97	6,76E-8
FADS3	0,59	5,60E-7
BTG2	-1,33	6,41E-7
IGFBP4	1,00	8,44E-7
GLIPR2	0,48	1,49E-6
TIMP2	0,55	2,12E-6
RHBDF2	0,55	2,67E-6
PHLDA3	0,59	1,01E-4
CAPN2	0,48	1,17E-4
EGFR	0,50	1,63E-4

Supplementary Figure 5. Senescence enriched genes in BA spatial WTA dataset. Significant enrichment of a published gene list in senescent HepG2 cells (Aravinthan et al 2014) was observed in all cholangiocytes subgroups (BA early vs controls; BA late vs controls; BA late vs BA early), indicating a progression of cholangiocytes senescence associated with disease stage in BA. The leading edge genes of the GSEA are highlighted in red in the volcano plots of each subgroup comparison. Detailed data are listed for the top 20 leading edge genes in each subgroup comparison. BA: biliary atresia; FC: fold change; GSEA: gene set enrichment analysis; padj: adjusted p-value; WTA: whole transcriptome analysis.

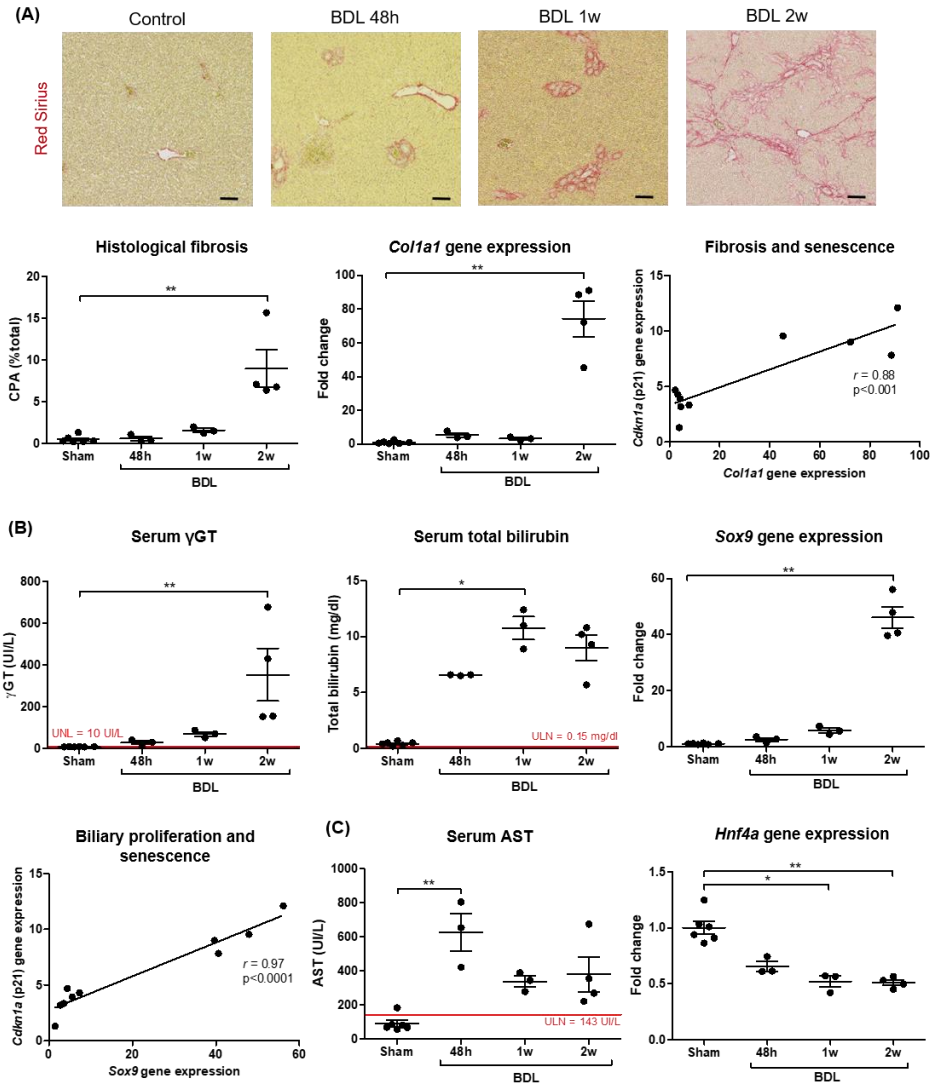

Supplementary Figure 6. Liver disease is correlated to senescence progression in BDL. (A) Liver fibrosis increases post-BDL and correlates with senescence progression. (B) Biliary damage (serum γGT) and proliferation (*Sox9)* increase in BDL rats and biliary proliferation correlates with senescence progression. (C) Serum AST maximal increase occurs 48 hours post-BDL and is followed by a loss of hepatocytes mass *(Hnf4a)*. BDL: bile duct ligation; CPA: collagen proportionate area; 48h – 1w – 2w : rats sacrificed 48 hours (n=3) – 1 week (n=3) – 2 weeks (n=4) after BDL surgery. Data is presented as mean ± SEM; *p≤0.05; **p<0.01. Scale bars = 100µm.

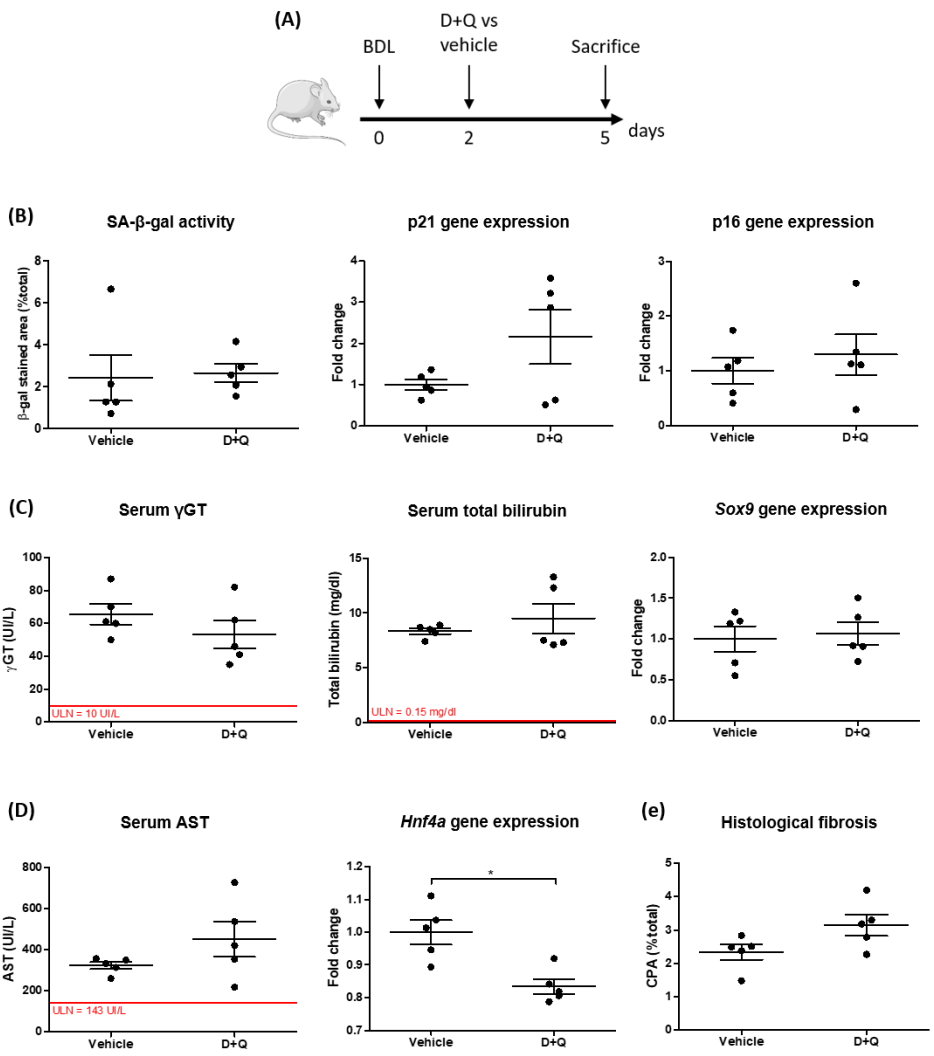

Supplementary Figure 7. D+Q administration in BDL rats. (A) Operated rats received D (5 mg/kg) + Q (50 mg/kg) by oral gavage (n=5) 48 hours after BDL and were compared to controls that received the vehicle (50% PEG400; n=5). (B) D+Q had no effect on liver senescence. (C) D+Q had no effect on biliary injury (serum γGT) and proliferation (*Sox9*) nor on biochemical cholestasis (serum total bilirubin). (D-E) D+Q worsened the hepatocytes mass loss *(Hnf4a)* and had no significant effect on hepatocytes injury (serum AST) nor on liver histological fibrosis. BDL: bile duct ligation; D: dasatinib: Q: quercetin; SA-β-gal: senescence-associated β-galactosidase; ULN: upper limit of normal. Data is presented as mean ± SEM; *p≤0.05.

Chapter 4: repeated senotherapeutics administration in a preclinical model of biliary cirrhosis

Introduction

In the previous chapter, we obtained encouraging results regarding the short-term HALPC effect on liver senescence and disease in the BDL model of biliary cirrhosis. Unexpectedly, the well-described senolytic combination D+Q did not have any beneficial on liver senescence and even seemed to worsen liver disease. Since liver senescence and disease progressively worsen in the BDL model, we hypothesized that more differences could be evidenced regarding the effect of HALPC or D+Q on liver senescence and disease in a longer experiment. In particular, we aimed at evidencing a potential effect of those treatments on markers of established senescence (such as p16 or SA-β-gal activity) that were not modified in the short-term experiment, and on liver fibrosis. In this chapter, we report the results obtained after repeated administrations of HALPC or D+Q in animals that were sacrificed two weeks after the BDL surgery.

Materials and methods

Methods were similar to Chapter 3 except for the fact that all the animals in the HALPC group were injected with 1.25 x 10^6 cell/kg. The effects of HALPC were comparable for low (1.25 x 10^6 cell/kg) and high (12.5 x 10^6 cell/kg) doses in previous experiments, which encouraged us select the low dose for further

experiments to avoid unnecessary side effects. D+Q regimens were unchanged (D 5 mg/kg and Q 50 mg/kg) as this combination is the best described in the literature in rats and in liver disease (1, 2). Of note, the HALPC donor was different as compared to the previous experiment (8 months old male donor versus 4 months old male donor in the previous experiment). The design of the experiment is presented in Figure 1. Repeated administrations of HALPC were performed because HALPC were not detected at 72 hours in liver homogenates in the previous experiment, probably due to the rapid clearance of human cells by the immune system of the rats in the absence of immunosuppression (data not shown). Repeated administrations were also selected for D+Q to perform a "hit and run" approach that would allow to remove senescent cells at multiple timepoints while limiting the side effects (3).

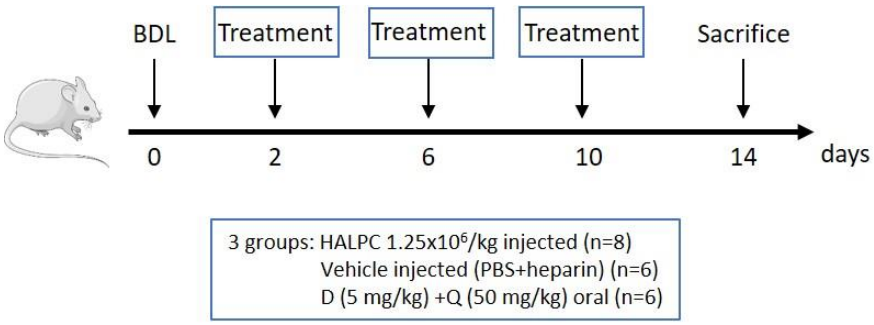

Figure 1. Design of the experiment. Operated rats received repeated administrations of HALPC (n=8) vs D+Q (n=6) vs vehicle (n=6) and were sacrificed 14 days after the BDL surgery. BDL: bile duct ligation; D: dasatinib; HALPC: human allogenic liver-derived progenitor cells; Q: quercetin.

Results

Repeated administrations of HALPC and D+Q did not have any effect on established senescence and SASP in the BDL model

Neither HALPC nor D+Q displayed an effect on liver senescence and SASP in the BDL model when the animals were sacrificed 14 days after the surgery (Figure 2).

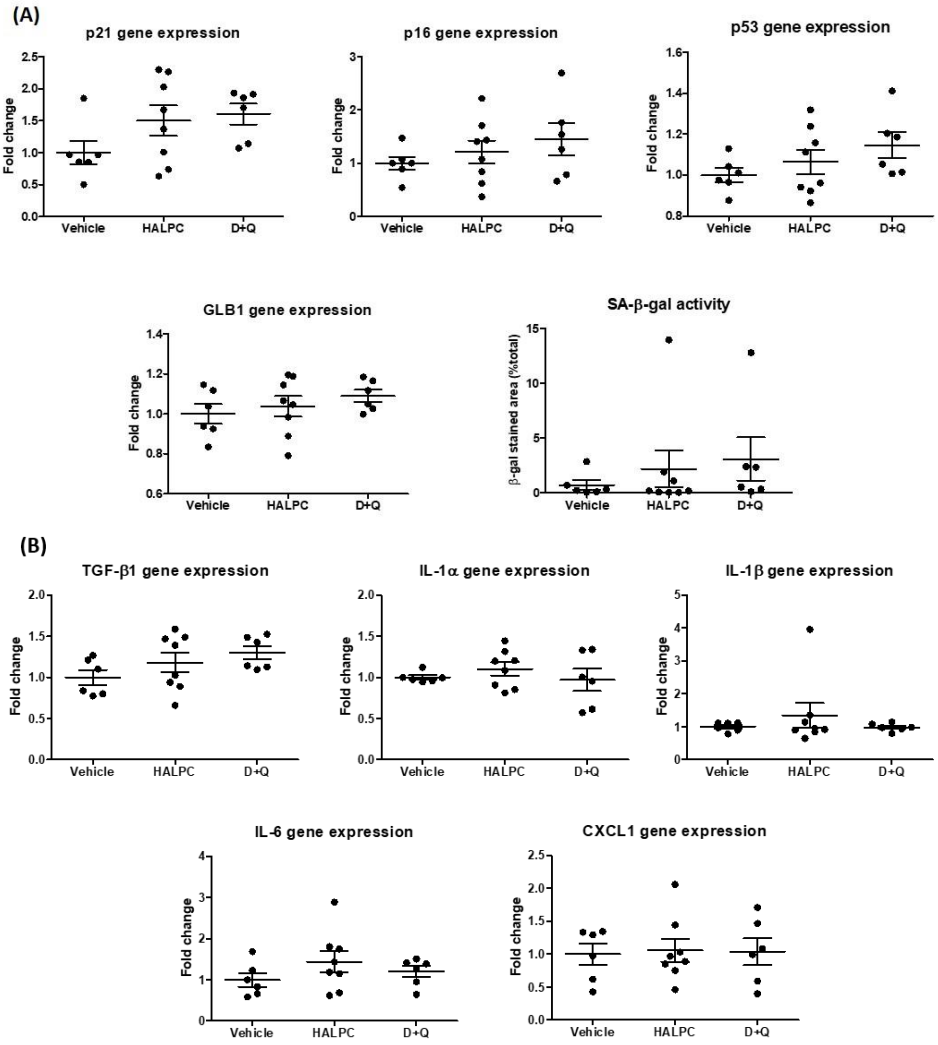

Figure 2. Effect of HALPC and D+Q on liver senescence and SASP in rats sacrificed 14 days after the BDL surgery. (A) HALPC and D+Q did not have any effect on senescence compared to animals that received the vehicle as demonstrated by p21, p16, p53 and GLB1 gene expression in liver homogenates and by SA-β-gal activity. (B) HALPC and D+Q did not have any effect on the SASP compared to the vehicle as demonstrated by TGF-β1, IL-1α, IL1-β, IL-6 and CXCL1 gene expression in liver homogenates. BDL: bile duct ligation; D: dasatinib; HALPC: human allogenic liver-derived progenitor cells; Q: quercetin; SA-β-gal: senescence-associated β-galactosidase. Data is presented as mean ± SEM.

Repeated administrations of HALPC and D+Q did not improve liver disease in the BDL model

Biochemical parameters of the animals did not improve with HALPC or D+Q administrations as compared to the vehicle (Figure 3).

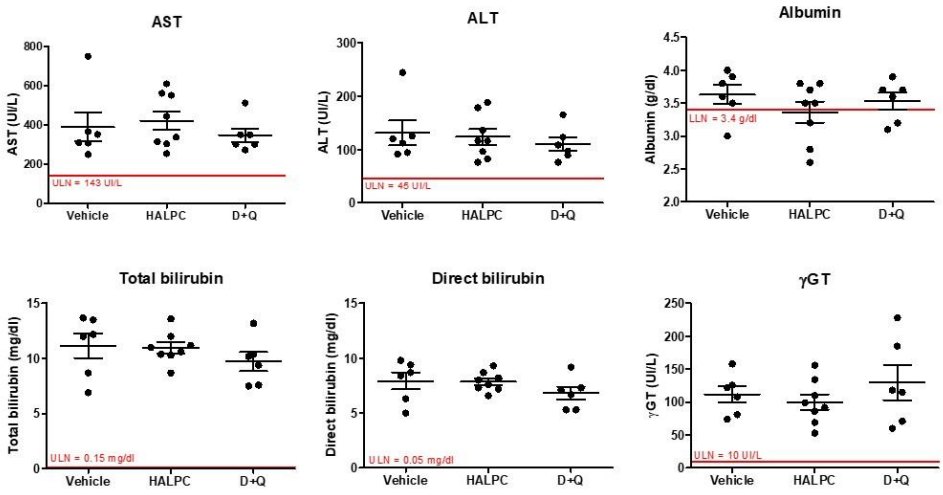

Figure 3. Effect of HALPC and D+Q on biochemical parameters of BDL rats sacrificed 14 days after the surgery. Neither HALPC nor D+Q had any effect on serum AST, ALT, albumin, bilirubin (total and direct) and γGT as compared to the vehicle. γGT: gamma-glutamyl transferase; ALT: alanine transaminase; AST: aspartate transaminase; D: dasatinib; HALPC: human allogenic liver-derived progenitor cells; LLN: lower limit of normal; Q: quercetin; ULN: upper limit of normal. Data is presented as mean ± SEM.

Treatment with HALPC or D+Q did not improve liver disease as well in respect of the results obtained on liver homogenates and liver sections (Figure 4). D+Q even tended to increase biliary proliferation (SOX-9 gene and protein expression) and significantly worsened histological liver fibrosis as compared to HALPC (Figure 4).

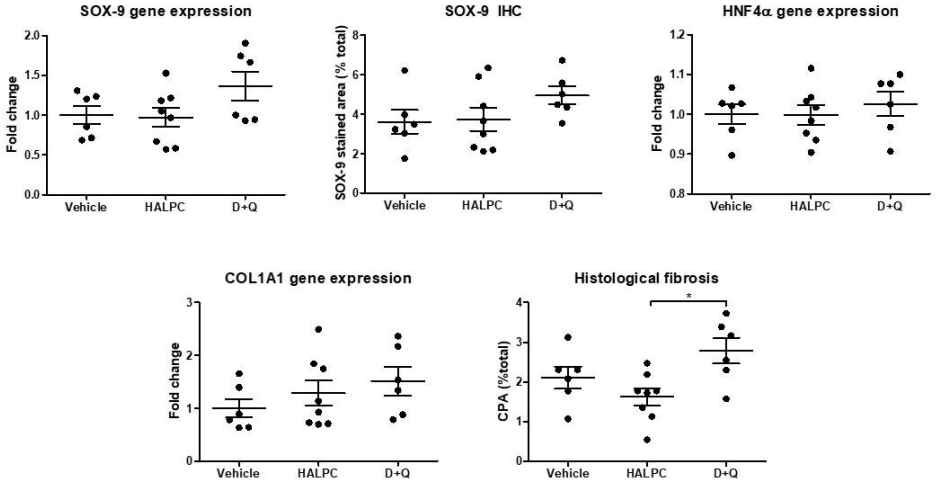

Figure 4. Effect of HALPC and D+Q on liver disease in BDL rats sacrificed 14 days after the surgery. HALPC and D+Q did not have any effect on biliary proliferation (SOX-9 gene and protein expression), hepatocytes mass (HNF4α gene expression) and liver fibrosis (COL1A1 gene expression and histological fibrosis) as compared to the vehicle. CPA: collagen proportionate area; D: dasatinib; HALPC: human allogenic liver-derived progenitor cells; Q: quercetin. Data is presented as mean ± SEM; $p<0.05$.

Discussion

Neither HALPC nor D+Q displayed any beneficial effect on liver senescence and disease in this prolonged experiment with repeated treatments. D+Q even worsened histological liver fibrosis with regard to HALPC. No specific control for D+Q was included in this experiment as the vehicle injected was HALPC vehicle only due to technical considerations, but this result is in line with previous study underlying the potential deleterious effect of removing senescent cells without targeting a specific cell-type (4). The encouraging effects obtained on liver senescence and disease 72 hours after a single HALPC administration in BDL rats were not confirmed in rats that were sacrificed 14 days after the surgery and received HALPC three times. This might have been related to the complete and irreversible mechanical damage induced on the extrahepatic biliary tract in the BDL model, causing a level of disease that could be too severe to observe any improvement related to therapeutic interventions. In this context, the use of milder preclinical models of BA as for example the reassortant RRV mice model might be an interesting option (5). However, the low survival rate at 14 days (less than 50%) and the lack of systematic fibrotic evolution would make the long-term assessment of liver senescence and disease evolution very challenging in this model as well. Of note, the change of HALPC donor might also have participated in the different results observed in the short-term versus long-term experiments.

HALPC anti-senescence properties will have to be validated in a model of advanced biliary senescence before considering to use them as senotherapeutics in clinical application. This generates a need for preclinical models of biliary senescence that would be severe enough to benefit from senotherapies, but with a slow progression that would better mimic BA and potentially allow to obtain a proof of efficacy regarding senotherapeutic interventions. Since such BA models do not exist for the

moment to our knowledge, other models of hepatobiliary senescence will have to be investigated and developed in the future.

Acknowledgements

Many thanks to Eliano Bonaccorsi for operating the rats and performing cell injections and oral gavages. We also thank Jonathan Evraerts and Joachim Ravau for their technical assistance.

References

1. Krzystyniak A, Wesierska M, Petrazzo G, Gadecka A, Dudkowska M, Bielak-Zmijewska A, et al. Combination of dasatinib and quercetin improves cognitive abilities in aged male Wistar rats, alleviates inflammation and changes hippocampal synaptic plasticity and histone H3 methylation profile. Aging (Albany NY). 2022;14(2):572-95.
2. Ogrodnik M, Miwa S, Tchkonia T, Tiniakos D, Wilson CL, Lahat A, et al. Cellular senescence drives age-dependent hepatic steatosis. Nat Commun. 2017;8:15691.
3. Gasek NS, Kuchel GA, Kirkland JL, Xu M. Strategies for Targeting Senescent Cells in Human Disease. Nat Aging. 2021;1(10):870-9.
4. Grosse L, Wagner N, Emelyanov A, Molina C, Lacas-Gervais S, Wagner KD, et al. Defined p16(High) Senescent Cell Types Are Indispensable for Mouse Healthspan. Cell Metab. 2020;32(1):87-99 e6.
5. Mohanty SK, Lobeck I, Donnelly B, Dupree P, Walther A, Mowery S, et al. Rotavirus Reassortant-Induced Murine Model of Liver Fibrosis Parallels Human Biliary Atresia. Hepatology. 2020;71(4):1316-30.

Chapter 5: Alagille syndrome livers display premature senescence

Giulia Jannone[1], Catherine de Magnée[2], Roberto Tambucci[2], Jonathan Evraerts[1], Joachim Ravau[1], Mustapha Najimi[1], Etienne Marc Sokal[1]

[1]Pediatric Hepatology and Cell Therapy Unit, Institut de Recherche Expérimentale et Clinique, UCLouvain, Brussels, Belgium
[2]Pediatric Surgery and Transplantation Unit, Department of Surgery, Cliniques Universitaires Saint-Luc, UCLouvain, Brussels, Belgium

This work was submitted for publication

Summary

Introduction: Alagille syndrome (ALGS) is an autosomal dominant disease characterized by a multisystem involvement including bile duct paucity and cholestasis, and caused by *JAG1* or *NOTCH2* mutations in most of the cases. Jagged1-Notch2 interactions are known to be crucial for intrahepatic biliary tract development, but the Notch signaling pathway is also involved in the juxtacrine transmission of senescence and in the induction and modulation of the senescence-associated secretory phenotype (SASP).

Aim: Our aim was to investigate premature senescence in ALGS liver to better understand the involvement of Notch in senescence and SASP development.

Methods: Liver tissue from ALGS patients was prospectively obtained at the time of liver transplantation (n=5) and compared to control livers (n=5).

Results: We evidenced advanced premature senescence in the livers of five *JAG1* mutated ALGS pediatric patients through increased senescence-associated beta-galactosidase activity ($p<0.05$), increased p16 and p21 gene expression ($p<0.01$),

and increased p16 and γH2AX protein expression ($p<0.01$). Senescence was located in hepatocytes of the whole liver parenchyma as well as in remaining bile ducts. The classical SASP markers TGF-β1, IL-6, and IL-8 were not overexpressed in the livers of our patients, but other SASP markers were upregulated in ALGS livers in a published RNA sequencing dataset.

Conclusions: We demonstrate for the first time that ALGS livers display important premature senescence despite Jagged1 mutation, underlying the complexity of senescence and SASP development pathways.

Introduction

Alagille syndrome (ALGS) is an autosomal dominant disease characterized by a multisystem involvement including bile duct paucity and cholestasis. The penetrance is highly variable and clinical manifestations can also consist in cardiovascular defects, renal anomalies, characteristic facial features, vertebral arch/other skeletal defects and ocular features (typically posterior embryotoxon) (1). In the presence of ALGS-related initial cholestasis, more than 75% of the patients need a liver transplantation before the age of 18 years (2). A mutation in *JAG1*, which encodes the protein Jagged1, explains the phenotype in more than 90% of the cases. *NOTCH2* mutations are found in up to 4% of the patients in the absence of *JAG1* anomalies (2, 3). Jagged1-Notch2 interactions are known to be crucial for intrahepatic biliary tract development (4). The Notch signaling pathway also demonstrated to have major effects in senescence induction and propagation, especially through Notch1 (5). Jagged1-Notch1 interactions induce a juxtacrine transmission of senescence and Notch1 mediates a switch between TGF-β-rich secretome and pro-inflammatory secretome during senescence (6). Activation of Notch2 also induced premature senescence in vitro in human primary endothelial

cells (7). It was therefore relevant to investigate the presence of premature senescence and senescence-associated secretory phenotype (SASP) in ALGS livers.

Materials and methods

Liver samples

Five patients with genetically confirmed ALGS who underwent liver transplantation were prospectively recruited in the Pediatric Gastroenterology and Hepatology Unit of Cliniques Universitaires Saint-Luc between 2018 and 2022. A fragment of the explanted liver was collected during the surgery and biochemical data were obtained the day before the procedure. Five control liver fragments were provided by the Cliniques Universitaires Saint-Luc biobank when consent for research purposes was given. One control liver fragment was obtained from an explanted liver during liver transplantation for hyperoxaluria type 1 (metabolic defect in a structurally healthy liver), while the four others were obtained from diseased donors when no compatible organ receiver was identified. Biochemical data was not available for control patients. This project was approved by the Ethics Committee of Cliniques Universitaires Saint-Luc (registration number B403201938739). Written informed consent was obtained for all study participants.

Senescence-associated β-galactosidase activity assay

Senescence-associated β-galactosidase (SA-β-gal) activity assay was performed on cryopreserved liver tissue at pH 4 for one hour (37C) as previously described (8). Stained sections were washed with PBS before performing immunohistochemical staining when indicated.

Immunohistochemistry

Five µm formalin-fixed paraffin-embedded (FFPE) liver sections were deparaffinized and rehydrated in xylene and graded alcohol series. After a 1 hour blocking step in 5% BSA (Merck, Darmstadt, Germany) ± 5% normal goat serum (Thermo Fisher Scientific, Waltham, MA, USA), sections were incubated at 37C with primary antibody for 1 hour (Supplementary Table 1) followed by species-specific secondary antibodies incubation (Dako EnVision+ System HRP; Agilent, Santa Clara, CA, USA) and 3,3'-diaminobenzidine (DAB) chromogen detection. Digital quantification of staining was assessed on x20 magnification scanned sections by using the image analysis tool Author version 2017.2 (Visiopharm, Hørsholm, Denmark) as previously described (8).

Reverse transcription quantitative polymerase chain reaction

Liver homogenates were obtained from liver biopsies with the FastPrep-24 Classic Instrument (MP Biomedicals, Irvine, CA, USA). Total RNA was extracted from liver homogenates using Tripure isolation reagent (Roche, Basel, Switzerland) and retro-transcribed using the high-capacity cDNA reverse transcription kit (Applied Biosystems, Waltham, CA, USA). Quantitative PCR was carried out in duplicate using TaqMan universal MasterMix (Applied Biosystems) and pre-designed TaqMan probes (Supplementary Table 2). Relative gene expression was determined with the ΔΔCt method using *TBP* and *PPIA* as housekeeping genes (9).

Statistical analysis

Statistical analysis was conducted using Graphpad Prism 5.0 (GraphPad Software, La Jolla, CA, USA). Continuous variables were presented as mean ± standard deviation (SD). The non-parametric Mann-Whitney U test was used to compare

continuous variables between subgroups. A two-tailed p-value < 0.05 was considered to indicate statistical significance for all analysis.

Results

Description of the study population is presented in Table 1. All the ALGS patients were transplanted at a pediatric age, while 2/5 controls were adults. All control livers were structurally normal (no inflammation nor fibrosis). A heterozygous mutation of *JAG1* was evidenced in all ALGS patients. Two ALGS patients were transplanted for end-stage liver disease with cirrhosis and portal hypertension, and three patients were transplanted due to poor quality of life mainly related to pruritus and jaundice, in the absence of established cirrhosis (Metavir F2-F3). Advanced premature senescence was evidenced in ALGS livers as demonstrated by an increase in p16 and γH2AX protein expression, as well as an increase in p16 and p21 gene expression (Figs 1 and 2A). Gene expression of the SASP-associated markers TGF-β1, IL-6 and IL-8 was not increased in ALGS livers (Fig 2B). One ALGS patient (patient number 5) had markedly increased liver gene expression of those three SASP markers, but we could not evidence any relevant clinical, biochemical or histological differences in this patient as compared to the four others except for the presence of hypoalbuminemia and marked hyperbilirubinemia (Table 1).

	Alagille syndrome				
	Patient 1	**Patient 2**	**Patient 3**	**Patient 4**	**Patient 5**
Age (years)	1	11	4	5	5
Gender	F	F	M	F	M
AST (UI/L) (< 80)	196	321	326	325	757
ALT (UI/L) (< 35)	153	381	394	235	242
γGT (UI/L) (< 40)	335	460	692	131	133
Total bilirubin (mg/dL) (< 1.2)	14.8	1.4	15.6	25.4	36.3
Albumin (g/L) (>34)	38	43	45	38	29
INR (0.8-1.2)	1.01	1.01	1.12	1.4	1.58
Histological fibrosis (Metavir)	F2	F2	F3	F4	F4
Liver transplant indication	Quality of life	Quality of life	Quality of life	End-stage liver disease	End-stage liver disease
JAG1 mutation	c.551G>A / p.(Arg184His)	c.550C>T / p.(Arg184Cys)	c.2122_2125del, p.(Gln708Valfs*34)	c.2455A>G (p.Ile819Val)	c.886+1G>A
Other anomalies:					
Heart	No	Yes	Yes	Yes	Yes
Kidneys	No	No	Yes	Yes	Yes
Vertebral	No	No	Yes	Yes	Yes
Ophtalmic	No	Yes	Yes	No	No
Typical facies	Yes	Yes	Yes	Yes	Yes
	Controls				
	Control 1	**Control 2**	**Control 3**	**Control 4**	**Control 5**
Age (years)	4	28	0	15	41
Gender	M	F	M	M	F
Histological fibrosis (Metavir)	F0	F0	F0	F0	F0
Liver transplant indication	/	/	/	Hyperoxaluria type 1	/
Cause of death	Status epilepticus	Motor vehicle accident	Neonatal asphyxia	/	Hemorragic stroke

Table 1. Description of the study population. Standard values are indicated for all biochemical parameters.

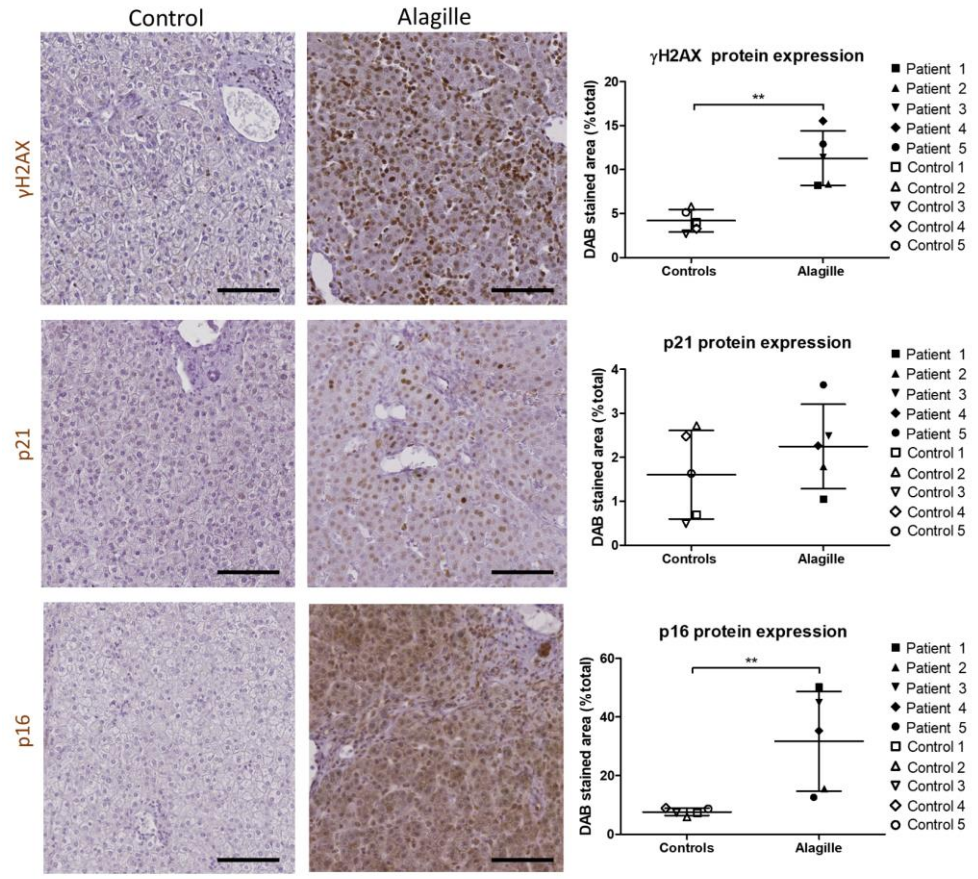

Fig 1. Protein expression of senescence markers in ALGS livers. Protein expression of γH2AX and p16 increases in ALGS as compared to controls. No significant change is observed regarding p21 protein expression. ALGS: Alagille syndrome; DAB: 3,3'-diaminobenzidine. Data is presented as mean ± SD; **p<0.01. Scale bars = 100 µm.

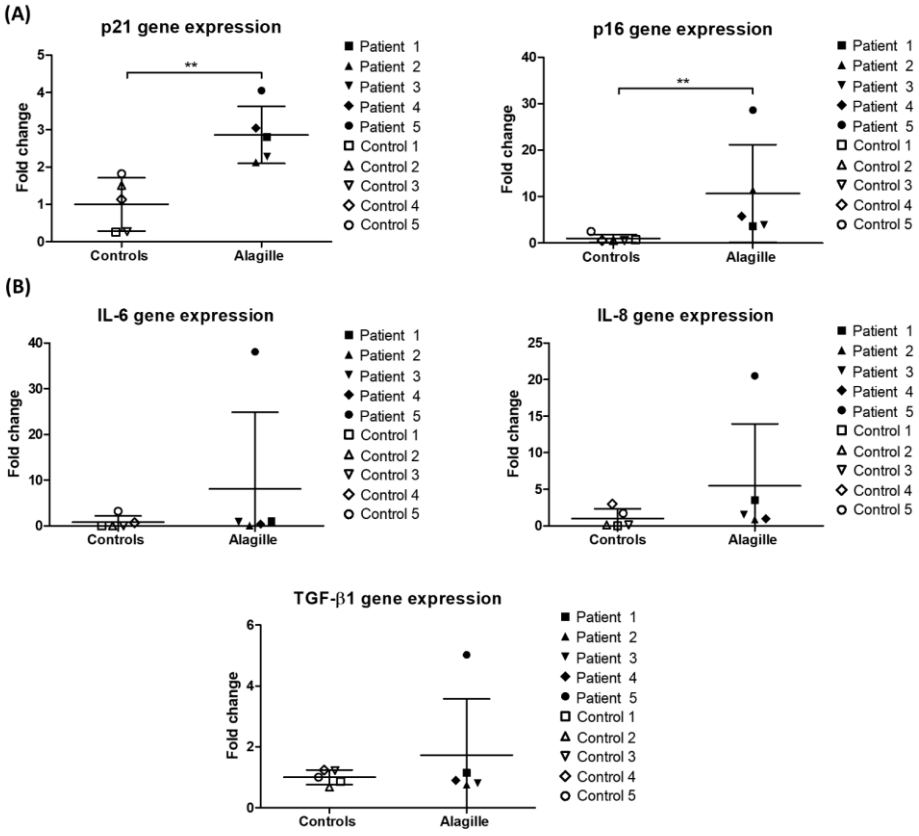

Fig 2. Gene expression of senescence and SASP markers in ALGS livers. (A) Gene expression of p21 and p16 increases in ALGS livers. (B) Gene expression of SASP markers TGF-β1, IL-6 and IL-8 is unchanged in ALGS livers. ALGS: Alagille syndrome; SASP: senescence-associated secretory phenotype. Data is presented as mean ± SD; **p<0.01.

SA-β-gal activity confirmed the presence of senescence in ALGS livers and co-staining of SA-β-gal activity and CK-19 immunohistochemistry located senescence in the whole liver parenchyma and pointed out the disappearance of bile ducts in ALGS livers (Figs 3A and 3B). However, remaining bile ducts were senescent as well as demonstrated by serial staining of p16 and CK-19 (Fig 3C). Of note, levels of senescence appeared comparable between adult and pediatric control livers, as

expected since cholangiocytes and hepatocytes do not suffer from telomere shortening and replicative senescence in physiological conditions (Figs 1-3) (10).

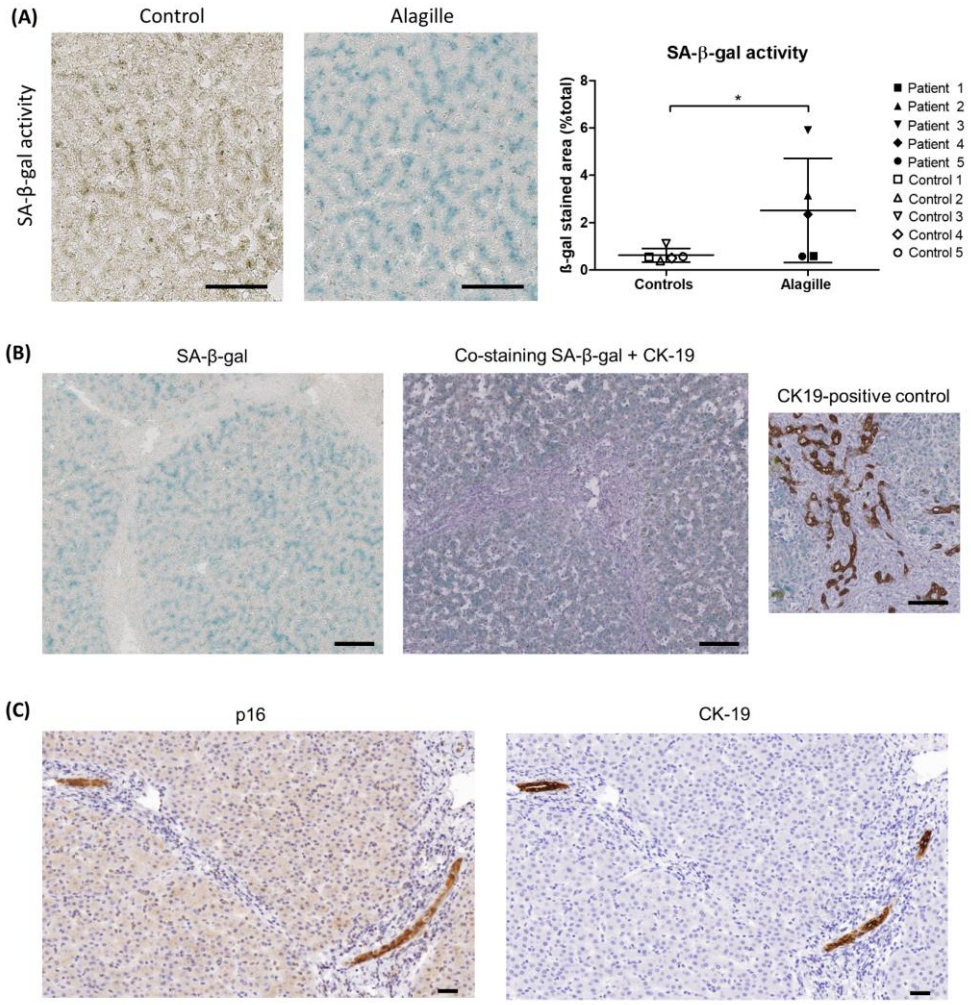

Fig 3. Senescence localization in ALGS livers. (A) SA-β-gal activity increases in ALGS livers as compared to controls. (B) Co-staining of SA-β-gal activity and CK-19 IHC shows senescence in the whole liver parenchyma of ALGS livers, with disappearance of intrahepatic bile ducts as demonstrated by the absence of CK-19 staining on this liver section. (C) Serial IHC staining of p16 and CK-19 evidences senescence in the remaining bile ducts of ALGS livers. ALGS: Alagille syndrome; IHC: immunohistochemistry; SA-β-gal: senescence-associated beta-galactosidase. Data is presented as mean ± SD; *p<0.05. Scale bars = 100 µm.

Finally, we investigated the expression of senescence and SASP-related genes in a published RNA sequencing dataset obtained from pediatric ALGS (n=5) and cholestatic (n=2)/non-cholestatic (n=2) control livers (GSE104873) (11). We only considered the results of the differential expression analysis comparing ALGS to non-cholestatic controls since oxidative stress due to bile acids accumulation can *per se* lead to premature senescence in cholestatic diseases (12). Also, ALGS and cholestatic livers clustered together in the principal component analysis of the study and were distinct from the transcriptomes of the two non-cholestatic controls suffering from autoimmune hepatitis (11). Amongst the 370 genes that were upregulated in the differential expression analysis of ALGS livers versus non-cholestatic controls, 14 genes were previously described as SASP components, including *CXCL8* (IL-8) (Table 2) (13-15). Only 2/5 ALGS patients had a marked upregulation of all the 14 SASP-related genes. *CDKN1A* (p21), *CDKN2A* (p16), *TGFB1* (TGF-β1) and *IL6* (IL-6) were not significantly upregulated in the differential expression analysis, but seemed overexpressed in some ALGS patients when the detailed database was investigated. Those observations underlie the heterogeneity of senescence and SASP-related transcriptomes in ALGS patients.

Gene	LogFC	*p*-value
CXCL8	7.06	2.99×10^{-15}
CCL20	6.65	3.22×10^{-11}
CCL3	4.04	7.8×10^{-5}
PDGFA	3.75	1.91×10^{-11}
IGFBP1	3.2	1.51×10^{-7}
PLAU	3.12	6.3×10^{-4}
LIF	3.08	1.1×10^{-3}
CCL2	3.07	1.84×10^{-4}
IL32	3.05	9.56×10^{-7}
MMP2	2.96	8.69×10^{-6}
PLAUR	2.7	1.12×10^{-3}
TIMP1	1.9	5.83×10^{-4}
ICAM1	1.87	4.18×10^{-4}
MMP14	1.45	3.09×10^{-3}

Table 2. SASP-related genes upregulated in ALGS livers versus non-cholestatic controls. This table was extracted from the differential expression analysis of a published RNA sequencing dataset (11). SASP genes were identified based on existing literature (13-15). ALGS: Alagille syndrome; FC: fold change; SASP: senescence-associated secretory phenotype.

Discussion

Our results demonstrate for the first time that ALGS livers display advanced premature senescence from early life. Senescence is located in the whole liver parenchyma, and predominates in hepatocytes in the presence of a major intrahepatic ductular paucity inherent to the disease. Our observations are in line with the increased SA-β-gal activity that was evidenced in livers from jag1b/2b mutants zebrafish (jag1b$^{-/-}$; jag2b$^{-/-}$), in which the developmental loss of intrahepatic cholangiocytes and the subsequent cholestasis of ALGS are phenocopied (16). Due to Jagged1 mutation, a reduction of the juxtacrine transmission of senescence mediated by Jagged1-Notch1 interactions would be expected in ALGS (6). Jagged1 deficiency might also affect the transient increase in Notch1 and in the active Notch1 intracellular domain (N1ICD) necessary to induce

the TGF-β1-rich primary SASP, TGF-β being an important promotor of the paracrine transmission of senescence in liver disease (6, 17, 18). This transient increase is normally followed by N1ICD downregulation, which allows the production of a pro-inflammatory SASP containing inflammatory cytokines such as IL-6 and IL-8 through the de-repression of C/EBPβ (5). The SASP markers TGF-β1, IL-6 and IL-8 were not overexpressed in ALGS livers in our cohort – except for one patient – and TGF-β1 was not differentially expressed in ALGS versus control livers in a published RNA sequencing dataset (11). Jagged1/Notch/TGF-β-independent mechanisms thus lead to the important premature senescence that we observe in ALGS livers, in the absence of the classically described mechanisms of juxtacrine and paracrine transmission of senescence. However, other SASP components promoting the paracrine transmission of senescence such as CCL2 and CCL20 were upregulated in ALGS livers RNA sequencing dataset, underlying the fact that other senescence pathways might compensate the abnormal Notch signaling (11, 19, 20). Also, we observed an important interpatient variability regarding the expression of senescence and SASP-related genes in our cohort and in a published dataset about ALGS livers. The senescence and SASP profiles can vary widely according to the cell type and senescence-inducing stress, but the interpatient variability that we observed could also be related to the high phenotypic variability inherent to ALGS (15). Finally, senescence markers were expressed to various extent within one patient, corroborating the fact that a combination of markers is required to confirm the senescent phenotype (21). Further studies will be needed to deeply investigate pathways involved in senescence and SASP regulation, especially since the number of patients included in this preliminary study was very small with high interpatient variability. In particular, comparing *JAG1*- and *NOTCH2*-mutated ALGS livers could be of high interest to discriminate Notch1 and Notch2 involvement in senescence and SASP. In conclusion, ALGS livers display important premature senescence

despite Jagged1 mutation, underlying the complexity of senescence and SASP development pathways.

Acknowledgements

We thank the IREC 2IP platform for the use of laboratory facilities, and especially Caroline Bouzin for designing the Visiopharm APPs necessary for the digital quantification of histological staining. Giulia Jannone, Catherine de Magnée, Roberto Tambucci and Etienne Sokal are members of the European Reference Networks Rare-Liver and/or TransplantChild.

References

1. Ayoub MD, Kamath BM. Alagille Syndrome: Diagnostic Challenges and Advances in Management. Diagnostics (Basel). 2020;10(11).
2. Kamath BM, Ye W, Goodrich NP, Loomes KM, Romero R, Heubi JE, et al. Outcomes of Childhood Cholestasis in Alagille Syndrome: Results of a Multicenter Observational Study. Hepatol Commun. 2020;4(3):387-98.
3. Gilbert MA, Bauer RC, Rajagopalan R, Grochowski CM, Chao G, McEldrew D, et al. Alagille syndrome mutation update: Comprehensive overview of JAG1 and NOTCH2 mutation frequencies and insight into missense variant classification. Hum Mutat. 2019;40(12):2197-220.
4. Lemaigre FP. Development of the Intrahepatic and Extrahepatic Biliary Tract: A Framework for Understanding Congenital Diseases. Annu Rev Pathol. 2020;15:1-22.
5. Ito Y, Hoare M, Narita M. Spatial and Temporal Control of Senescence. Trends Cell Biol. 2017;27(11):820-32.
6. Hoare M, Ito Y, Kang TW, Weekes MP, Matheson NJ, Patten DA, et al. NOTCH1 mediates a switch between two distinct secretomes during senescence. Nat Cell Biol. 2016;18(9):979-92.
7. Venkatesh D, Fredette N, Rostama B, Tang Y, Vary CP, Liaw L, et al. RhoA-mediated signaling in Notch-induced senescence-like growth arrest and endothelial barrier dysfunction. Arterioscler Thromb Vasc Biol. 2011;31(4):876-82.
8. Jannone G, Rozzi M, Najimi M, Decottignies A, Sokal EM. An Optimized Protocol for Histochemical Detection of Senescence-associated Beta-galactosidase Activity in Cryopreserved Liver Tissue. J Histochem Cytochem. 2020:22155420913534.

9. Livak KJ, Schmittgen TD. Analysis of relative gene expression data using real-time quantitative PCR and the 2(-Delta Delta C(T)) Method. Methods. 2001;25(4):402-8.
10. Verma S, Tachtatzis P, Penrhyn-Lowe S, Scarpini C, Jurk D, Von Zglinicki T, et al. Sustained telomere length in hepatocytes and cholangiocytes with increasing age in normal liver. Hepatology. 2012;56(4):1510-20.
11. Andersson ER, Chivukula IV, Hankeova S, Sjoqvist M, Tsoi YL, Ramskold D, et al. Mouse Model of Alagille Syndrome and Mechanisms of Jagged1 Missense Mutations. Gastroenterology. 2018;154(4):1080-95.
12. Meadows V, Baiocchi L, Kundu D, Sato K, Fuentes Y, Wu C, et al. Biliary Epithelial Senescence in Liver Disease: There Will Be SASP. Front Mol Biosci. 2021;8:803098.
13. Freund A, Orjalo AV, Desprez PY, Campisi J. Inflammatory networks during cellular senescence: causes and consequences. Trends Mol Med. 2010;16(5):238-46.
14. Irvine KM, Skoien R, Bokil NJ, Melino M, Thomas GP, Loo D, et al. Senescent human hepatocytes express a unique secretory phenotype and promote macrophage migration. World J Gastroenterol. 2014;20(47):17851-62.
15. Hernandez-Segura A, de Jong TV, Melov S, Guryev V, Campisi J, Demaria M. Unmasking Transcriptional Heterogeneity in Senescent Cells. Curr Biol. 2017;27(17):2652-60 e4.
16. Zhao C, Lancman JJ, Yang Y, Gates KP, Cao D, Barske L, et al. Intrahepatic cholangiocyte regeneration from an Fgf-dependent extrahepatic progenitor niche in a zebrafish model of Alagille Syndrome. Hepatology. 2022;75(3):567-83.
17. Bird TG, Muller M, Boulter L, Vincent DF, Ridgway RA, Lopez-Guadamillas E, et al. TGFbeta inhibition restores a regenerative response in acute liver injury by suppressing paracrine senescence. Sci Transl Med. 2018;10(454).
18. Ferreira-Gonzalez S, Lu WY, Raven A, Dwyer B, Man TY, O'Duibhir E, et al. Paracrine cellular senescence exacerbates biliary injury and impairs regeneration. Nat Commun. 2018;9(1):1020.
19. Acosta JC, Banito A, Wuestefeld T, Georgilis A, Janich P, Morton JP, et al. A complex secretory program orchestrated by the inflammasome controls paracrine senescence. Nat Cell Biol. 2013;15(8):978-90.
20. Sasaki M, Miyakoshi M, Sato Y, Nakanuma Y. Modulation of the microenvironment by senescent biliary epithelial cells may be involved in the pathogenesis of primary biliary cirrhosis. J Hepatol. 2010;53(2):318-25.
21. Gorgoulis V, Adams PD, Alimonti A, Bennett DC, Bischof O, Bishop C, et al. Cellular Senescence: Defining a Path Forward. Cell. 2019;179(4):813-27.

Supplementary tables

Primary antibody	Company	Cat. No	Species	Ag retrieval	Dilution
p21 WAF1/Cip1	Agilent	M7202	M mAb	T 1 hour 98C	IHC 1/400
p16 INK4a	Abcam	ab108349	Rb mAb	T 1 hour 98C	IHC 1/1000
gamma H2A.X (Ser139)	Abcam	ab81299	Rb mAb	C 35 min 98C	IHC 1/500
CK19	Dako	M0888	M mAb	C 35 min 98C	IHC 1/100

Supplementary Table 1. Primary antibodies. Ag: antigen; C: citrate; M: mouse; mAb: monoclonal antibody; pAb: polyclonal antibody; Rb: rabbit; T: Tris-EDTA.

Gene of interest	Company	Reference
CDKN1A	Thermo Fisher Scientific	Hs00355782_m1
CDKN2A	Thermo Fisher Scientific	Hs00923894_m1
IL6	IDT	Hs.PT.58.40226675
CXCL8	IDT	Hs.PT.58.38869678.g
TGFB1	IDT	Hs.PT.58.39813975

Supplementary Table 2. Pre-designed TaqMan probes used for reverse transcription quantitative polymerase chain reaction.

Chapter 6: general discussion and conclusions

Discussion

Cholestatic liver diseases – and especially BA – are the first cause of liver transplantation in the pediatric population since there are currently no alternatives to this heavy procedure in case of end-stage liver disease (1). It is now well established that premature liver senescence occurs in adult chronic hepatobiliary diseases and worsens the prognosis by aggravating liver tissue remodeling and hepatic dysfunction (2-4). Some evidence suggests that premature senescence also occurs in pediatric BA livers, but no study ever investigated the possibility of using anti-senescence therapies in pediatric biliary cirrhosis (5-7). In this context, our aim was to investigate premature senescence and SASP in pediatric biliary cirrhosis and to test senotherapeutics that could be translated to clinical applications in a preclinical model of biliary cirrhosis.

We demonstrated that premature senescence occurs in BA and ALGS livers, two main causes of pediatric end-stage liver disease due to chronic cholestasis. BA livers displayed advanced premature senescence already at diagnosis, but senescence continued to progress until liver transplantation, underlying the potential interest of developing anti-senescence therapies to limit the worsening of the disease related to senescence. HALPC decreased the early marker of senescence p21 and improved liver disease in the BDL preclinical model of biliary senescence, providing promising results regarding the use of senotherapeutics in biliary cirrhosis. HALPC were tested as senotherapeutics because other MSC types demonstrated to have

anti-senescence properties in other organs, but those cells have well-described anti-inflammatory, anti-fibrotic and pro-regenerative paracrine properties that could have participated to the observed disease improvement (8-10). Also, the anti-senescence properties of HALPC observed on the early marker of senescence p21 will have to be confirmed on established senescence markers before considering HALPC as true senotherapeutics. Therapies that specifically target senescent cells and thereby improve established senescence and liver disease will need to proof their efficacy before considering to translate senotherapeutics to pediatric biliary cirrhosis.

The first step of the project was to develop an easy and reproducible test to detect senescence on human and rat liver tissue. In order to do that, we adapted the well-described SA-β-gal activity detection protocol to be able to use it on cryopreserved tissue (11). Our innovative protocol uses the optimal pH of the β-gal enzyme at shorter incubation times and allowed us to compare human samples that were collected over time due to limited availability. Since no markers of senescence are completely specific, we also developed IHC/IF and RTqPCR methods to evidence protein and/or gene expression of cell cycle inhibitors (p21 and p16), DNA/telomere-damage foci (γH2AX ± TRF2) and SASP markers (TGF-β1, IL-6, IL-8, IL-1β) (12).

We next investigated the presence of premature liver senescence in BA, which is the first cause of liver transplantation in children (13). We demonstrated for the first time through multiple markers and techniques that BA livers display advanced premature senescence. Senescence was predominant in cholangiocytes and in perinodular hepatocytes, and SASP markers were elevated in whole liver tissue homogenates. To confirm our observations, we performed the first DSP analysis on BA livers, which allowed us to investigate the whole transcriptome with regard to

the investigated cell type (cholangiocytes versus hepatocytes). This analysis confirmed that senescence and SASP predominated in cholangiocytes and continued to progress until liver transplantation. It also allowed us to conclude that the senescent transcriptome of hepatocytes and cholangiocytes shared many similarities, while it was very different from other cell types in line with previous reports underlying the heterogeneity of senescence and SASP transcriptomes (14). The localization of senescence in cholangiocytes and surrounding perinodular hepatocytes as well as the predominance of senescence in cholangiocytes in our BA livers are in line with the hypothesis of a paracrine transmission of senescence from cholangiocytes to hepatocytes through the SASP, hypothesis that was previously demonstrated in a preclinical model of biliary senescence (15). This is especially true since CCL2 and TGF-β1 – two SASP components that are widely incriminated in the paracrine transmission of senescence – were elevated in our BA livers (3, 15, 16).

Since senescence was confirmed in BA livers and continued to progress until liver transplantation, we aimed at developing a preclinical model of biliary cirrhosis and senescence that would mimic BA and allow us to test anti-senescence therapies. We chose the BDL model in two-month-old rats, which generates a rapid and constant progression to biliary cirrhosis (17). We observed that liver disease and senescence progression in this model were in many points comparable to BA, allowing us to proceed with the administration of HALPC or D+Q, two senotherapeutic options that could be translated to clinical applications. When we treated the animals once 48 hours after BDL surgery and sacrificed them 72 hours after the treatment, we observed that HALPC decreased the gene expression of the early marker of senescence p21, possibly through anti-oxidative properties since *Gpx1* liver gene expression was reduced in treated animals. HALPC also reduced the biliary damage (serum γGT and *Sox9* gene expression) and slightly improved the

hepatocytes mass (*Hnf4a*). In contrast, the well-described senolytic combination D+Q did not have any effect on liver senescence and even seemed to worsen liver disease as it decreased the hepatocytes mass. This underlies the deleterious potential of senolytic therapies when a particular senescent cell type is not specifically targeted, in line with the literature (18, 19). Identifying specific senescent cell types to remove in selected diseases and developing senotherapies that are able to target those cells remains an enormous challenge to address. Methods to increase the specificity of senotherapies for senescent cells are being developed, for example through galactose-conjugated nanoparticles or prodrugs cleaved in cells with increased SA-β-gal activity (20). Another example is the successful immune-mediated clearance of senescent cells through cytotoxic CAR T cells primed against uPAR, a cell-surface protein that is broadly induced during senescence (21). However, context-specific biomarkers that could identify senescent cells within a particular cell type are currently lacking. Such markers will be essential to increase specificity and limit off-target effects of senotherapies in the future.

Given the encouraging results obtained with HALPC on senescence and liver disease in BDL rats, we further investigated the effect of HALPC and D+Q by administrating repeated treatments to the animals. Operated rats received three HALPC or D+Q administrations (days 2-6-10 post-surgery) and were sacrificed two weeks after BDL surgery. In this extended experiment, HALPC and D+Q did not have any effect on senescence nor liver disease. Those results might have been related to the lack of senotherapeutic properties of the administrated substances, but the severity of the BDL model might also have been involved since complete and irreversible anatomical damage is induced by resecting the common bile duct. This observation underlies the difficulty of generating a preclinical model that would be severe enough to induce biliary cirrhosis and senescence, but with a progression that

would be slow enough to evidence potential beneficial effects related to senotherapeutic interventions. Such models would better mimic pediatric chronic cholestasis and would allow to assess the effect of senotherapies on established senescence and biliary disease. The reassortant RRV ($RRV^{(VP2,VP4)}$-TUCH) mice model of BA is an improved version of the original RRV model as it allowed to lower the mortality rate and increase fibrosis development (22). However, senescence was never investigated in this model and the low survival rate at 14 days (less than 50%) as well as the lack of systematic fibrotic evolution would make the assessment of liver senescence and disease evolution very challenging. Another model of biliary disease that could be considered is the multidrug resistance 2 (Mdr2) gene (*Abcb4*) knockout mice ($Mdr2^{-/-}$), in which bile acid leakage into portal tracts due to the absence of phospholipids in the bile results in portal inflammation and periductal fibrosis (23). Ductular reaction, cholangiocytes senescence and mild biliary fibrosis were described in this model in three-weeks-old mice, with slow progression of fibrosis from periportal areas and high survival rate, making it an interesting model to explore (24, 25). Established biliary cirrhosis was absent in the original model even after several months, but the genetic backcross of $Mdr2^{-/-}$ mice onto the highly fibrosis-susceptible BALB/c substrain allowed to observe early signs of biliary cirrhosis at 3 months of age (26). However, the Mdr2 knockout model has been classically used to mimic PSC or PFIC rather than BA, and the primary hepatocytes dysfunction would have to be taken into account as this feature is absent in BA. Other models were recently developed to mimic BA such as the biliatresone mouse model, intra-hepatic *Pkd1l1* knockout mice or human cholangiocytes organoids derived from BA livers (27-29). Biliatresone injection in neonatal mice induces a very severe BA phenotype as the mortality rate reaches 50% before 7 days of age and only asymptomatic mice survive after 18 days (27). The liver-specific $Pkd1l1^{-/-}$ mouse model induces delayed biliary maturation and a reduction in primary cilia, with progressive cholangiocyte proliferation and peribiliary fibro-inflammation

(28). Cholangiocytes senescence was also demonstrated in this model, which could be very suitable to study syndromic BA in future research. Finally, cholangiocytes organoids derived from BA livers – in which delayed epithelial development and disruption of the apical-basal polarization were demonstrated – allow to extensively study diseased human cholangiocytes *in vitro*, but not the interactions of cholangiocytes with other cell types (29). Various preclinical models of BA and biliary cirrhosis exist, and careful selection of the most suitable models will have to be performed before testing new senotherapeutic options in the future as new models are constantly developed.

Finally, we reported for the first time that ALGS livers display premature senescence at the time of liver transplantation. The degree of cellular senescence was advanced in those livers despite the mutation of Jagged1, which is involved in the juxtacrine transmission of senescence (30). However, we could not evidence any increase of classical SASP markers gene expression in those livers, possibly due to a dysfunction in the Notch pathway that plays a critical role in SASP induction and modulation or to SASP heterogeneity depending on the pathological conditions (30). Future research about senescence in ALGS livers of Jagged1 versus Notch2 mutated patients could be of great interest to better understand the involvement of the Notch pathway in senescence and SASP development.

Perspectives

This work demonstrates that senescence occurs in BA and ALGS – two main causes of neonatal cholestasis – and allows an advanced understanding of the physiopathology of premature senescence related to pediatric biliary cirrhosis. The deleterious effects of senescence progression on the disease evolution and the lack

of therapeutic alternatives to liver transplantation make the use of senotherapies very appealing in pediatric biliary diseases, but substantial work remains to be done before delivering clinically validated senotherapies to cholestatic children. The first aspect that will need to be further explored before translating senotherapies is the identification of specific senescent cell types to remove in selected diseases, in this case in pediatric biliary cirrhosis. This point will be crucial to avoid off-target side effects of senotherapies, particularly in liver diseases since not all senescent cell types are deleterious for liver homeostasis as previously mentioned (18, 31, 32). In this purpose, single-cell RNA sequencing on fresh tissue would allow to precisely identify the liver senescent cell types by correlating senescence and cell-type specific markers in preclinical models and in human liver disease. Transgenic models such as the p16-3MR mouse model could also be of high interest to observe the progressive accumulation of senescent cells *in vivo* and the effect of senescent cells removal on liver disease. P16-3MR mice express a trimodal reporter of synthetic luciferase, red fluorescent protein and herpes simplex virus 1 thymidine kinase under the control of p16 promotor, which allows tracking, sorting and ganciclovir-induced elimination of p16-expressing senescent cells (33). Biliary damage and senescence could be induced in p16-3MR mice through mechanical damage (BDL) or viral (RRV)/toxic (biliatresone) BA induction and the model would allow to follow the progression of senescence, to identify the senescent cell-types and to remove p16-expressing senescent cells. The next step would be to selectively remove the identified senescent cell types one by one to evidence which cell types are beneficial or deleterious for the tissue. To achieve this goal, strategies built on the recent developments in the field of senotherapies – such as senolytics coated with galactose-conjugated nanoparticles – could be considered (20). For example, bilirubin conjugation could be used to selectively kill senescent hepatocytes through ganciclovir coated with indirect bilirubin and administrated to BDL p16-3MR mice. However, it is likely that such strategies will not be possible to

adapt for all liver cell types. In this context, the identification of specific biomarkers to target deleterious senescent cell types seems essential to develop cell-type specific senotherapies that would have the potential to be translated to clinical applications. This is true for pediatric biliary cirrhosis, but also for age-related disorders and for every disease in which premature senescence occurs. The constant improvement of transcriptomic and proteomic screening techniques will hopefully help in this process, and allow to identify or engineer new senotherapeutic drugs that would specifically target those biomarkers. Finally, if such senotherapeutics can be developed, careful selection of the most suitable preclinical models will have to be performed to test the drugs according to the specific human disease(s) that are targeted (e.g. *Pkd1l1* deletion for syndromic BA, *Mdr2* deletion for PFIC or *Jag1* missense mutation for ALGS) (26, 28, 34). There is still a long way to go before considering the clinical translation of senotherapies to pediatric biliary cirrhosis, but constant progress is made in the field of senescence and this very exciting challenge will hopefully be addressed in the coming years.

Conclusion

In conclusion, this PhD thesis work provides the first report suggesting a potential interest of anti-senescence therapies in pediatric biliary cirrhosis. Premature senescence was evidenced in BA and ALGS livers, and spatial transcriptomic analysis revealed that senescence and SASP predominated in cholangiocytes in BA and progressed between diagnosis and liver transplantation. Since premature senescence worsens the prognosis of adult chronic hepatobiliary diseases, implementing senotherapies after hepatoportoenterostomy could help to limit the liver dysfunction and tissue remodeling related to senescence in BA and thereby allow to postpone or avoid liver transplantation. HALPC decreased the early marker of senescence p21 and improved liver disease in the BDL preclinical model of biliary

cirrhosis and senescence, providing promising results regarding the use of senotherapeutics in biliary cirrhosis. However, our study did not report any effect of the senolytic combination D+Q on liver senescence and even seemed to worsen liver disease. Consistent experimental work remains to be conducted in order to identify and develop senotherapeutics that would have the following properties: (1) specificity for senescent cells and for targeted cell type(s) in a particular disease, (2) beneficial effects on the disease related to identified anti-senescence mechanisms and (3) translatability to clinical application. Although senotherapies are promising therapeutic tools to develop in pediatric biliary cirrhosis, it is clear that such therapies will have to be further developed and improved before reaching clinical practice.

References

1. Feldman AG, Sokol RJ. Neonatal cholestasis: emerging molecular diagnostics and potential novel therapeutics. Nat Rev Gastroenterol Hepatol. 2019;16(6):346-60.
2. Cazzagon N, Sarcognato S, Floreani A, Corra G, De Martin S, Guzzardo V, et al. Cholangiocyte senescence in primary sclerosing cholangitis is associated with disease severity and prognosis. JHEP Rep. 2021;3(3):100286.
3. Sasaki M, Miyakoshi M, Sato Y, Nakanuma Y. Modulation of the microenvironment by senescent biliary epithelial cells may be involved in the pathogenesis of primary biliary cirrhosis. J Hepatol. 2010;53(2):318-25.
4. Aravinthan A, Scarpini C, Tachtatzis P, Verma S, Penrhyn-Lowe S, Harvey R, et al. Hepatocyte senescence predicts progression in non-alcohol-related fatty liver disease. J Hepatol. 2013;58(3):549-56.
5. Gutierrez-Reyes G, del Carmen Garcia de Leon M, Varela-Fascinetto G, Valencia P, Perez Tamayo R, Rosado CG, et al. Cellular senescence in livers from children with end stage liver disease. PLoS One. 2010;5(4):e10231.
6. Sasaki M, Kuo FY, Huang CC, Swanson PE, Chen CL, Chuang JH, et al. Increased expression of senescence-associated cell cycle regulators in the progression of biliary atresia: an immunohistochemical study. Histopathology. 2018;72(7):1164-71.
7. Sanada Y, Aida J, Kawano Y, Nakamura K, Shimomura N, Ishikawa N, et al. Hepatocellular telomere length in biliary atresia measured by Q-FISH. World J Surg. 2012;36(4):908-16.
8. Sana G, Lombard C, Vosters O, Jazouli N, Andre F, Stephenne X, et al. Adult human hepatocytes promote CD4(+) T-cell hyporesponsiveness via interleukin-10-producing allogeneic dendritic cells. Cell Transplant. 2014;23(9):1127-42.

9. Najimi M, Berardis S, El-Kehdy H, Rosseels V, Evraerts J, Lombard C, et al. Human liver mesenchymal stem/progenitor cells inhibit hepatic stellate cell activation: in vitro and in vivo evaluation. Stem Cell Res Ther. 2017;8(1):131.
10. Herrero A, Prigent J, Lombard C, Rosseels V, Daujat-Chavanieu M, Breckpot K, et al. Adult-Derived Human Liver Stem/Progenitor Cells Infused 3 Days Postsurgery Improve Liver Regeneration in a Mouse Model of Extended Hepatectomy. Cell Transplant. 2017;26(2):351-64.
11. Debacq-Chainiaux F, Erusalimsky JD, Campisi J, Toussaint O. Protocols to detect senescence-associated beta-galactosidase (SA-betagal) activity, a biomarker of senescent cells in culture and in vivo. Nat Protoc. 2009;4(12):1798-806.
12. Gorgoulis V, Adams PD, Alimonti A, Bennett DC, Bischof O, Bishop C, et al. Cellular Senescence: Defining a Path Forward. Cell. 2019;179(4):813-27.
13. Elisofon SA, Magee JC, Ng VL, Horslen SP, Fioravanti V, Economides J, et al. Society of pediatric liver transplantation: Current registry status 2011-2018. Pediatr Transplant. 2020;24(1):e13605.
14. Hernandez-Segura A, de Jong TV, Melov S, Guryev V, Campisi J, Demaria M. Unmasking Transcriptional Heterogeneity in Senescent Cells. Curr Biol. 2017;27(17):2652-60 e4.
15. Ferreira-Gonzalez S, Lu WY, Raven A, Dwyer B, Man TY, O'Duibhir E, et al. Paracrine cellular senescence exacerbates biliary injury and impairs regeneration. Nat Commun. 2018;9(1):1020.
16. Acosta JC, Banito A, Wuestefeld T, Georgilis A, Janich P, Morton JP, et al. A complex secretory program orchestrated by the inflammasome controls paracrine senescence. Nat Cell Biol. 2013;15(8):978-90.
17. Kountouras J, Billing BH, Scheuer PJ. Prolonged bile duct obstruction: a new experimental model for cirrhosis in the rat. Br J Exp Pathol. 1984;65(3):305-11.
18. Grosse L, Wagner N, Emelyanov A, Molina C, Lacas-Gervais S, Wagner KD, et al. Defined p16(High) Senescent Cell Types Are Indispensable for Mouse Healthspan. Cell Metab. 2020;32(1):87-99 e6.
19. Raffaele M, Kovacovicova K, Frohlich J, Lo Re O, Giallongo S, Oben JA, et al. Mild exacerbation of obesity- and age-dependent liver disease progression by senolytic cocktail dasatinib + quercetin. Cell Commun Signal. 2021;19(1):44.
20. Morsli S, Doherty GJ, Munoz-Espin D. Activatable senoprobes and senolytics: Novel strategies to detect and target senescent cells. Mech Ageing Dev. 2022;202:111618.
21. Amor C, Feucht J, Leibold J, Ho YJ, Zhu C, Alonso-Curbelo D, et al. Senolytic CAR T cells reverse senescence-associated pathologies. Nature. 2020;583(7814):127-32.
22. Mohanty SK, Lobeck I, Donnelly B, Dupree P, Walther A, Mowery S, et al. Rotavirus Reassortant-Induced Murine Model of Liver Fibrosis Parallels Human Biliary Atresia. Hepatology. 2020;71(4):1316-30.
23. Fickert P, Fuchsbichler A, Wagner M, Zollner G, Kaser A, Tilg H, et al. Regurgitation of bile acids from leaky bile ducts causes sclerosing cholangitis in Mdr2 (Abcb4) knockout mice. Gastroenterology. 2004;127(1):261-74.
24. Zhou T, Wu N, Meng F, Venter J, Giang TK, Francis H, et al. Knockout of secretin receptor reduces biliary damage and liver fibrosis in Mdr2(-/-) mice by diminishing senescence of cholangiocytes. Lab Invest. 2018;98(11):1449-64.

25. Nishio T, Hu R, Koyama Y, Liang S, Rosenthal SB, Yamamoto G, et al. Activated hepatic stellate cells and portal fibroblasts contribute to cholestatic liver fibrosis in MDR2 knockout mice. J Hepatol. 2019;71(3):573-85.
26. Ikenaga N, Liu SB, Sverdlov DY, Yoshida S, Nasser I, Ke Q, et al. A new Mdr2(-/-) mouse model of sclerosing cholangitis with rapid fibrosis progression, early-onset portal hypertension, and liver cancer. Am J Pathol. 2015;185(2):325-34.
27. Yang Y, Wang J, Zhan Y, Chen G, Shen Z, Zheng S, et al. The synthetic toxin biliatresone causes biliary atresia in mice. Lab Invest. 2020;100(11):1425-35.
28. Hellen DJ, Bennett A, Malla S, Klindt C, Rao A, Dawson PA, et al. Liver-restricted deletion of the biliary atresia candidate gene Pkd1l1 causes bile duct dysmorphogenesis and ciliopathy. Hepatology. 2023.
29. Amarachintha SP, Mourya R, Ayabe H, Yang L, Luo Z, Li X, et al. Biliary organoids uncover delayed epithelial development and barrier function in biliary atresia. Hepatology. 2021.
30. Hoare M, Ito Y, Kang TW, Weekes MP, Matheson NJ, Patten DA, et al. NOTCH1 mediates a switch between two distinct secretomes during senescence. Nat Cell Biol. 2016;18(9):979-92.
31. Krizhanovsky V, Yon M, Dickins RA, Hearn S, Simon J, Miething C, et al. Senescence of activated stellate cells limits liver fibrosis. Cell. 2008;134(4):657-67.
32. Cheng N, Kim KH, Lau LF. Senescent hepatic stellate cells promote liver regeneration through IL-6 and ligands of CXCR2. JCI Insight. 2022;7(14).
33. Demaria M, Ohtani N, Youssef SA, Rodier F, Toussaint W, Mitchell JR, et al. An essential role for senescent cells in optimal wound healing through secretion of PDGF-AA. Dev Cell. 2014;31(6):722-33.
34. Andersson ER, Chivukula IV, Hankeova S, Sjoqvist M, Tsoi YL, Ramskold D, et al. Mouse Model of Alagille Syndrome and Mechanisms of Jagged1 Missense Mutations. Gastroenterology. 2018;154(4):1080-95.

Annexes

Annex 1: list of publications

- Jannone G, Bonaccorsi Riani E, de Magnée C, et al. Senescence and senotherapies in biliary atresia and biliary cirrhosis. *Submitted.*
- Jannone G, de Magnée C, Tambucci R, et al. Alagille syndrome livers display premature senescence. *Submitted.*
- Najimi M, de Bodt G, Jannone G, et al. Mesenchymal stem cells Transplantation for liver regenerative medicine. In: Regenerative hepatology and liver transplantation (2d volume of the Regenerative and Transplant Medicine series). Paulo Martins & Pedro Baptista, 1st edition. 2023.
- Jannone G, Scheers I, Smets F, et al. Everolimus is Safe as a Second-/Third-Line Therapy in Pediatric Autoimmune Hepatitis. JPGN Reports. 2022 Aug;3(3):227-231.
- Jannone G, Stephenne X, Scheers I, et al. Nasobiliary Drainage Prior to Surgical Biliary Diversion in Progressive Familial Intrahepatic Cholestasis Type II. Eur J Pediatr. 2020 Apr 14.
- Jannone G, Rozzi M, Najimi M, et al. An Optimized Protocol for Histochemical Detection of Senescence-associated Beta-galactosidase Activity in Cryopreserved Liver Tissue. J Histochem Cytochem. 2020 Apr;68(4):269-278.
- Jannone G, van Dievoet MA, Coppin L, et al. Vitamin K May Be A-OK, in Kids and Cholestatic Patients. P T. 2019 Jun;44(6):318-319.

Annex 2: nasobiliary drainage prior to surgical biliary diversion in progressive familial intrahepatic cholestasis type II

European Journal of Pediatrics
https://doi.org/10.1007/s00431-020-03646-z

ORIGINAL ARTICLE

Nasobiliary drainage prior to surgical biliary diversion in progressive familial intrahepatic cholestasis type II

Giulia Jannone[1] · Xavier Stephenne[1] · Isabelle Scheers[1] · Françoise Smets[1] · Catherine de Magnée[2] · Raymond Reding[2] · Etienne M. Sokal[1]

Received: 27 December 2019 / Revised: 18 March 2020 / Accepted: 27 March 2020

Abstract

Progressive familial intrahepatic cholestasis (PFIC) can cause intense pruritus that is refractory to medical therapy. Surgical biliary diversion techniques, including partial internal biliary diversion (PIBD), have been developed over the years to relieve pruritus without requiring liver transplantation. No clinical or genetic features can currently predict postoperative pruritus response. We present three PFIC type 2 (PIFC 2) patients who underwent transient endoscopic nasobiliary drainage (NBD) prior to PIBD surgery. Two patients repeatedly responded to NBD and presented with complete pruritus resolution after subsequent PIBD. NBD failed technically in the third patient, and PIBD was partially successful. Mild post-endoscopic biological pancreatitis occurred in 2/6 NBD procedures and resolved spontaneously. The only adverse effect observed within 7 years post-PIBD was very mild transient osmotic diarrhea.

Conclusion: Our limited data suggest that NBD is a safe and effective way to predict pruritus response before performing permanent biliary diversion surgery in PFIC patients.

What is Known:
- *Surgical biliary diversion techniques have been developed to relieve intractable pruritus in progressive familial intrahepatic cholestasis (PFIC).*
- *No clinical or genetic features can currently predict pruritus response to surgery.*

What is New:
- *Our data suggest that nasobiliary drainage could be a safe and effective tool to predict pruritus response to biliary diversion and avoid unnecessary surgery in PFIC patients.*

Keywords Biliary diversion · Nasobiliary drainage · Familial cholestasis · Pruritus · Bile acids

Communicated by Peter de Winter

✉ Giulia Jannone
giulia.jannone@uclouvain.be

Xavier Stephenne
xavier.stephenne@uclouvain.be

Isabelle Scheers
isabelle.scheers@uclouvain.be

Françoise Smets
francoise.smets@uclouvain.be

Catherine de Magnée
catherine.demagnee@uclouvain.be

Raymond Reding
raymond.reding@uclouvain.be

Etienne M. Sokal
etienne.sokal@uclouvain.be

[1] Department of Pediatrics, Pediatric Gastroenterology and Hepatology Unit, Cliniques Universitaires Saint-Luc, Avenue Hippocrate 10, Brussels 1200, Belgium

[2] Department of Surgery, Pediatric Surgery and Transplantation Unit, Cliniques Universitaires Saint-Luc, Brussels, Belgium

Published online: 14 April 2020

Abbreviations

ERCP	Endoscopic retrograde cholangiopancreatography
MARS	Molecular adsorbents recirculating system
NBD	Nasobiliary drainage
PEBD	Partial external biliary diversion
PFIC	Progressive familial intrahepatic cholestasis
PIBD	Partial internal biliary diversion
TBA	Serum total bile acids

Introduction

Progressive familial intrahepatic cholestasis (PFIC) refers to a group of autosomal recessive disorders, which result in liver cholestasis caused by hepatocellular defects in the secretion of bile components. Patients may experience extremely intense pruritus despite medical therapy; this was originally an indication for liver transplantation [1, 2]. Over the years, various surgical techniques for biliary diversion have been developed to relieve pruritus without liver transplantation [3]. Among those surgical techniques, partial internal biliary diversion (PIBD) has shown very promising results and has the advantage of avoiding external stoma and related infections [4, 5]. Despite the efficacy and safety of this procedure, some patients do not respond to the surgery and there is currently no method for predicting response according to genotype or other clinical parameters. Ramachadran et al. observed pruritus improvement in seven out of ten PFIC 1 and PFIC 2 patients after PIBD [4]. Erginel et al. observed pruritus reduction in five out of six PFIC 1 and PFIC 2 patients after PIBD, and suggested that outcomes may be better in PFIC 1 patients after biliary diversion [5]. However, PIBD can be a useless permanent intervention in patients who do not show any post-operative pruritus improvement, with subsequent risk of osmotic diarrhea [4, 6]. Endoscopic nasobiliary drainage (NBD) is a reversible procedure, which may improve pruritus in various cholestatic diseases, including primary biliary cirrhosis or benign recurrent intrahepatic cholestasis [7, 8]. This procedure has proven to be safe even for long-term use, the principal adverse effect being post-endoscopic pancreatitis [7, 9]. It has already been suggested that NBD could be an efficient way to evaluate pruritus response to biliary drainage before performing a surgical procedure with permanent effects [10]. To our knowledge, no clinical case has been published to confirm this hypothesis.

We present three PFIC 2 patients who underwent NBD to evaluate their clinical response to biliary drainage prior to PIBD surgery. NBD was inconclusive in one patient, since no bile was ever drained by the catheter. The two other patients displayed full response to NBD and then underwent PIBD successfully, with complete resolution of pruritus.

Materials and methods

Inclusion criteria

Patients were retrospectively identified in the Pediatric Hepatology database of the Cliniques Universitaires Saint-Luc. The inclusion criteria were:(1) confirmed diagnosis of cholestatic liver disease and (2) NBD followed by surgical biliary diversion. No age restrictions were applied. We identified three patients diagnosed with PFIC 2 who underwent NBD prior to PIBD between 2011 and 2019.

Endoscopic nasobiliary drainage

A catheter (size 5 French in children and 7 French in adults) was placed in the common bile duct by endoscopic retrograde cholangiopancreatography (ERCP) under general anesthesia (Fig. 1a). No sphincterotomy was performed. The position of the nasobiliary catheter was confirmed by contrast product injection through the catheter.

Partial internal biliary diversion surgery

Right subcostal laparotomy was performed to place a jejunal conduit of 25 cm between the gallbladder fundus and the transverse colon (Fig. 1b). Jejunal continuity was restored through jejunal termino-lateral anastomosis. Antibiotic prophylaxis with cefuroxime and metronidazole was administered to the patients for 4 days after surgery coupled with long-term fat-soluble vitamin supplementation.

Pruritus score

Pruritus was assessed according to the scale of Whitington et al., modified as follows: 0 = none; 1 = rubbing or mild scratching when undistracted; 2 = active scratching without evident skin abrasions; 3 = abrasions evident; 4 = cutaneous mutilation and scarring evident, impaired quality of life [11].

Results

Clinical case no. 1

The first patient was a Caucasian female diagnosed with PFIC 2 based on the presence of two compound heterozygous mutations identified in the *ABCB11* gene: c.1548T>G (p.Ile516Met) and c.1622T>C (p.Ile541Thr). She suffered from mild jaundice and intense pruritus since her first year of life. Pruritus caused her major sleep and concentration troubles. Various pharmaceutical interventions were unsuccessfully tested, including rifampicin, cholestyramine, ursodeoxycholic acid, phenobarbital, simvastatin, anti-

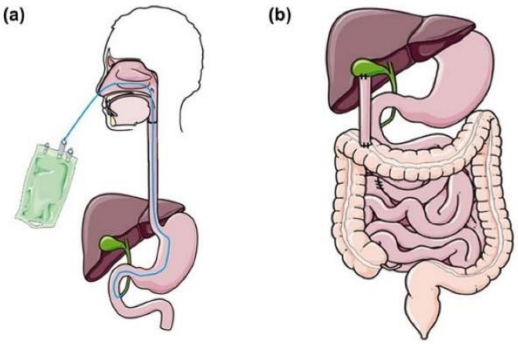

Fig. 1 **a** Nasobiliary drainage; **b** partial internal biliary diversion. Illustrations are modified from Servier Medical Art

histamines, and zinc. Liver transplantation was considered but never performed due to normal liver function and histology. In another attempt to relieve pruritus, Molecular Adsorbents Recirculating System (MARS—also termed albumin dialysis) was tried at the age of 24 years. The first attempt (two cycles in 2 days) improved her pruritus (score 4 decreased to 2), but its intensity returned to baseline (score 4) 15 days after the first dialysis. One month later, a second MARS attempt (three cycles in 3 days) only mildly improved pruritus (score 4 decreased to 3) for a few days. Seven months later, ERCP-guided NBD was performed in this patient. At the time, she had normal total serum bilirubin levels and gamma-GT, with elevated serum total bile acids (TBA) (93.7 μmol/L; normal value < 10 μmol/L). Her liver transaminases and liver function were normal. A few hours after the procedure, the pruritus drastically decreased (score 4 decreased to 0), and TBA levels normalized to 5.0 μmol/L after 24 h. The patient developed mild biological post-endoscopic pancreatitis, which resolved without any treatment. The catheter spontaneously dislodged from the biliary tree after 3 days, leading to pruritus recurrence. A second NBD was performed 1 month later to assess reproducibility. Pruritus markedly improved again (score 4 decreased to 1), and TBA levels decreased from 90.0 to 14.0 μmol/L. Post-endoscopic pancreatitis did not occur. Three months later, at 25 years of age, she underwent PIBD surgery. At the time, her liver transaminases and liver histology were still completely normal (Metavir score F0). The pruritus resolved completely a few hours after surgery (score 4 decreased to 0), and TBA levels decreased from 282.0 μmol/L before surgery to 40.7 μmol/L 3 days after surgery (Table 1). Two weeks after surgery, TBA levels were 103 μmol/L and pruritus was still absent. Two months after surgery, she complained about mild osmotic diarrhea, with excellent response to cholestyramine therapy and rapid resolution. Three years after surgery, she experienced transient pruritus (score 2) during a constipation episode, which spontaneously resolved after a few weeks. Seven years after surgery, she is still free of pruritus and does not present any adverse effects due to the surgery. Her liver function and enzymes remain normal, with normal bilirubinemia and improved TBA levels (11.9 μmol/L).

Clinical case no. 2

The second patient was a Caucasian male diagnosed with PFIC 2 at the age of 6 months. The following compound heterozygous mutations were identified in the *ABCB11* gene: c.2178+1G>A and c.389+8G>A. His major symptoms during childhood were pruritus and failure to thrive. Around the age of 12 years, the pruritus became severely debilitating, despite medical therapy with rifampicin, cholestyramine, and ursodeoxycholic acid. Liver transplantation was not formally indicated, since his liver function was normal, and liver biopsy showed only very mild fibrosis (Metavir score F0-F1). He first underwent NBD at 27 years of age. At the time, he had total bilirubin levels of 1.6 mg/dL (normal value 1.2 mg/dL), with normal gamma-GT, and elevated TBA levels (178.0 μmol/L). His liver transaminases were slightly elevated (AST 60 U/L and ALT 54 U/L; normal values < 40 U/L). A few hours after the procedure, the pruritus completely resolved (score 4 to 0), TBA levels decreased slightly to 140.0 μmol/L, and liver transaminases almost completely normalized (AST 42 U/L and ALT 31 U/L). The nasobiliary catheter remained for 6 days, and pruritus recurred 4 days after catheter removal. Two more NBDs were performed in this patient, 2 months and 4 months after the first attempt. Both procedures completely abrogated the patient's pruritus (scores 4 decreased to 0), until a few days after the removal of the catheter. None of the three NBD procedures caused post-ERCP pancreatitis. Four months later, at 28 years of age, he underwent PIBD surgery. The

Table 1 Serum TBA levels and pruritus scores before and after PIBD. Last follow-up was 7 years after the surgery for patient 1, 1 month after the surgery for patient 2, and 6 months after the surgery for patient 3. Normal TBA levels < 10 μmol/L. *PIBD*, partial internal biliary diversion; *TBA*, serum total bile acids

	Pre-PIBD		3 days post-PIBD		15 days post-PIBD		Last follow-up	
	TBA (μmol/L)	Pruritus score	TBA (μmol/L)	Pruritus score	TBA (μmol/L)	Pruritus score	TBA (μmol/L)	Pruritus score
Patient 1	282	4	40.7	0	103	0	11.9	0
Patient 2	314.4	4	220.9	0	382.5	0	304.6	0
Patient 3	402	4	267	0	635.8	3	533	1–2

pruritus resolved completely a few hours after surgery (score 4 decreased to 0), and TBA levels decreased from 314.4 to 220.9 μmol/L 3 days after surgery (Table 1). Two weeks after surgery, TBA levels returned to 382.5 μmol/L without pruritus recurrence. One month after surgery, the patient was well and free of pruritus. TBA levels were 304.6 μmol/L.

Clinical case no. 3

The third patient was a Caucasian male diagnosed with PFIC 2 at the age of 3 months (homozygous mutation C1810-3C>G in the *ABCB11* gene). Because of intense pruritus refractory to medical therapy, it was decided to try biliary diversion. He underwent NBD at the age of 2 years and 9 months. At the time, total bilirubin levels were 2 mg/dL, gamma-GT levels were normal, and TBA levels were elevated (414 μmol/L). His liver transaminases were elevated (AST 213 U/L and ALT 177 U/L). Liver histopathology showed marked fibrosis with occasional nodules (Metavir score F3-F4). A 5-French catheter introduced in the common bile duct never drained any bile and was removed 17 h later because of increased lipase levels. Biological pancreatitis resolved spontaneously a few days after catheter removal. TBA levels were unchanged (402 μmol/L, 24 h after the procedure). No pruritus improvement was noticed during NBD, but the procedure was considered inconclusive, as no bile was ever drained. No further NBD was attempted, and the patient underwent PIBD 1 month later. Pruritus markedly improved following surgery (score 4 decreased to 0,) and TBA levels decreased to 267 μmol/L after 48 h. Five days post-surgery, total bilirubin decreased to 1.4 mg/dl and transaminases were improved (AST 58 U/L and ALT 47 U/L). Fifteen days after surgery, pruritus recurred (score 0 increased to 3) during an episode of constipation with enlargement of the jejunal conduit used for the diversion (TBA levels, 635.8 μmol/L). The pruritus fully responded to laxative therapy. Six months after surgery, the patient complained about mild pruritus (score 1–2). His TBA levels were 533 μmol/L with total bilirubin at 1.7 mg/dl and elevated transaminases (AST 135 U/L and ALT 114 U/L). Liver histology was stable.

Discussion

Our experience suggests that NBD is a safe way to predict pruritus response to PIBD in PFIC 2 patients. We observed two mild transient occurrences of post-endoscopic pancreatitis over the six NBD procedures, with rapid and spontaneous resolution. When performed after successful NBD, PIBD drastically improved the quality of life of our patients. The only adverse effect observed up to 7 years post-surgery was very mild osmotic diarrhea, which was easily treated with cholestyramine.

Biliary diversion techniques were originally developed to improve pruritus through interruption of biliary enterohepatic circulation [11, 12]. Bile acids are normally excreted by the liver in the bile, and then mostly reabsorbed in the small intestine to return to the liver through the hepatic portal circulation. In cholestatic disease, it was hypothesized that pruritus resulted from intradermal bile acid accumulation secondary to elevated serum TBA levels [4]. Enterohepatic cycle interruption through biliary diversion would lead to an excretion of bile acids, with progressive depletion of the total bile acids pool and pruritus improvement. Unexpectedly, a correlation between pruritus and TBA levels was never demonstrated [13]. Kremer et al. reported that TBA levels can rise back to baseline values during NBD without associated recurrence of pruritus [13]. In the same study, MARS strongly decreased pruritus severity, while TBA levels were not significantly reduced. In our experience, complete pruritus resolution occurred after biliary diversion through NBD or PIBD, even with moderate reduction in TBA levels. We also observed that TBA levels could rise back to baseline values after biliary diversion without pruritus recurrence. Regarding MARS, one of our patients underwent several cycles on two occasions. As already suggested for cholestatic disease, the decrease in pruritus experienced after dialysis was only transient [14]. In our patient, pruritus relief was stronger following NBD compared to MARS [13]. An alternative hypothesis suggesting how biliary diversion reduces pruritus involves the lysophospholipase autotaxin (ATX) as a potential mediator of cholestatic pruritus [15]. It was observed that pruritus and serum ATX reduction are directly correlated following NBD and MARS [13]. Since no ATX was detected in the bile, it was hypothesized that an ATX-inducing factor exists in the bile and is removed from the enterohepatic

circulation by the biliary diversion [13]. This mechanism could explain the rapid resolution of pruritus that we observed in our patients after NBD and PIBD. However, the ATX-inducing factor remains to be identified and the physiopathology of pruritus in cholestatic diseases is still not completely understood.

The first surgical technique for biliary diversion developed to treat pruritus was partial external biliary diversion (PEBD). Whitington et al. demonstrated that PEBD not only showed excellent results on pruritus but that histological cholestasis and portal fibrosis resolution were observed a few years after surgery [11]. Those results were corroborated by Arnell et al., who observed successive reductions in histological cholestasis and then fibrosis after PEBD in 12 PFIC patients [16]. Moreover, Schukfeh et al. reported no progression of biochemical cholestasis in 13 out of 17 PFIC patients who underwent PEBD surgery without liver cirrhosis [17]. One year after surgery, those patients had reduced TBA and total bilirubin levels, with stable liver transaminases. On the contrary, all seven cirrhotic patients who underwent PEBD needed subsequent liver transplantation within 1 year after PEBD [17]. Over the years, PEBD has become a fist-line therapy in PFIC types 1 and 2 in the absence of established cirrhosis [18]. PEBD and PIBD are both partial biliary diversion techniques, with very similar physio-pathological outcomes. In our first patient, biochemical cholestasis did not progress in 7 years of follow-up post-PIBD. In the future, PIBD could become an indication not only for the relief of severe refractory pruritus in PFIC but also for the slowing down of the progression of cholestasis and fibrosis in early disease stages.

PIBD has the advantage of avoiding external stoma and related complications but increases the concentration of bile acids in the colon. This might cause bile acid diarrhea, which usually responds well to cholestyramine therapy. Previous publications suggested that patients with colorectal cancers might have higher fecal bile acid levels than controls [19]. To our knowledge, no study has ever demonstrated that patients suffering from bile acid malabsorption are at higher risk for developing colorectal cancer. In the general population, the fraction of bile acids that are not reabsorbed by enterocytes, and thereby end up in the feces, represents approximately 5% of the total bile acid pool [20]. Due to BSEP mutations, the concentration of bile acids in the bile is very low in PFIC 2 patients (< 1% of normal) [21]. In this context, it is very unlikely that PFIC 2 patients who underwent PIBD would be at higher risk of colorectal cancer, as compared to the general population. Nonetheless, further research will be needed to investigate the potential risk of colorectal cancer related to PIBD in cholestatic patients.

In PFIC type 2 patients who underwent PEBD, common missense mutations (patients heterozygous or homozygous for p.Asp482Gly and/or p.Glu297Gly BSEP mutations) had been suggested to predict a better outcome compared to other BSEP mutations [22–24]. Our two patients who underwent successful NBD did not carry common missense BSEP mutations and still presented with good clinical outcomes following PIBD surgery. No correlation between PFIC genotype and post-surgical outcomes has been demonstrated to date in PIBD, but NBD could be a useful tool to help predict clinical outcomes after biliary diversion procedures.

The principal limitation of our work is the small number of participants. Of our three patients, two underwent successful NBD, and the procedure was inconclusive in the third patient. We observed that the two patients who responded to NBD underwent successful PIBD, but we cannot state that NBD failure leads to unsuccessful PIBD. In the same way, the number of patients that we present is too small to conclude that effective NBD will always lead to pruritus resolution after PIBD. Nonetheless, our results are encouraging and highlight NBD as a promising tool for predicting PIBD outcomes. It is also important to note that the successful NBD procedures that we describe were performed on two adult patients. Successful NBD and PIBD have already been described in pediatric patients, but the technical challenge of performing NBD in pediatric patients will have to be considered in future research [4, 25].

In conclusion, our limited experience suggests that NBD is an excellent way to test pruritus response to biliary diversion before performing permanent biliary diversion surgery in PFIC patients. Further research will have to be conducted to corroborate our data and to extend PIBD indication from refractory pruritus to disease progression in the absence of cirrhosis.

Authors' contributions GJ contributed to study conception and design, to data collection and analysis, drafted the manuscript and approved the final manuscript. XS contributed to study conception and design and to material preparation, revised the manuscript and approved the final manuscript. IS contributed to study conception and design and to material preparation, revised the manuscript and approved the final manuscript. FS contributed to study conception and design and to material preparation, revised the manuscript and approved the final manuscript. CDM contributed to study conception and design and to material preparation, revised the manuscript and approved the final manuscript. RR contributed to study conception and design and to material preparation, revised the manuscript and approved the final manuscript. ES contributed to study conception and design and to material preparation, revised the manuscript and approved the final manuscript.

Funding information GJ is supported by the Fonds National de la Recherche Scientifique et Médicale (FNRS, Belgium) through an FRIA grant (number FC29559). IS is supported by FNRS and Fondation contre le Cancer grants.

Compliance with ethical standards These procedures were considered as standard medical care and did not require prior ethical committee approval.

Conflict of interest The authors declare that they have no conflicts of interest.

References

1. Wanty C, Joomye R, Van Hoorebeek N, Paul K, Otte JB, Reding R, Sokal EM (2004) Fifteen years single center experience in the

management of progressive familial intrahepatic cholestasis of infancy. Acta Gastroenterol Belg 67(4):313–319
2. Ismail H, Kalicinski P, Markiewicz M, Jankowska I, Pawlowska J, Kluge P, Eliadou E, Kaminski A, Szymczak M, Drewniak T, Revillon Y (1999) Treatment of progressive familial intrahepatic cholestasis: liver transplantation or partial external biliary diversion. Pediatr Transplant 3(3):219–224
3. Davis AR, Rosenthal P, Newman TB (2009) Nontransplant surgical interventions in progressive familial intrahepatic cholestasis. J Pediatr Surg 44(4):821–827. https://doi.org/10.1016/j.jpedsurg.2008.07.018
4. Ramachandran P, Shanmugam NP, Sinani SA, Shanmugam V, Srinivas S, Sathiyasekaran M, Tamilvanan V, Rela M (2014) Outcome of partial internal biliary diversion for intractable pruritus in children with cholestatic liver disease. Pediatr Surg Int 30(10): 1045–1049. https://doi.org/10.1007/s00383-014-3559-x
5. Erginel B, Soysal FG, Durmaz O, Celik A, Salman T (2018) Long-term outcomes of six patients after partial internal biliary diversion for progressive familial intrahepatic cholestasis. J Pediatr Surg 53(3):468–471. https://doi.org/10.1016/j.jpedsurg.2017.10.055
6. Nicastro E, Stephenne X, Smets F, Fusaro F, de Magnee C, Reding R, Sokal EM (2012) Recovery of graft steatosis and protein-losing enteropathy after biliary diversion in a PFIC 1 liver transplanted child. Pediatr Transplant 16(5):E177–E182. https://doi.org/10.1111/j.1399-3046.2011.01514.x
7. Hegade VS, Krawczyk M, Kremer AE, Kuczka J, Gaouar F, Kuiper EM, van Buuren HR, Lammert F, Corpechot C, Jones DE (2016) The safety and efficacy of nasobiliary drainage in the treatment of refractory cholestatic pruritus: a multicentre European study. Aliment Pharmacol Ther 43(2):294–302. https://doi.org/10.1111/apt.13449
8. Stapelbroek JM, van Erpecum KJ, Klomp LW, Venneman NG, Schwartz TP, van Berge Henegouwen GP, Devlin J, van Nieuwkerk CM, Knisely AS, Houwen RH (2006) Nasobiliary drainage induces long-lasting remission in benign recurrent intrahepatic cholestasis. Hepatology 43(1):51–53. https://doi.org/10.1002/hep.20998
9. Appleby VJ, Hutchinson JM, Davies MH (2015) Safety and efficacy of long-term nasobiliary drainage to treat intractable pruritus in cholestatic liver disease. Frontline Gastroenterol 6(4):252–254. https://doi.org/10.1136/flgastro-2014-100489
10. Jacquemin E (2012) Progressive familial intrahepatic cholestasis. Clin Res Hepatol Gastroenterol 36(Suppl 1):S26–S35. https://doi.org/10.1016/S2210-7401(12)70018-9
11. Whitington PF, Whitington GL (1988) Partial external diversion of bile for the treatment of intractable pruritus associated with intrahepatic cholestasis. Gastroenterology 95(1):130–136. https://doi.org/10.1016/0016-5085(88)90301-0
12. Bustorff-Silva J, Sbraggia Neto L, Olimpio H, de Alcantara RV, Matsushima E, De Tommaso AM, Brandao MA, Hessel G (2007) Partial internal biliary diversion through a cholecystojejunocolonic anastomosis–a novel surgical approach for patients with progressive familial intrahepatic cholestasis: a preliminary report. J Pediatr Surg 42(8):1337–1340. https://doi.org/10.1016/j.jpedsurg.2007.03.029
13. Kremer AE, van Dijk R, Leckie P, Schaap FG, Kuiper EM, Mettang T, Reiners KS, Raap U, van Buuren HR, van Erpecum KJ, Davies NA, Rust C, Engert A, Jalan R, Oude Elferink RP, Beuers U (2012) Serum autotaxin is increased in pruritus of cholestasis, but not of other origin, and responds to therapeutic interventions. Hepatology 56(4):1391–1400. https://doi.org/10.1002/hep.25748
14. Pares A, Herrera M, Aviles J, Sanz M, Mas A (2010) Treatment of resistant pruritus from cholestasis with albumin dialysis: combined analysis of patients from three centers. J Hepatol 53(2):307–312. https://doi.org/10.1016/j.jhep.2010.02.031
15. Kremer AE, Martens JJ, Kulik W, Rueff F, Kuiper EM, van Buuren HR, van Erpecum KJ, Kondrackiene J, Prieto J, Rust C, Geenes VL, Williamson C, Moolenaar WH, Beuers U, Oude Elferink RP (2010) Lysophosphatidic acid is a potential mediator of cholestatic pruritus. Gastroenterology 139(3):1008–1018, e1001. https://doi.org/10.1053/j.gastro.2010.05.009
16. Arnell H, Papadogiannakis N, Zemack H, Knisely AS, Nemeth A, Fischler B (2010) Follow-up in children with progressive familial intrahepatic cholestasis after partial external biliary diversion. J Pediatr Gastroenterol Nutr 51(4):494–499. https://doi.org/10.1097/MPG.0b013e3181df99d5
17. Schukfeh N, Metzelder ML, Petersen C, Reismann M, Pfister ED, Ure BM, Kuebler JF (2012) Normalization of serum bile acids after partial external biliary diversion indicates an excellent long-term outcome in children with progressive familial intrahepatic cholestasis. J Pediatr Surg 47(3):501–505. https://doi.org/10.1016/j.jpedsurg.2011.08.010
18. Verkade HJ, Bezerra JA, Davenport M, Schreiber RA, Mieli-Vergani G, Hulscher JB, Sokol RJ, Kelly DA, Ure B, Whitington PF, Samyn M, Petersen C (2016) Biliary atresia and other cholestatic childhood diseases: advances and future challenges. J Hepatol 65(3):631–642. https://doi.org/10.1016/j.jhep.2016.04.032
19. Tong JL, Ran ZH, Shen J, Fan GQ, Xiao SD (2008) Association between fecal bile acids and colorectal cancer: a meta-analysis of observational studies. Yonsei Med J 49(5):792–803. https://doi.org/10.3349/ymj.2008.49.5.792
20. Li T, Chiang JY (2014) Bile acid signaling in metabolic disease and drug therapy. Pharmacol Rev 66(4):948–983. https://doi.org/10.1124/pr.113.008201
21. Jansen PL, Strautnieks SS, Jacquemin E, Hadchouel M, Sokal EM, Hooiveld GJ, Koning JH, De Jager-Krikken A, Kuipers F, Stellaard F, Bijleveld CM, Gouw A, Van Goor H, Thompson RJ, Muller M (1999) Hepatocanalicular bile salt export pump deficiency in patients with progressive familial intrahepatic cholestasis. Gastroenterology 117(6):1370–1379. https://doi.org/10.1016/s0016-5085(99)70287-8
22. Bull LN, Pawlikowska L, Strautnieks S, Jankowska I, Czubkowski P, Dodge JL, Emerick K, Wanty C, Wali S, Blanchard S, Lacaille F, Byrne JA, van Eerde AM, Kolho KL, Houwen R, Lobritto S, Hupertz V, McClean P, Mieli-Vergani G, Sokal E, Rosenthal P, Whitington PF, Pawlowska J, Thompson RJ (2018) Outcomes of surgical management of familial intrahepatic cholestasis 1 and bile salt export protein deficiencies. Hepatol Commun 2(5):515–528. https://doi.org/10.1002/hep4.1168
23. Davit-Spraul A, Fabre M, Branchereau S, Baussan C, Gonzales E, Stieger B, Bernard O, Jacquemin E (2010) ATP8B1 and ABCB11 analysis in 62 children with normal gamma-glutamyl transferase progressive familial intrahepatic cholestasis (PFIC): phenotypic differences between PFIC1 and PFIC2 and natural history. Hepatology 51(5):1645–1655. https://doi.org/10.1002/hep.23539
24. van Wessel DBE, Thompson RJ, Gonzales E, Jankowska I, Sokal E, Grammatikopoulos T, Kadaristiana A, Jacquemin E, Spraul A, Lipinski P, Czubkowski P, Rock N, Shagrani M, Broering D, Algoufi T, Mazhar N, Nicastro E, Kelly DA, Nebbia G, Arnell H, Bjorn F, Hulscher JBF, Serranti D, Arikan C, Polat E, Debray D, Lacaille F, Goncalves C, Hierro L, Munoz Bartolo G, Mozer-Glassberg Y, Azaz A, Brecelj J, Dezsofi A, Calvo PL, Grabhorn E, Sturm E, van der Woerd WJ, Kamath BM, Wang JS, Li L, Durmaz O, Onal Z, Bunt TMG, Hansen BE, Verkade HJ, course NA, Prognosis of P, Effect of biliary Diversion c (2020) Genotype correlates with the natural history of severe bile salt export pump deficiency. J Hepatol. https://doi.org/10.1016/j.jhep.2020.02.007
25. Zellos A, Lykopoulou L, Polydorou A, Tanou K, Jirsa M, Roma E, Knisely AS (2012) Nasobiliary drainage in an episode of intrahepatic cholestasis in a child with mild ABCB11 disease. J Pediatr Gastroenterol Nutr 55(1):88–90. https://doi.org/10.1097/MPG.0b013e31822f2bda

Annex 3: everolimus is safe as a second-/third-line therapy in pediatric autoimmune hepatitis

OPEN

Everolimus is Safe as a Second-/Third-Line Therapy in Pediatric Autoimmune Hepatitis

Giulia Jannone, MD, Isabelle Scheers, MD, PHD, Françoise Smets, MD, PHD, Xavier Stephenne, MD, PHD, and Etienne M Sokal, MD, PHD

ABSTRACT

Objectives: Autoimmune hepatitis (AIH) can lead to progressive fibrosis in patients refractory to conventional therapy with prednisolone and azathioprine. The use of mammalian target of rapamycin (mTOR) inhibitors has recently emerged in refractory AIH, but no data have been published about everolimus in pediatric AIH to date. Our aim was to share our experience about everolimus as a second-/third-line therapy in pediatric AIH.

Methods: Pretransplant AIH patients aged 0–18 years who received everolimus therapy from 2014 to 2021 were retrospectively identified. All patients underwent regular plasma monitoring of everolimus trough levels to avoid toxicity and assess adherence. Special attention was paid to the clinical and biochemical occurrence of everolimus-related adverse events.

Results: We report six difficult-to-treat AIH patients who received everolimus therapy for 8–46 months (median 28 months). No side effects were reported when everolimus plasma trough levels were in the therapeutic range. Liver transaminases improved in 5 of 6 patients at everolimus introduction and significantly decreased at the last follow-up (FU) in our cohort ($P < 0.05$). None of our patients achieved complete biochemical remission at the last FU and 3 of 6 admitted to have suboptimal adherence to therapy.

Conclusions: Our data bring preliminary safety for the use of everolimus as a second-/third-line therapy in pediatric AIH. Although liver transaminases improved in our cohort, prospective studies are needed to determine if everolimus can induce long-term remission.

Key Words: autoimmune hepatitis, corticosteroids, everolimus, mTOR inhibitors, pediatric

What Is Known

- New second-line therapies are needed in pediatric autoimmune hepatitis (AIH) refractory to conventional immunosuppressive therapy with prednisolone and azathioprine.
- The use of mammalian target of rapamycin (mTOR) inhibitors has recently emerged in refractory AIH.

What Is New

- Our work suggests that everolimus can be safely used in difficult-to-treat pediatric AIH.

INTRODUCTION

Autoimmune hepatitis (AIH) is a chronic inflammatory liver disorder, which leads to progressive fibrosis and cirrhosis. Conventional immunosuppressive therapy consists in prednisolone and azathioprine, the latter being used alone as well for long-term maintenance after remission (1,2). Treatment alternatives such as mycophenolate mofetil (MMF, in replacement of azathioprine), budesonide, cyclosporine, or tacrolimus can be administered in the event of intolerable adverse effects or persistent disease activity despite standard therapy. The use of second-line therapies is based on case series reports and experience rather than on randomized controlled trials, which explains why the level of current guidelines recommendations about rescue therapies is low (1,3). The efficacy of those medications is variable in difficult-to-treat patients, and therefore, there is a need for developing new treatment alternatives.

The use of mammalian target of rapamycin (mTOR) inhibitors has recently emerged in refractory AIH (4). A central element in AIH pathogenesis is the loss of immunoregulation related to defective regulatory T cells (5,6). mTOR inhibitors sirolimus and everolimus were originally administered to prevent rejection in solid organ transplantation based on their antiproliferative properties on T cells (7). However, those drugs induce a selective proliferation of regulatory T cells, making them very promising tools in AIH treatment strategies (8,9). mTOR inhibitors also decrease dendritic cells and lymphocytes B maturation, result in a reduced antibodies production, and induce autophagy (10). Sirolimus and everolimus have related chemical structures but display different properties, including differences in pharmacokinetics and drug–target protein interactions (11). Very scarce and rather disappointing retrospective case reports have been published about sirolimus in refractory AIH. Two reports of five and two adult patients respectively showed sustained liver transaminases improvement in 2 of 5 and 0 of 2 patients, with side effects justifying sirolimus withdrawal in one patient (12,13). A pediatric report about sirolimus in AIH showed biochemical improvement in 2 of 4 patients (14). The only case series published about everolimus in difficult-to-treat AIH showed liver transaminases improvement in 6 of 7 adult patients (15). Those 6 patients had their corticosteroids doses reduced and 4 of them displayed complete biochemical response to everolimus. A follow-up (FU) liver biopsy was performed after 3–5 years of everolimus therapy in the 4 patients who responded to the treatment, showing histological stability in 2 patients and fibrosis reduction in the other 2. No major side effects were reported. To our knowledge, no data were ever published about everolimus in pediatric AIH.

Received February 8, 2022;accepted May 28, 2022.

From the Department of Pediatrics, Pediatric Gastroenterology and Hepatology Unit, Cliniques Universitaires Saint-Luc, Université Catholique de Louvain, Brussels, Belgium.

Correspondence: Giulia Jannone, MD, Cliniques Universitaires Saint-Luc, Département de Pédiatrie, Service de Gastroentérologie et Hépatologie Pédiatrique, Avenue Hippocrate, 10, 1200 Brussels, Belgium. E-mail: giulia.jannone@uclouvain.be.

The authors report no conflicts of interest.

JPGN Reports (2022) 3:3(e227)
ISSN: 2691-171X
DOI: 10.1097/PG9.0000000000000227

Considering the lack of data about the use of mTOR inhibitors in pediatric AIH and the promising results obtained with everolimus in adults, our aim was to share our experience about everolimus as a second-/third-line therapy in pediatric AIH. We report 6 AIH/autoimmune sclerosing cholangitis (ASC) children who received everolimus due to poor response to other medications or to related adverse events.

METHODS

Inclusion Criteria

AIH patients who received everolimus (Certican; Novartis, Switzerland) therapy between 2014 and 2021 were retrospectively identified from the Pediatric Hepatology database of the Cliniques Universitaires Saint-Luc (Brussels, Belgium). The inclusion criteria were: diagnosis of definite AIH or ASC according to the ESPGHAN juvenile AIH/ASC scoring system (score ≥ 8, retrospectively applied), patients aged 0–18 at the time of everolimus introduction and pretransplant state (1). Everolimus was introduced in patients refractory to first-/second-line therapies or in patients who suffered from adverse events related to those medications. This research project was assessed and approved by the Biomedical Ethics Committee of the Université catholique de Louvain (Brussels, Belgium; no. 2020/04SEP/445).

Everolimus Regimen and Monitoring

Everolimus was introduced in replacement of azathioprine/MMF or in addition to other immunosuppressant, depending on the patients' clinical and biochemical situations. Based on previous reports in pediatric liver transplantation, everolimus initial dose was 0.8–1.6 mg/m^2/d (16,17). The initial dose was subsequently adapted according to clinical and biochemical response to achieve plasma trough levels of 3–6 ng/ml, as published in adult AIH (15). Everolimus plasma trough levels >2 ng/ml were tolerated in patients who reached biochemical stability and in patients with multiple immunosuppressive therapy to limit infectious side effects. Patients were submitted to regular monitoring of everolimus plasma trough levels to avoid drug toxicity and to assess the adherence. Side effects and disease evolution were investigated clinically and biochemically every 2 weeks at everolimus introduction. Once patients reached stability, clinical and biochemical controls were progressively reduced. Laboratory testing included liver and hematological parameters, kidney function, and blood glucose. Special attention was payed to the clinical and biological occurrence of everolimus most frequent side effects observed in the pediatric population: infections (upper respiratory tract, pneumonia, gastroenteritis, Epstein-Barr), diarrhea, vomiting, mouth ulceration, chronic cough, dermatitis, edema, dyslipidemia, proteinuria, and increase of hepatic enzymes (16,18).

Statistical Analysis

Statistical analysis was conducted using GraphPad Prism 5.0 (GraphPad Software; La Jolla, CA). Continuous variables were presented as mean ± standard deviation or as median (range). The Wilcoxon signed-rank nonparametric test was used to compare repeated measures between subgroups. A two-tailed $P \leq 0.05$ was considered to indicate statistical significance for all analyses.

RESULTS

Description of the Study Population

Six AIH/ASC patients received everolimus therapy between 2014 and 2021. Clinical, biochemical, and histological characteristics of the study population at the time of diagnosis are summarized in Table 1. Three of the 4 AIH type 1 patients had positive pANCA, but showed no signs of sclerosing cholangitis in magnetic resonance cholangiograpy nor in liver biopsy. None of our patients had associated IBD. All patients displayed important fibrosis with incomplete/complete cirrhosis at diagnosis (Metavir score F3-F4). No biopsy was performed in our cohort during the course of everolimus therapy.

Everolimus Introduction

Conventional therapy with methylprednisolone and azathioprine had been tried in all patients before everolimus introduction, as well as budesonide (n = 1) and MMF (n = 4), the latter in replacement of azathioprine. Both ASC patients received ursodeoxycholic acid therapy from the moment of the diagnosis. The reason for everolimus introduction was poor response to first- and/or second-line medications in 4 patients requiring corticosteroids maintenance therapy (Table 2). Important side effects of corticosteroids/azathioprine or MMF justified the change of medication in the 2 other patients. Patient no. 2 suffered from diabetes secondary to high-dose methylprednisolone. She subsequently presented a cutaneous reaction and upper limb paresthesia that resolved at azathioprine withdrawal. Those side effects did not recur when azathioprine was added to everolimus therapy 2 years later. Patient no. 6 had intense abdominal pain that only resolved at MMF therapy interruption. Everolimus replaced azathioprine or MMF except for patients no. 3 and 4, who had everolimus added to standard therapy with methylprednisolone and azathioprine due to very poor control of the disease. Median FU duration under everolimus therapy was 28 months (range 8–46 months).

Everolimus Monitoring and Side Effects

The mean everolimus plasma trough levels in our cohort was 3.4 ± 1.4 ng/ml. Three patients admitted to have suboptimal adherence to therapy and repeatedly displayed low/undetectable everolimus plasma trough levels (Table 2). During the first month following everolimus introduction, all patients were adherent according to their everolimus plasma trough levels. No clinical side effects were reported during the course of everolimus therapy when plasma trough levels were in the therapeutic range. Specifically, none of our patients suffered from severe/frequent infections, mouth ulcerations, chronic cough, or dermatitis. Patient no. 6 had an elevation of aspartate aminotransferase (AST) levels associated to high everolimus plasma trough levels (10.6 ng/ml) one month after everolimus introduction. Her AST levels improved shortly after adapting everolimus regimen. Everolimus was not associated to dyslipidemia, hyperglycemia, or renal function alteration/proteinuria in our cohort.

Corticosteroids During Everolimus Therapy

Methylprednisolone was stopped in 2 patients during the course of everolimus therapy: patient no. 3 due to biochemical stability and patient no. 5 in an attempt to improve the adherence to the rest of the treatment (Table 2). Two patients (no. 4 and 6) were receiving a well-tolerated low dose of methylprednisolone at everolimus introduction, which was unchanged to avoid subsequent relapse. Budesonide and azathioprine were added to the treatment of patient no. 2 due to insufficient disease control under everolimus alone and to previous diabetes secondary to methylprednisolone therapy. Finally, budesonide replaced methylprednisolone in patient no. 1 due to dependence to steroids.

Clinical and Biochemical Evolution During Everolimus Therapy

Four patients had very high liver transaminases plasma levels at everolimus introduction (between 7-fold and 20-fold elevation) and showed biochemical improvement within one month of therapy without normalization (2- to 5-fold elevation of alanine aminotransferase [ALT] after 1 month) (Fig. 1A, B). The other two patients (no.

TABLE 1. Characteristics of the study population at the time of AIH diagnosis

	Patient 1	Patient 2	Patient 3	Patient 4	Patient 5	Patient 6
AIH type	Type 1	Type 1	Type 1	Type 1	ASC	ASC
Gender	F	F	F	F	M	F
Age (years)	11	12	9	14	11	12
Juvenile AIH/ASC score*	9	11	11	10	12	11
Autoantibodies	ANA	ANA	ANA	ANA	ANA	ANA
	SMA	SMA	SMA	pANCA	SMA	SMA
		pANCA	pANCA		pANCA	pANCA
γ-globulins (g/L) (<15)	NA	41.4	31.7	71.5	44.4	23.1
ALT (UI/L) (<35)	1520	95	1062	255	311	206
AST (UI/L) (<35)	1380	106	990	592	399	142
GGT (UI/L) (<40)	568	33	69	167	201	324
Fibrosis (Metavir score)	F3	F4	F3	F3-F4	F3	F3
Other immune diseases	None	Coombs-positive hemolytic anemia	Celiac disease	Coombs-positive hemolytic anemia, AI pancreatitis	None	None

*Definite AIH/ASC: score ≥ 8 (4).

AI = autoimmune; AIH = autoimmune hepatitis; ALT = alanine aminotransferase; ANA = antinuclear antibodies; ASC = autoimmune sclerosing cholangitis; AST = aspartate aminotransferase; GGT = gamma-glutamyl transferase; LKM-1 = anti-liver kidney microsome type 1 antibodies; NA = not available; pANCA = perinuclear antineutrophil cytoplasmic antibodies; SMA = antismooth muscle antibodies.

TABLE 2. Everolimus introduction and follow-up

	Patient 1	Patient 2	Patient 3	Patient 4	Patient 5	Patient 6
Reason for EV introduction	Poor control	Side effects	Poor control	Poor control	Poor control	Side effects
Age at EV introduction (years)	14	12	9	15	16	16
FU under EV (months)	30	46	15	8	27	28
EV mean plasma trough levels (ng/ml)	3.3 ± 0.8	3.1 ± 2	2.6 ± 0.5	1.5 ± 0.6	3.8 ± 3.4	5.8 ± 3.2
EV side effects	No	No	No	No	No	Yes
Admitted adherence issues	No	Yes	No	Yes	Yes	No
Number of EV plasma trough levels < 2 ng/ml	0/8 (0%)	5/21 (24%)	1/12 (8%)	6/8 (75%)	4/12 (33%)	0/12 (0%)
Treatment before EV introduction	MMF, mPred	Aza	Aza, mPred	Aza, mPred	Aza, mPred	MMF, mPred
Treatment at EV introduction	EV, mPred	EV	EV, Aza, mPred	EV, Aza, mPred	EV, mPred	EV, mPred
Treatment at last FU	EV, Budes	EV, Aza, Budes	EV, Aza	EV, Aza, mPred	EV	EV, mPred
Steroid dosage during EV therapy (mg/kg/d)	0.5 → 0.1	0 → 0.1	0.1 → 0	0.1	0.3 → 0	0.03

Aza = azathioprine; Budes = budesonide; EV = everolimus; FU = follow-up; MMF = mycophenolate mofetil; mPred = methylprednisolone; NA = not available.

2 and 6) had up to 3-fold elevation of transaminases when everolimus was introduced due to side effects related to other medications. The transaminases levels of patient no. 2 very slightly decreased after one month, while patient no. 6 had an initial elevation of AST levels associated to high everolimus plasma trough levels. Gammaglobulins levels evolution during everolimus therapy were variable and GGT levels tended to improve after one month except for patients no. 4 (AIH type 1) and 5 (ASC) (Fig. 1C, D).

At last FU, all but one patient had a marked decrease (n = 3) or normalization (n = 2) of ALT levels (Fig. 1A). The remaining patient with ASC (patient no. 5) had no biochemical improvement in the context of poor adherence to therapy. When we considered the whole cohort, ALT, AST, and gammaglobulins levels significantly improved at the last FU compared to the levels observed at everolimus introduction ($P < 0.05$) (Fig. 1E). Four patients still displayed moderately elevated gammaglobulins at last FU (maximum 1.3-fold increase), and none of our patients achieved a persistent normalization of autoantibodies titers during FU. Clinically, all patients were in remission except for patient no. 5 who still presented intense fatigue.

DISCUSSION

We report 6 AIH/ASC patients aged 9–16 years, who received everolimus as a rescue therapy due to disease poor control despite first-/second-line medications or to intolerable side effects. No adverse events were reported in our cohort when everolimus plasma

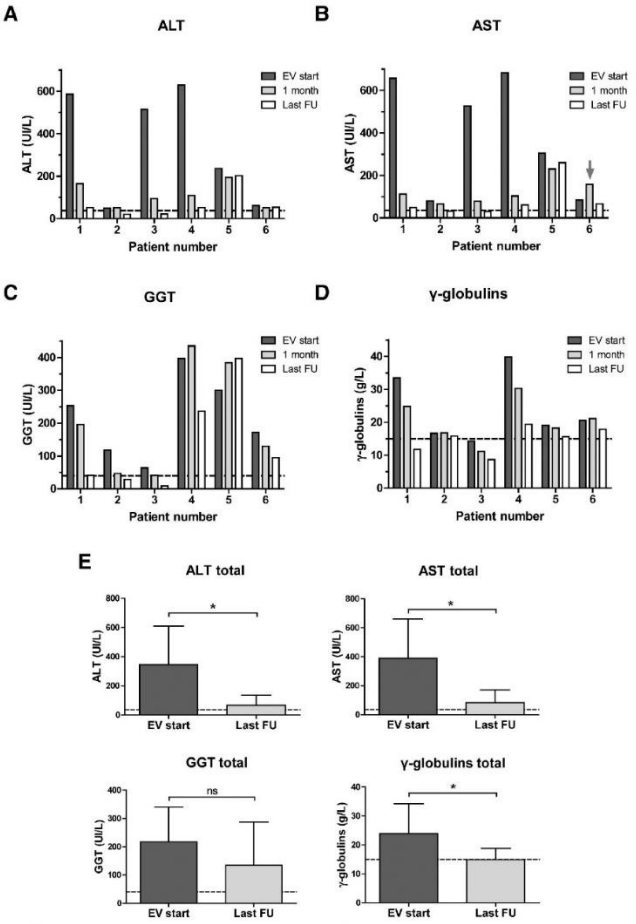

FIGURE 1. Evolution of biochemical parameters during the course of everolimus therapy. A) ALT plasma levels. Normal levels < 35 UI/L (discontinued line); (B) AST plasma levels. Normal levels < 35 UI/L (discontinued line). The grey arrow shows the AST elevation that was associated to high everolimus plasma levels; (C) GGT plasma levels. Normal levels < 40 UI/L (discontinued line); (D) γ-globulins plasma levels. Normal levels < 15 g/L (discontinued line); (E) Evolution of the whole cohort biochemical parameters between everolimus introduction and the last FU. Discontinued lines represent the upper limit of normal levels for each parameter. Data are presented as mean ± standard deviation; *$P < 0.05$. ALT = alanine aminotransferase; AST = aspartate aminotransferase; EV = everolimus; FU = follow-up; GGT = γ-glutamyl transferase; ns = not significant.

trough levels were in the therapeutic range. Everolimus improved liver transaminases in our patients without inducing biochemical remission.

Plasma monitoring of everolimus was regularly performed to avoid drug toxicity and to verify the adherence. None of our patients suffered from clinical/biochemical adverse events associated to

everolimus when plasma trough levels were in the therapeutic range. In particular, no dyslipidemia, proteinuria, frequent/severe infections, mouth ulcerations, chronic cough, or dermatitis were reported in our cohort. Everolimus plasma trough levels were kept in the inferior limit of the therapeutic range in patients receiving multiple immunosuppressive therapy, to limit infectious side effects. This might have contributed to the very low occurrence of clinical/biochemical adverse events associated to everolimus in our cohort. Three of our 6 patients admitted to have suboptimal adherence and displayed a high variability in everolimus plasma trough levels during FU. However, those patients did not suffer from any side effects when adherence was good and everolimus plasma trough levels were in the therapeutic range. We observed that adherence seemed to be better when patients were seen more regularly due to therapeutic changes or poor disease control. Based on this observation, a systematic closer FU in nonadherent patients could maybe help to improve adherence issues. Nonadherence remains a major problem in the management of juvenile AIH and made the assessment of everolimus efficacy as a long-term remission inducer even more challenging in our cohort (19).

Liver transaminases improved in 5 of 6 patients within 1 month of everolimus introduction, when adherence was good in all patients. The last patient had initial elevation of AST associated to high trough levels of plasma everolimus, which resolved once everolimus dosage returned in the target range. At the last FU, 5 of 6 patients showed liver transaminases improvement, of which 2 AIH type 1 patients displayed ALT complete normalization. The last ASC patient had insignificant biochemical improvement in the context of adherence issues, and still suffered from important fatigue at the last FU. When we considered our whole cohort, ALT, AST, and gammaglobulins levels improved between everolimus introduction and the last FU. Still, existing guidelines define biochemical remission as the normalization of liver transaminases and γ-globulins levels, in the presence of low or negative autoantibodies titles (1, 20). According to this definition, none of our patients achieved biochemical remission at the last FU. No FU biopsies were performed during the course of everolimus therapy in our cohort.

Important limitations of our study are the retrospective design and the small number of included patients. The retrospective study design and the complexity of the clinical cases explain that the patients' therapeutic regimens varied during the course of everolimus therapy. Those differences must be noted as they limit the ability to evaluate the efficacy of everolimus alone. In addition, our cohort includes AIH type 1 and ASC patients, offering interesting information but further limiting the number of patients for each subtype. ASC patients have poorer prognosis as compared to AIH type 1 due to the progression of biliary lesions despite immunosuppressive therapy (21,22). Our AIH type 1 patients seemed to have a better biochemical response to everolimus as compared to ASC, but larger studies are needed to corroborate those preliminary results. The mean FU duration of patients receiving everolimus therapy was 28 months in our cohort, which allowed us to obtain appreciable information about the clinical and biochemical evolution of our patients. Due to the rarity of the condition and the lack of published data about everolimus in pediatric AIH, we believe that our small case series report is a substantial contribution to the existing literature.

In conclusion, we present the first pediatric report about everolimus in difficult-to-treat AIH type 1/ASC patients. Liver transaminases improved in 5 of 6 patients following everolimus introduction and significantly decreased at the last FU. Everolimus was safe when plasma trough levels were in the therapeutic range, but did not allow to achieve biochemical remission in our cohort. Our results bring preliminary safety for the use of everolimus as a second-/third-line therapy in pediatric AIH, and open the way to a proper controlled trial.

REFERENCES

1. Mieli-Vergani G, Vergani D, Baumann U, et al. Diagnosis and management of pediatric autoimmune liver disease: ESPGHAN hepatology committee position statement. *J Pediatr Gastroenterol Nutr*. 2018;66:345–360.
2. Johnson PJ, McFarlane IG, Williams R. Azathioprine for long-term maintenance of remission in autoimmune hepatitis. *N Engl J Med*. 1995;333:958–963.
3. Mack CL, Adams D, Assis DN, et al. Diagnosis and management of autoimmune hepatitis in adults and children: 2019 practice guidance and guidelines from the american association for the study of liver diseases. *Hepatology*. 2020;72:671–722.
4. Terziroli Beretta-Piccoli B, Mieli-Vergani G, Vergani D. Autoimmune hepatitis: standard treatment and systematic review of alternative treatments. *World J Gastroenterol*. 2017;23:6030–6048.
5. Mieli-Vergani G, Vergani D, Czaja AJ, et al. Autoimmune hepatitis. *Nat Rev Dis Primers*. 2018;4:18017.
6. Ferri S, Longhi MS, De Molo C, et al. A multifaceted imbalance of T cells with regulatory function characterizes type 1 autoimmune hepatitis. *Hepatology*. 2010;52:999–1007.
7. Neuhaus P, Klupp J, Langrehr JM. mTOR inhibitors: an overview. *Liver Transpl*. 2001;7:473–484.
8. Battaglia M, Stabilini A, Roncarolo MG. Rapamycin selectively expands CD4+CD25+FoxP3+ regulatory T cells. *Blood*. 2005;105:4743–4748.
9. Gedaly R, De Stefano F, Turcios L, et al. mTOR inhibitor everolimus in regulatory T Cell expansion for clinical application in transplantation. *Transplantation*. 2019;103:705–715.
10. Thomson AW, Turnquist HR, Raimondi G. Immunoregulatory functions of mTOR inhibition. *Nat Rev Immunol*. 2009;9:324–337.
11. Klawitter J, Nashan B, Christians U. Everolimus and sirolimus in transplantation-related but different. *Expert Opin Drug Saf*. 2015;14:1055–1070.
12. Chatrath H, Allen L, Boyer TD. Use of sirolimus in the treatment of refractory autoimmune hepatitis. *Am J Med*. 2014;127:1128–1131.
13. Rubin JN, Te HS. Refractory autoimmune hepatitis: beyond standard therapy. *Dig Dis Sci*. 2016;61:1757–1762.
14. Kurowski J, Melin-Aldana H, Bass L, et al. Sirolimus as rescue therapy in pediatric autoimmune hepatitis. *J Pediatr Gastroenterol Nutr*. 2014;58:e4–e6.
15. Ytting H, Larsen FS. Everolimus treatment for patients with autoimmune hepatitis and poor response to standard therapy and drug alternatives in use. *Scand J Gastroenterol*. 2015;50:1025–1031.
16. Ganschow R, Ericzon BG, Dhawan A, et al. Everolimus and reduced calcineurin inhibitor therapy in pediatric liver transplant recipients: results from a multicenter, prospective study. *Pediatr Transplant*. 2017;21.
17. Nielsen D, Briem-Richter A, Sornsakrin M, et al. The use of everolimus in pediatric liver transplant recipients: first experience in a single center. *Pediatr Transplant*. 2011;15:510–514.
18. Dumortier J, Couchonnal E, Lacaille F, et al. mTOR inhibitors in pediatric liver transplant recipients. *Clin Res Hepatol Gastroenterol*. 2019;43:403–409.
19. Kerkar N, Annunziato RA, Foley L, et al. Prospective analysis of nonadherence in autoimmune hepatitis: a common problem. *J Pediatr Gastroenterol Nutr*. 2006;43:629–634.
20. Manns MP, Czaja AJ, Gorham JD, et al; American Association for the Study of Liver Diseases. Diagnosis and management of autoimmune hepatitis. *Hepatology*. 2010;51:2193–2213.
21. Gregorio GV, Portmann B, Karani J, et al. Autoimmune hepatitis/sclerosing cholangitis overlap syndrome in childhood: a 16-year prospective study. *Hepatology*. 2001;33:544–553.
22. Jannone G, Stephenne X, Castanares-Zapatero D, et al. Fibrosis and inflammation histology scores predict disease remission in pediatric autoimmune hepatitis. *JSM Hepatitis*. 2017;2:1006.